ISSN 2079-1372 *DOI: 10.31891/2079-1372*

THE INTERNATIONAL SCIENTIFIC JOURNAL

PROBLEMS OF TRIBOLOGY

Volume 31 ***No 1/119-2026***

МІЖНАРОДНИЙ НАУКОВИЙ ЖУРНАЛ

ПРОБЛЕМИ ТРИБОЛОГІЇ

PROBLEMS OF TRIBOLOGY

INTERNATIONAL SCIENTIFIC JOURNAL

Published since 1996, four time a year

Volume 31 No 1/119-2026

Establishers:
Khmelnytskyi National University (Ukraine)
Lublin University of Technology (Poland)

Associated establisher:
Vytautas Magnus University (Lithuania)

Editorial board address:
International scientific journal "Problems of Tribology",
Khmelnytskyi National University,
Instytutska str. 11, Khmelnytskyi, 29016, Ukraine
phone +380975546925

Indexed: CrossRef, DOAJ, Ulrichsweb, ASCI, Google Scholar, Index Copernicus

E-mail: tribology@khmnu.edu.ua

Internet: http://tribology.khnu.km.ua

ПРОБЛЕМИ ТРИБОЛОГІЇ

МІЖНАРОДНИЙ НАУКОВИЙ ЖУРНАЛ

Видається з 1996 р. ***Виходить 4 рази на рік***

Том 31 **№ 1/119-2026**

Співзасновники:
Хмельницький національний університет (Україна)
Університет Люблінська Політехніка (Польща)

Асоційований співзасновник:

Університет Вітовта Великого (Литва)

Адреса редакції:
Україна, 29016, м. Хмельницький, вул. Інститутська 11, к. 4-401
Хмельницький національний університет, редакція журналу "Проблеми трибології"
тел. +380975546925, **E-mail**: tribology@khmnu.edu.ua

Internet: http://tribology.khnu.km.ua

Зареєстровано Міністерством юстиції України
Свідоцтво про держреєстрацію друкованого ЗМІ: Серія КВ № 1917 від 14.03. 1996 р.
(перереєстрація № 24271-14111ПР від 22.10.2019 року)

Входить до переліку наукових фахових видань України
(Наказ Міністерства освіти і науки України № 612/07.05.19. Категорія Б.)

Індексується в МНБ: CrossRef, DOAJ, Ulrichsweb, ASCI, Google Scholar, Index Copernicus

Рекомендовано до друку рішенням вченої ради ХНУ, протокол № 14 від 12.03.2026 р.

ISSN 2079-1372 Problems of Tribology, V. 31, No 1/119-2026

Problems of Tribology
Website: http://tribology.khnu.km.ua/index.php/ProbTrib
E-mail: tribosenator@gmail.com

CONTENTS

***ISSN 2079-1372 Problems of Tribology**, V. 31, No 1/119-2026*

Problems of Tribology
Website: http://tribology.khnu.km.ua/index.php/ProbTrib
E-mail: tribosenator@gmail.com

ЗМІСТ

ISSN 2079-1372 Problems of Tribology, V. 31, No 1/119-2026, 6-15

Problems of Tribology
Website: http://tribology.khnu.km.ua/index.php/ProbTrib
E-mail: tribosenator@gmail.com

DOI: https://doi.org/10.31891/2079-1372-2026-119-1-6-15

Tribochemistry of damage to metal joints during fretting corrosion

V.V. Shevelya[*] 0000-0002-5462-3524, **V.P. Oleksandrenko** 0000-0002-2404-2104, **O.V. Dykha** 0000-0003-3020-9625, **K.S. Sokolan** 0000-0002-3513-8312
Khmelnytskyi National University, Ukraine
[*]*E-mail: valeriy.shevelya@gmail.com*

Received: 30 November 2025: Revised 12 December 2025: Accept: 10 January 2026

Abstract

The patterns of fretting wear of a number of structural materials and galvanic coatings were researched, taking into account their mechanical and physicochemical properties. The influence of the composition of the gas environment (air, oxygen) on the intensity of fretting wear was assessed, as well as the contact load with the corresponding temperature recording in the friction zone. Data were obtained indicating the possibility of low-amplitude fretting of metals in an air environment along with the oxidative processes of electrochemical corrosion. The physicochemical prerequisites for the initiation of electrochemical processes in the zone of vibrational contact during the formation of an ultradisperse oxide layer, which becomes a catalyst for the accelerated chemisorption of oxygen and air moisture in radical and ion-radical forms, are considered. As a result, according to the electronic theory of adsorption and catalysis on semiconductors (oxides), contact phenomena begin to develop through the mechanism of autocatalytic corrosion. After a latent period of oxide accumulation, conditions are created for electrochemical processes that contribute to corrosion-fatigue failure of mating surfaces. The results of the study expand existing ideas about the nature of corrosion processes during partial and mixed sliding, focusing on the possibility of using traditional methods of electrochemical protection to increase the fretting resistance of friction units operating under vibration conditions.

Keywords: fretting wear, friction coefficient, fretting resistance, adsorption, corrosion, electrochemistry, chemical-thermal treatment

Introduction

In many industrial equipment devices, machines, and instruments, the cause of failure is often fretting corrosion, which affects nominally stationary or low-movement couplings during their relative oscillatory motion with a small amplitude [1-4]. Such joints include, for example, bolted, splined, and threaded connections; gear couplings and lock joints; press and hot fits on shafts of discs, bearings, and wheel hubs; pipe fittings, etc. [5-10]. The cause of relative slippage in connections is vibration of the entire structure or the connection performing its working functions. In addition to loss of fit due to fretting wear, destruction due to fretting fatigue poses a great danger.

It is generally accepted that fretting wear develops as a result of the synergistic superposition of a number of contact phenomena, including adhesion (bonding), abrasive wear, delamination (surface delamination), contact fatigue, and oxidation processes [11-14]. In addition to the strength and viscoelastic properties of structural materials, their resistance to fretting wear is also influenced by chemical resistance, which, in combination with the corrosive activity of the external environment and the physicochemical properties of wear products (oxides), determines the specific vulnerability of metal joints [15-17]. However, the tribochemistry of fretting resistance of friction contact under vibration conditions has not been sufficiently studied. In particular, the problem of the influence of the nature of contact corrosion processes responsible for the degradation and destruction of mechanical tribosystems during “dry” fretting in an air working environment remains relevant. While the development of chemical corrosion (oxidation) during metal fretting in an air atmosphere is undisputed, there is no consensus regarding electrochemical corrosion. It is known that the occurrence and rate of electrochemical corrosion depend mainly on atmospheric humidity and temperature [18]. However, the question of how these factors affect the electrochemical corrosion mechanism under fretting conditions remains open due to conflicting

experimental data. In some cases, an increase in air humidity or temperature increased fretting wear, while in others it decreased it. For example, studies in which the rate of fretting wear decreased with increasing temperature [2,19] indicate the possibility of electrochemical corrosion. However, on the other hand, there is data showing that when the temperature was increased to 300°C, the wear rate during impact fretting increased by an order of magnitude compared to room temperature [20].

Experiments in which a more than 10-fold decrease in the fretting fatigue life of metal in air compared to vacuum was observed [4] support the idea that electrochemical corrosion can develop during fretting in a normal air environment. Earlier [21], when studying the fretting resistance of joints consisting of a number of alloys in contact with steel 45, it was shown that the more positive the electrode potential of the alloy relative to steel 45, the less it wore out. Simultaneously with the increase in the nobility of the alloy, the wear of the counterbody – steel 45, increased. This effect was associated with the accumulation of highly dispersed oxides in the vibration contact zone, which actively adsorbed moisture and oxygen from the air, resulting in electrochemical corrosion superimposed on the chemical corrosion (oxidation) process.

Thus, the role of electrochemical processes in fretting corrosion of nominally stationary or low-mobility joints remains controversial and requires further research. Obviously, much depends on the nature of the friction pair materials, the amplitude-load operating mode, the composition and properties of wear products, and the stage of fretting process development. The limited experimental data complicates the modeling of the physicochemical processes leading to the failure of the mechanical tribosystems under consideration.

The **aim of this work** is to research the contribution and role of chemical and electrochemical corrosion in the wear process of metal friction pairs under low-amplitude fretting conditions.

Research materials and methodology

The fretting resistance (fretting wear) of armco iron and a number of steels with mechanical and physicochemical properties acquired as a result of heat treatment under standard conditions (Table 1) was researched.

Table 1

Researched steels and their mechanical properties

Mechanical properties	Steel 45	ShKh15	DI-3A	16KhGTA	38KhA	30KhGSA	40KhNMA
$\sigma_в$. MPa	1450	2200	1100	1050	1050	1200	1090
σ_{-1}. MPa	550	800	540	600	500	650	490
HV	420	770	430	310	460	440	500
φ. V	-0.35	-0.36	-0.37	-0.38	-0.38	-0.40	-0.30

The fretting wear of a number of electrolytic coatings on steel 45 (Zn, Cd, Pb, Sn, Ag) was also studied.

The tests were carried out on an МФК friction machine (Fig. 1*a*) in accordance with GOST 23.211-80 [23], according to which fretting corrosion was caused in a flat ring contact during oscillatory-rotational motion around the axis of the bushing end face (movable sample) relative to the end face of a stationary fixed cylindrical sample made of the material under study (Fig. 1*b*).

In all cases, the material of the moving sample (bushing) was steel 45, hardened and tempered to *HV* = 600; at the same time, the weight wear of both the stationary and moving samples was evaluated with simultaneous control of the friction coefficient. In addition to air, oxygen was used as a gas medium, which was blown through the gas chamber of the experimental setup, after which its flow was set with a slight excess pressure before the experiment.

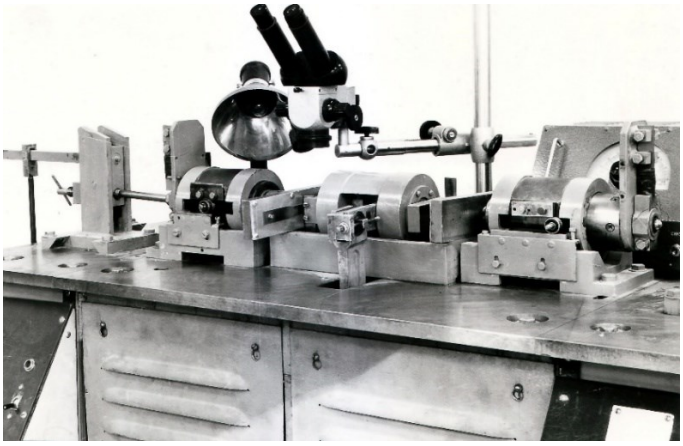

***a*)**

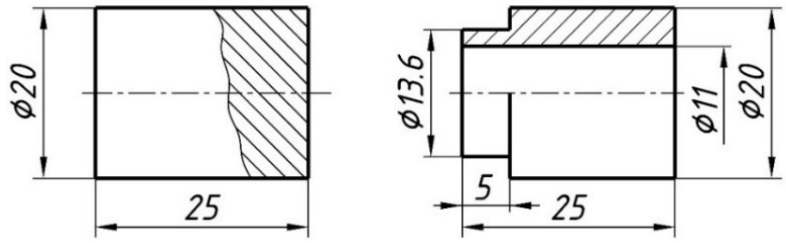

***b*)**

Fig. 1. General view of the МФК setup (*a*) and samples (*b*) for testing metals for fretting corrosion

To evaluate the electrochemical activity of the studied steels, the steady-state electrode potentials in a 3% NaCl solution (φ, V) were determined relative to a standard hydrogen electrode, and a potentiostatic method was used to record the anodic polarization curves.

Research results and discussion

Given the vibrational, alternating nature of contact interaction that causes fretting corrosion, it is natural to assume that the main cause of metal surface destruction under fretting conditions (apart from adhesion and abrasive wear) is fatigue and corrosion processes. Obviously, the degree of structural damage to metals, as well as the role of chemical factors, can vary significantly depending on the loading parameters (number of fretting cycles, specific load, sliding amplitude, oscillation frequency), the aggressiveness of the external environment, and the stage of development of the fretting process. It can be expected that the intensity of fretting wear at a certain stage of damage will be related to the degree of dispersion of the surface layers in the contact zone. The disordered ultradisperse structure of the metal acquires increased chemical and electrochemical activity in the presence of a suitable environment.

Fig. 2 compares the fretting wear kinetics of armco iron and 45 steel, which reveals the following pattern: up to a certain critical number of test cycles, armco iron wears out faster than steel, and above that number of cycles, steel wears out more intensively. It can be assumed that in the initial stages of fretting, when corrosion processes are not yet sufficiently developed, the wear resistance of the material is determined by its contact strength. Naturally, steel 45 is more wear-resistant under these conditions due to its greater ability to resist plastic deformation. The greater wear of steel compared to iron in the subsequent stages of fretting corrosion is obviously associated with the activation of chemical processes in the contact zone, which should lead to a change in friction conditions. Indeed, as fretting corrosion develops, a monotonic decrease in the friction coefficient is observed for both materials (Fig. 3), and by the time the friction regime has stabilized, when the chemical factor begins to manifest itself more significantly, the degree of decrease in the friction coefficient for steel 45 is always greater due to the increased effectiveness of the shielding action of corrosion products.

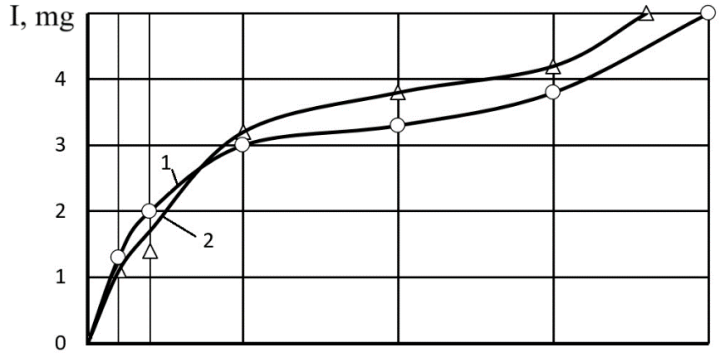

Fig. 2. Dependence of fretting wear of armco iron (1) and steel 45 (2) on the number of loading cycles: A = 0,05 mm; P = 25 MPa; f = 25 Hz

With an increase in the number of test cycles, steel wear increases compared to armco iron, which may indicate the development of a corrosion process in the contact zone that is different from chemical oxidation. It is quite likely that the wear products concentrated between the contacting surfaces initiate a series of corrosion processes, and in the later stages, the development of electrochemical corrosion.

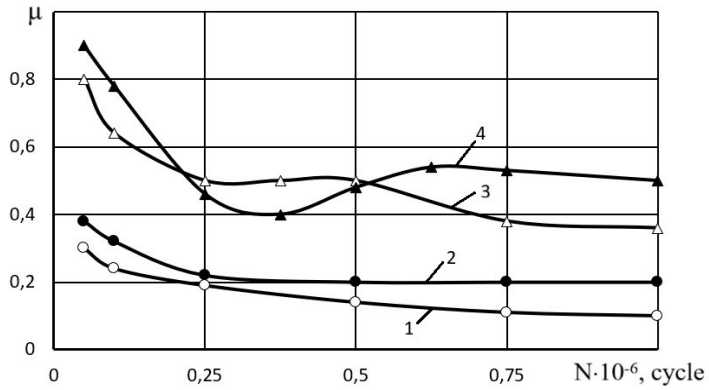

Fig. 3. Change in the friction coefficient during the development of fretting corrosion of steel 45 (1.3) and armco iron (2.4): 1,2 - *P* = 10 MPa; 3,4 - *P* = 50 MPa

From an electrochemical point of view, steel 45, unlike armco iron, has a large amount of cathodic impurities (cementite), which create an additional amount of microgalvanic couples. The effect of such impurities depends on the nature of the corrosion process control [18]. With cathodic control, cathodic impurities will increase the corrosion rate: the more cathodic impurities in the metal (steel 45) and the greater the potential difference between the cathodic and anodic components of the metal, the higher the corrosion rate. Thus, it can be concluded that at the beginning of fretting corrosion, chemical (gas) corrosion processes predominate, and with an increase in the number of loading cycles, electrochemical processes may occur in the friction zone.

Comparative tests in air and oxygen (no moisture removal) of steel 45 (Fig. 4) demonstrated the possibility of electrochemical processes developing under fretting corrosion conditions.

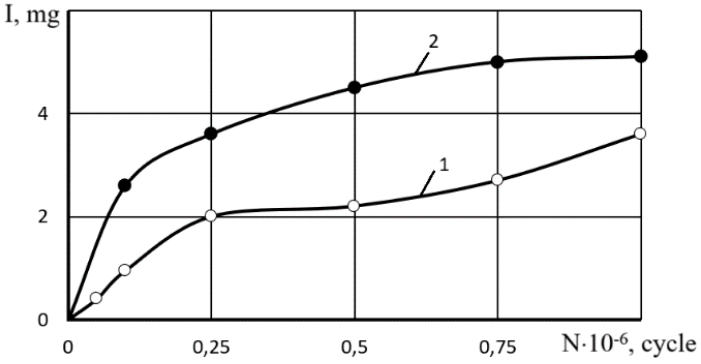

Fig. 4. Dependence of fretting wear of steel 45 on the number of loading cycles in air (1) and in oxygen (2): *P* = 10 MPa; *A* = 0,05 mm; *f* = 25 Hz

At the very beginning of fretting corrosion, when the chemical factor manifests itself in the predominant oxidation processes, with an excess of oxygen in the external environment, a material with increased chemical activity (45 steel) is more susceptible to fretting wear. Obviously, at this stage, due to the formation of an oxide layer, the mechanical factor plays a secondary role, since friction conditions are facilitated. The latter is evidenced by a decrease in the friction coefficient during tests in oxygen compared to air at the stage of wear stabilization. On steel, which is more chemically active than armco iron, oxide films form and break down more quickly in oxygen, which contributes to the earlier development of electrochemical processes.

In electrochemical corrosion with oxygen depolarization, when the cathodic process is the controlling factor, an increase in the concentration of the cathodic depolarizer (oxygen) in the friction zone intensifies corrosion. With an increase in load, the development of electrochemical processes begins at earlier stages of fretting corrosion, since the corrosion rate with oxygen depolarization (which occurs in our case) is usually determined by the rate of oxygen diffusion to the corroding metal surface [18]. As the contact load increases, the access of atmospheric oxygen to the contact zone becomes more difficult, thereby significantly increasing the concentration polarization of oxygen, i.e., cathodic control occurs earlier. Under such conditions, an increase in the concentration of oxygen (cathodic depolarizer) in the environment leads to an observable increase in the destruction of contacting surfaces due to the activation of electrochemical processes. In addition, it should be noted that as the load increases, the processes of formation and subsequent destruction of primary oxide films accelerate, so that the oxide layer between the contacting surfaces forms more quickly. Accordingly, electrochemical corrosion begins to develop earlier due to the active adsorption of moisture and oxygen by oxides.

Fig. 5 shows the change in the intensity of fretting wear of the metals under study depending on the specific load. The number of cycles ($N = 3 \cdot 10^5$) corresponding to the stabilization of wear values, when corrosion processes prevail and the behavior of the material is significantly determined by its chemical activity, was taken as the basis for testing.

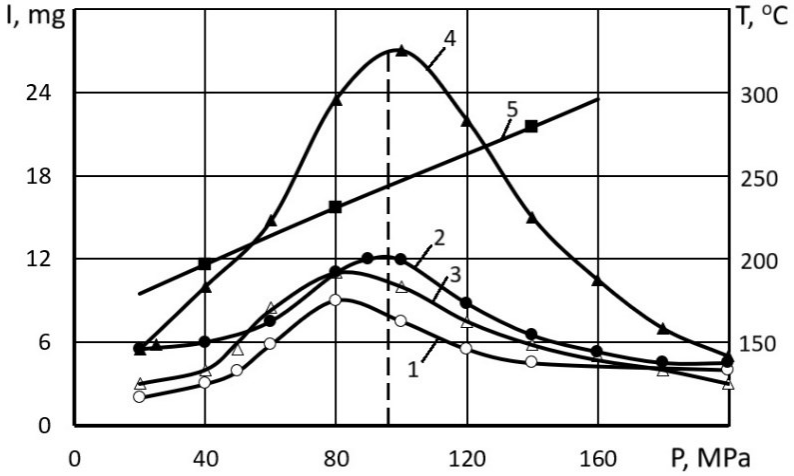

Fig. 5. Dependence of fretting wear of armco iron (1,2) and steel 45 (3,4) on contact load in air (1,3) and in oxygen (2,4); 5 – change in contact temperature: $N = 3 \cdot 10^5$ cycles; A = 0,05 mm; f = 25 Hz

The dependence of wear on specific load is parabolic in nature: the amount of wear increases up to a load of about 80 MPa, and then decreases. It should be emphasized that the sliding amplitude remained constant at all load levels. Obviously, at specific loads corresponding to the ascending branches of the characteristics, the oxidizing environment enters the friction zone relatively more easily. The reduction in wear at loads above critical values may be due, firstly, to the difficulty of access of the oxidizing environment to the contact zone and the activation of the setting process, and secondly, to the increase in temperature at the contact, which can significantly worsen the conditions for the formation of a corrosive environment. Indeed, the effect of reducing fretting wear of the materials under study upon reaching a certain critical contact pressure (80-100 MPa) can be associated with an increase in temperature to 230-250°C recorded in the contact zone (using a thermocouple), which is precisely the temperature limit for the removal of adsorbed moisture and oxygen [24]. Dehydration of the oxide surface leads to a decrease in adsorption activity.

A comparison of the rate of deterioration of iron and steel 45 depending on the specific load during tests in air and oxygen (see Fig. 5) shows that the lower wear of these materials in air compared to oxygen could be explained (given the higher friction coefficient for air) by the greater intensity of adhesive bonding and mutual transfer of metal from one surface to another. Considering that armco iron has reduced hardness, the adhesion factor for this material should be most significant. However, the wear of armco iron in both environments differs little, while steel 45 deteriorates more in oxygen and to a greater extent the higher the pre-critical load. Obviously, in this case, the tendency of the material to electrochemical corrosion plays a decisive role. In fact, for chemically inactive armco iron, an increase in the oxygen content in the external environment does not significantly intensify fretting wear. At the same time, for a more corrosion-active material (steel 45), the role of an environment with a strong oxidizing effect becomes decisive in the destruction of the joint.

Obviously, if contact is made between materials of the same name, electrochemical corrosion should be caused by microgalvanic couples (structural heterogeneity, different crystal orientation, structural imperfections, etc.). It is natural to assume that electrochemical processes will manifest themselves more clearly if contact is made between dissimilar materials that differ in their electrochemical properties (macrogalvanic couple). When a corrosion-active environment arises in the contact zone, electrochemical processes should develop according to the mechanism of contact corrosion [18].

To verify this possibility, a study was conducted, the first stage of which examined the fretting corrosion of 45 steel in contact with electrolytic coatings (Zn, Cd, Pb, Sn, Ag). The counterbody (movable sample) was 45 steel – hardened.

The following pattern was established: the more noble the surface in contact with the steel, the less wear that surface experienced and, in turn, the more fretting wear the steel itself experienced (Fig. 6).

It can be seen that the coatings with which steel 45 worked are arranged in an electrochemical series in order of increasing positivity of their electrode potential. Coatings with a more negative electrode potential than steel 45 (Zn, Cd), while protecting the steel from corrosion, are themselves intensively destroyed: steel itself begins to play a similar role when it is in contact with tin and silver. It is noteworthy that at a relatively low specific load (P = 10 MPa), steel samples in contact with zinc showed not only no wear, but also an increase in weight.

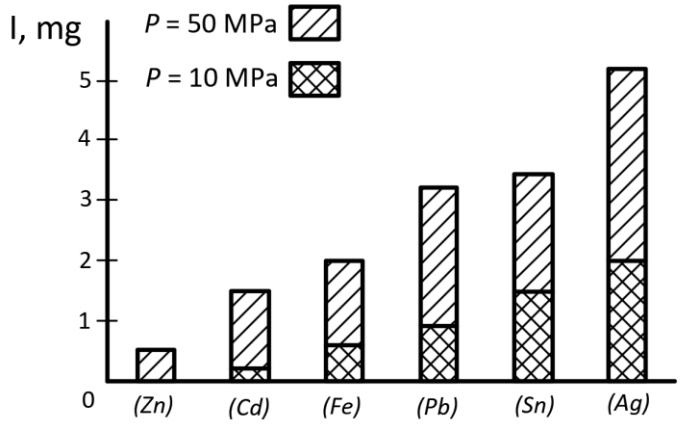

Fig. 6. Dependence of fretting wear of steel 45 on the nature of metals in contact with it, arranged in an electrochemical series: $N = 5 \cdot 10^5$ cycle; $A = 0{,}05$ mm; $f = 30$ Hz

Considering that under normal test conditions (air), intermetallic contact in fretting corrosion is quickly disrupted due to the formation of an oxide layer, and also taking into account the observed strong dependence of the intensity of destruction on the composition of the external environment (oxygen concentration, humidity), preference should be given not to a series of contact potential differences, but to a series of normal electrode potentials. In the second stage, the effect on fretting wear of 45 series steels with different mechanical and physicochemical properties acquired as a result of hardening heat treatment using the technology commonly accepted for each material and having a similar electrode potential (Table 1) was researched. For each of these materials, the tangent of the slope of the anodic polarization curve (Tafel constant - *b*), which characterizes the activation overpotential of electrochemical dissolution, was additionally determined using a potentiostat [18]. It turned out that the higher the Tafel constant of the material in contact with steel 45, the more the steel wears out, and vice versa (Fig. 7).

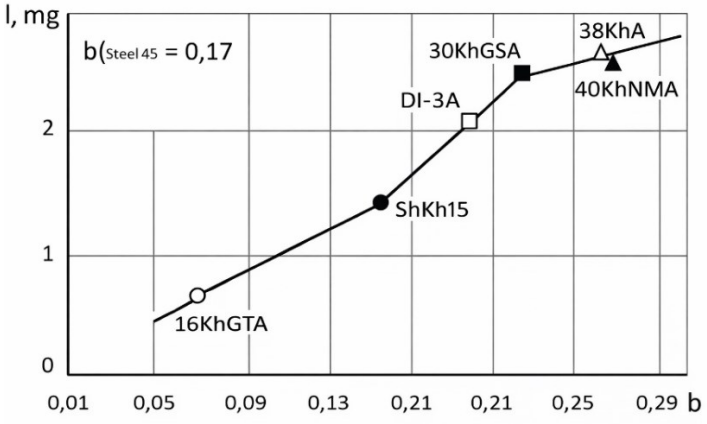

Fig. 7. Fretting wear of steel 45 depending on the value of the Tafel constant (*b*) of the counterbody: $N = 5 \cdot 10^5$ cycles; $P = 10$ MPa; $A = 0{,}05$ mm; $f = 30$ Hz

The patterns observed indicate that electrochemical factors play a significant (and sometimes leading) role in low-amplitude fretting [22]. The peculiarity of the conditions of interaction between contacting surfaces during fretting corrosion (vibration, low sliding amplitude, preservation of wear products—oxides—in the friction zone) contributes to the occurrence of specific topochemical reactions, which, in turn, change the nature of contact. The transition of the surface layers of metal in the initial stage of fretting corrosion to an amorphous or near-amorphous (ultradisperse) state accelerates surface oxidation reactions [2]. The resulting degradation products in the form of oxides, which are usually semiconductors, can give the process an autocatalytic character (wear products accelerate oxidation and corrosion) [24]. Moreover, the fine grinding of oxides increases the free surface area and the number of active centers, which contributes to the activation of adsorption and catalysis processes. The catalytic effect of oxides manifests itself in the acceleration of oxygen and moisture adsorption, with the adsorbed molecules transforming into a more easily activated form under the influence of surface forces or available free valences. Indeed, the nature of molecules in the gas phase and in the chemisorbed state is different. According to the electronic theory of adsorption and catalysis on semiconductors, adsorbed molecules undergo significant deformation and weakening of intramolecular bonds, as well as involve free carriers (electrons and holes) in the

chemisorption bond. The localization of free carriers on the adsorbed particle converts it into a radical or ion-radical form, which has high reactivity due to the acquisition of a charge state (O_2^-, O^-, H_2O^+, etc.). Moreover, the adsorption of a molecule may be accompanied by its dissociation with the formation of new valence-saturated and unsaturated compounds. Thus, in chemisorbed water molecules in a state of coordination bond with the oxide surface, deformation results in the weakening of O-H bonds [24]. In this case, the water molecule is protonated, and at elevated temperatures it can even lose a proton and turn into an OH group. Protonated water molecules adsorbed by the coordination mechanism are new centers for subsequent water adsorption by the mechanism of hydrogen bond formation. During the adsorption of an oxygen molecule as a result of the transfer of two electrons from two negative ions of the oxide crystal lattice, the double bond of the molecule may break. Subsequently, the localization of the hole or the recombination of the hole and the free electron of the oxide may convert the oxygen atom into a reactive radical form. In addition to acquiring anomalous properties, adsorbed water and oxygen molecules change the electrophysical properties of the oxide and, in particular, charge its surface. Chemosorbed oxygen molecules, being acceptors, localize free electrons, charging the semiconductor surface negatively. The adsorption of H_2O molecules (donor particles) charges the surface positively and increases the electrical conductivity of the oxide. The opposite nature (donor-acceptor) of the adsorbed water and oxygen molecules increases the adsorption activity of the oxide surface.

The processes of chemisorption of water and oxygen on oxides create conditions for the emergence of an electrochemical environment between contacting surfaces, capable of giving the fretting process the character of catalytic corrosion, when the mobility of surface metal atoms increases, resulting in the rapid redistribution of the substance between different areas of the surface. In particular, the activation polarization of the metal should decrease (the ionization overvoltage will decrease). The catalytic action of oxides manifests itself in the emergence of reactive radical and ion-radical forms of chemisorption on them. Indeed, our qualitative reaction to peroxide compounds in the products of fretting corrosion of steel, bronze, etc. (based on the reaction with solutions of starch in water and potassium iodide in acetic acid) showed the presence of peroxide forms, probably in the form of the ion radical O_2^-. Charged forms of chemisorption and induced reaction flows should activate electrochemical processes during fretting corrosion. Thus, the emergence of an accelerating field during oxygen adsorption (O_2^-, O^-) reduces the ionization overvoltage of the metal (facilitating the anodic process). The presence of radical forms of adsorbed moisture H_2O^+ and the course of topochemical reactions via the self-oxidation mechanism should accelerate the cathodic process. The oxides formed are capable of acting as a cathode, which, together with the emergence of elements of differential aeration (which is particularly favored by the conditions of the contact under study), creates additional prerequisites for the development of electrochemical corrosion.

Thus, it has been experimentally shown that under conditions of fretting corrosion, the intensity of destruction of contacting metals depends on their electrochemical properties, as well as on the presence of components in the external gas environment that affect the kinetics of electrochemical processes (oxygen, moisture). It has been established that fretting corrosion of metal surfaces creates conditions conducive to electrochemical processes, which, along with other factors (e.g., fatigue phenomena), determine the mechanism and selectivity of the destruction of contacting metals. Electrochemical corrosion develops due to the accumulation in the contact zone of a highly dispersed layer of oxides saturated with adsorbed oxygen and moisture in charged forms. From the point of view of the adsorption-electrochemical mechanism of fretting corrosion, a number of known experimental facts can be explained. Thus, in some experiments [2], when the relative humidity of the environment was increased to 30-40%, an increase in the intensity of fretting corrosion of steel was initially observed, and with a further increase in humidity, the damageability of the contacting surfaces decreased. Since the adsorption activity of oxides increases with the degree of surface hydration, an increase in the concentration of adsorbed oxygen and moisture molecules in the friction zone within certain limits should be accompanied by an increase in fretting corrosion from the point of view of the adsorption-electrochemical mechanism. However, with a further increase in the concentration of adsorbed oxygen, the corrosion rate should decrease due to the passivation of steel [18]. The growth in the intensity of fretting corrosion at low temperatures is obviously associated with an increase in the adsorption activity of oxides, and the usually observed high susceptibility to fretting corrosion of surfaces with an increased purity class [1,2] is probably explained by the fact that polished surfaces are more susceptible to electrochemical corrosion. Taking into account the possible development of contact fatigue and corrosion fatigue processes under fretting conditions, the protective effect of diffusion chemical-thermal coatings was researched, which are known to contribute to an effective increase in the corrosion fatigue strength of steel. In many cases, parts subjected to chemical-thermal treatment (CTT) do not require anti-corrosion protection. The interaction of compressive stresses created by diffusion coatings with stresses from external loads leads to a significant increase in resistance to cyclic loads. The creation of a surface diffusion layer during CTT increases the critical stress of dislocation sources and inhibits the processes of shear formation and plastic flow transfer from grain to grain. When two- or multi-phase structures with sharply different plasticity are formed, materials acquire high relaxation capacity under cyclic loads [12]. We studied the fretting resistance of normalized 45 steel treated with several types of diffusion saturation during CTT, as well as, for comparison, steel in a hardened state (Table 2). Chemical-thermal treatment was carried out in appropriate reaction mixtures using standard methods. A cylindrical (fixed) sample was treated (see Fig. 1 *b*), and the indenter was a movable sample made of 45 steel, hardened and tempered.

Table 2

Effect of chemical-thermal treatment of 45 steel on fretting resistance (P = 30 MPa; A = 0,05 mm; f = 30 Hz)

No.	Type of processing	Fretting resistance, $Q \cdot 10^{-3}$ cycle/μm
1	Steel 45 (normalization)	40
2	Steel 45 hardened	65
3	Vanadium coating	70
4	Siliconization	114
5	Boronization	120
6	Chromium plating	160
7	Alitization	175
8	Boronization	185
9	Borosilication	450

The criterion for fretting resistance Q was taken to be the ratio of the number of fretting cycles to the linear wear of the friction zone at a given specific load, slip amplitude, and vibration frequency (based on $N_f = 5 \cdot 10^5$ cycles). This value shows the number of load cycles required to destroy a surface layer of a unit depth. Of the types of CTT studied, chromium plating, alitization, boronization, and borosilication showed the most significant increase in fretting resistance. The positive effect of chromium plating is due to the fact that chromium is an easily passivated element, so that such alloying of the surface layer, along with substructural hardening and the creation of residual compressive stresses, leads to the inhibition of anodic processes, increasing the corrosion resistance of steel. The high fretting resistance of the aluminized layer is due to the ability of aluminum to form a stable Al_2O_3 oxide film during oxidation, which has high protective properties and protects the metal from corrosion. However, it is necessary to saturate to a depth of no more than 0.05 mm, since a greater saturation depth (0.1-0.2 mm) leads to a decrease in the fatigue strength of steel. It is important to note the high effectiveness of boron-containing coatings in resisting fretting corrosion. Indeed, conventional boronizing increases the fretting resistance of steel more than fourfold, while borosilicating increases it tenfold. After boronizing, the modified layer consisted mainly of two types of solid borides—FeB and Fe_2B—in the form of needles directed perpendicular to the saturated surface (Fig. 8*a*).

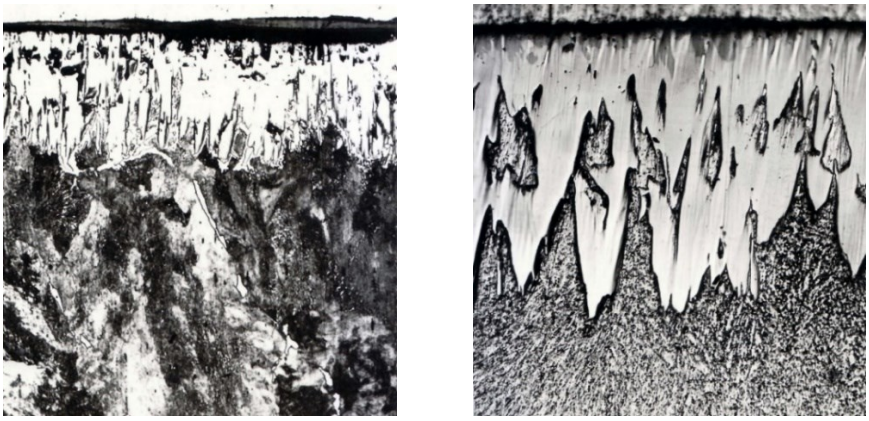

a) ***b***)

Fig. 8. Microstructure of diffusion coatings on 45 steel (×450): *a* – boronization; *b* - borosilication

To increase the load-bearing capacity of the transition zone, the boronized samples were subjected to hardening (from 840°C) and low-temperature tempering (200°C), which formed a tempered martensite structure in the boride substrate. Borosilication forms needles of iron borides (mainly Fe_2B) elongated in the direction of diffusion of the saturating elements, and in the space between them, a phase representing a solid solution of silicon and boron in iron (Fig. 8*b*). Such a compositionally heterogeneous structure with high hardness is characterized by high damping capacity (internal friction), which, in addition to corrosion protection, provides an increase in contact fatigue strength [12].

Conclusions

Data has been obtained that expands theoretical understanding in the field of physicochemical mechanics of contact interaction during low-amplitude fretting.

The susceptibility of metals to fretting corrosion develops in accordance with the following three stages:

1. Period of adhesion-deformation strengthening of contact surfaces and cyclic flow of subsurface layers with their transition to an ultradisperse (nanocrystalline) state with high reactivity (chemical corrosion).

2. Incubation period, which is accompanied by the accumulation of fatigue damage in the subsurface layer and the formation of a reaction-active interlayer of oxides in a highly dispersed state.

3. The period of corrosion-fatigue failure of mating surfaces, when conditions favorable for the development of electrochemical corrosion are created, which, along with fatigue phenomena, determines the mechanism and selectivity of fretting wear at this stage.

Electrochemical corrosion becomes the leading process after the formation of a highly dispersed oxide layer saturated with oxygen and moisture adsorbed in reactive radical forms in the contact zone. Metal oxides, as semiconductors, have specific properties that influence the processes of adsorption and catalysis in tribochemical reactions. These data expand the scope of application of traditional methods of electrochemical protection capable of changing the nature and kinetics of tribochemical reactions under fretting conditions.

References

1. Waterhouse R.B. Fretting Corrosion: Pergamon Press. 1972.

2. Golego N.L., Alab'ev A.Ya., Shevelya V.V. Fretting Korroziya Metallov (Fretting Corrosion of Metals). Kiev: Technika. 1974.

3. Shevelya V.V., Kalda G.S. Fretting Ustalost Metallov (Fretting Fatigue of Metals). Chmelnytskyi: Podillya. 1998.

4. Liskievicz T., Dini D. Fretting Wear and Fretting Fatigue. Fundamental Principles and Applications. Elsevier. 2023. DOI: 10.1016/C2020-0-00006-X

5. Sunde S.L., Berto F., Hacgen B. Predicting Fretting Fatigue in Engineering Design . Int. J. of Fatigue. 2018. v. 117: 314-326. https:.doi.org/10.1016/j.ijfatigue.2018.08.028

6. Croccolo, D., De Agostinis, M., Fini, S., Olmi, G., Robusto, F., & Scapecchi, C. (2022). Fretting Fatigue in Mechanical Joints: A Literature Review. *Lubricants*, *10*(4), 53. https:.doi.org/10.3390/lubricants10040053

7. Yan Y., Chai M. Sealing Failure and Fretting Fatigue Behaviour of Fittings Induced by Pipeline Vibration . International Journal of Fatigue. 2020. 136: 105602. https:.doi.org/10.1016/j.ijfatigue.2020.105602

8. Li D., Botto D., Xu C., Gola M. Fretting Wear of Bolted Joint Interfaces . Wear. 2020. 458-459. 203411. https:.doi.org/10.1016/j.wear.2020.203411

9. Oku Y., Sugino M., Ando Y., Makino T. Komoda R. Fretting Fatigue on Thread Root of Premium Threaded Connections . Tribology International. 2017. 108: 111-120. https:.doi.org/10.1016/j.triboint.2016.10.021

10. Pettigrew M.J., Taylor C.E. Vibration Analysis of Shell-and-Tube heat Exchangers: An Overview – Part 2: Vibration Response. Fretting-Wear. Guidelines . Journal of Fluids and Structures. 2003. 18(5): 485-500.

11. Waterhouse R.B. Fretting Fatigue . Inter. Mater. Reviews. 1992; 37(1): 77-98. https:.doi.org/10.1016/j.jfluidstructs.2003.08.008

12. Shevelya V.V., Oleksandrenko V.P. Tribochimiya i Reologiya Iznosostoikosti (Tribochemistry and Rheology of Wear Resistance). Chmelnytskyi: Chmelnytskyi National University. 2006.

13. Nowell D., Dini D., Hills D.A. Recent Developments in the Understanding of Fretting Fatigue . Engineering Fracture Mechanics. 2006. v. 73 (2): 2007-2022. https:.doi.org/10.1016/j.engfracmech.2005.01.013

14. Varenberg M., Halperin G., Etsion I. Different Aspects of the Role of Wear Debris in Fretting wear . Wear. 2002; 252: 902-910.

15. Zhu M.H., Zhou Z.R. On the Mechanisms of Various Fretting Wear Modes . Tribology International. 2011 (44). 11: 1378-1388.

16. Maich A.A., Gronsky R., Komvopoulos K. Microstructure Evolution and Fretting Wear Mechanisms of Steels Undergoing Oscillatory Sliding Contact in Dry Atmosphere . Materials. 2024; 17(8): 1737.

17. Zhou Z.R., Nakazawa K., Zhu M., Maruyama N., Kapsa P., Vincent L. Progress in Fretting Maps . Tribol. Int., 2006; 39(10): 1068-1073. https:.doi.org/10.1016/j.triboint.2006.02.001

18. Oh H.K. Yeon K.H., Kim H.Y. The Influence of Atmospheric Humidity on the Friction and Wear of Carbon Steels . J. Mater. Process Technol., 1999; 95: 10-16.

19. Ahmadi A., Sadeghi F., Shaffer S. In-situ Friction and Fretting Wear Measurement of Inconel 617 at Elevated Temperatures . Wear. 2018(410-411): 110-118. https:.doi.org/10.1016/j.wear.2018.06.007

20. Pearson S.R., Shipwaj P.H., Abere J.O. The Effect of Temperature on Wear and Friction of a Highstrength Steel in Fretting . Wear. 2013 (303): 622-631.

21. Shevelya, V.V., Ganzjuk, A.L., Kalda, G.S. *et al.* Contact Corrosion of Metals under Low Amplitude Fretting. *J. Frict. Wear* **42**, 23–29 (2021). https:.doi.org/10.3103/S1068366621010098.

23. GOST 23211-80. Method of Testing Materials for Wear during Fretting and Fretting Corrosion. 1982.

24. Miranda R., Michel E.G. Electronic Structure of Adsorbates on Semiconductors. Handbook of Surface Science. 2000. № 2; 863-897. https:.doi.org/10.1016/S1573-4331(00)80016-5

Шевеля В.В., Олександренко В.П., Диха О.В., Соколан К.С. Трибохімія ушкодження металевих сполучень при фреттинг-корозії

Досліджувались закономірності фреттинг-зносу ряду конструкційних матеріалів та гальванічних покриттів з урахуванням їх механічних та фізико-хімічних властивостей. Проводилась оцінка впливу на інтенсивність фреттинг-зносу складу газового середовища (повітр, кисень), а також контактного навантаження з однойменною реєстрацією температури в зоні тертя. Отримано дані, що свідчать про можливість розвитку при малоамплітудному фреттингу металів у повітряному середовищі поряд з окислювальними процесами електрохімічної корозії. Розглянуто фізико-хімічні передумови ініціювання в зоні вібраційного контакту електрохімічних процесів при формуванні ультрадисперсного прошарку оксидів, які стають каталізатором прискореної хемосорбції кисню і вологи у радикальних та іон-радикальних формах. В результаті, згідно з електронною теорією адсорбції та каталізу на напівпровідниках (окислах), контактні явища починають розвиватися за механізмом автокаталітичної корозії. Після латентного періоду накопичення оксидів створюються умови для електрохімічних процесів, що сприяють корозійно-втомному руйнуванню сполучених поверхонь. Результати дослідження розширюють уявлення про природу корозійних процесів при частковому та змішаному ковзанні, орієнтуючи на можливість застосування традиційних методів електрохімічного захисту для підвищення фреттингостійкості вузлів тертя, що працюють в умовах вібрації.

Ключові слова: фреттинг-знос, коефіцієнт тертя, фреттингостійкість, адсорбція, корозія, електрохімія, хіміко-термічна обробка

ISSN 2079-1372 Problems of Tribology, V. 31, No 1/119-2026, 16-22

Problems of Tribology
Website: http://tribology.khnu.km.ua/index.php/ProbTrib
E-mail: tribosenator@gmail.com

DOI: https://doi.org/10.31891/2079-1372-2026-119-1-16-22

Lifetime Improvement of Contact Brush Units of Automotive Power Machines. Part 2

A.H. Dovhal*[0000-0003-1300-0192], **O.M. Biliakovych**[0000-0003-3887-3715], **L.B. Pryimak**[0000-0003-4024-0941]

Kyiv aviation institute, Ukraine
andrii.dovhal@npp.kai.edu.ua

Received: 05 December 2025: Revised 18 December 2025: Accept: 15 January 2026

Abstract

Lifetime testing of contact brush units of automotive power machines is held. Friction contact of copper and graphite under working voltage and current within ordinary atmosphere environment was simulated on the friction test bench. Wear resistance and friction losses have been detected. Wear mechanisms and friction surfaces were investigated using the scanning electronic microscopy. This study allows recommendation the optimal surface treatment of copper elements of contact brush unit of alternators or commutator unit of power starters.

Keywords: AC power machines, alternator, vehicle starter, contact brush unit, friction in power contact

Introduction and review of publications

Formerly the optimal technological modes of electrospark coating of aluminium on copper substrate were detected. Kinetics of mass transfer and coating thickness were researched. Using the scanning electronic cmicroscopy the structure of acquired coating was thoroughly investigated. Presumption of good electric conductivity together with good adhesion to copper subsrate under moderate heating was made and as well. The last issue can be checked only during the benchmark friction testing with research of friction surfaces. Considerations of the latest investigations in this area are the following.

So in the research [1] sliding wear behavior of copper-graphite composite for maglev vehicles and high-speed railway train was investigated. The samples were formed by cold pressing at 300 MPa and by hot sintering (950°C × 3 h) in a hydrogen atmosphere. After specimens were cooled to room temperature with the furnace, further pressing at 300 MPa was performed. Wear tests were conducted with a specially designed sliding apparatus to simulate the tribological condition of sliding current collectors in a maglev system. The material was slid against a stainless steel band under unlubricated condition. Worn surfaces of the material were analyzed by SEM and field-emission-gun environment SEM equipped with an energy dispersive X-ray spectroscopy. Within the studied range of normal pressure and electrical current, wear loss increased with increasing normal pressure and electrical current. Adhesive wear, abrasive wear and arc erosion were the dominant mechanisms during electrical sliding. It provides principle for designing suitable sliding counter parts for the current collection device in maglev system.

The publicaion [2] is about that copper-graphite is an important tribological material used in the applications of electrical sliding contact like generators and electrical brushes. A series of experimental tests were conducted on a pin-disc tribometer in air and dry sliding condition. The pair of material was subjected to electric current ranging from 0 to 10A, normal loads of 5 to 30N and sliding speed of 0.5 m/s. The duration of each test was 30 minutes. Experimental results indicated that the friction coefficient decreases and wear rate increases with increasing load with and without applied electric current. The changes in surface chemistry and topography of the tribo-surfaces were characterized using Raman spectroscopy, scanning electron microscopy (SEM) and energy dispersive spectrometer (EDS). This later technique was used to analyze the transfer of pin materials to the counterface, and also to understand how copper and graphite influence the tribological properties. Results indicated that, electric current and normal load have more or less significant influence on the tribological behavior of the pair of materials and the effect of oxide layer created at interface of the pairs in contact.

As stated in article [3] the copper matrix composites were prepared by spark plasma sintering (SPS). The current-carrying friction and wear tests were carried out on a self-made HST-100 high-speed current-carrying

friction and wear tester, and the effect of the graphite content on the current-carrying friction and wear properties of the composite material was studied. The results show that with an increase in graphite content, the average friction coefficient and wear rate of the two materials decreased significantly, the fluctuation amplitude of the friction coefficient was also significantly reduced, and the average friction coefficient of copper-coated graphite composite with graphite content of 10 wt.% was 0.100; when the graphite content was the same and more than 5.0 wt.%, the average friction coefficient and wear rate of copper–graphite composites were slightly higher than copper–copper-coated graphite composites; the current-carrying efficiency and current-carrying stability of the copper matrix composite were obviously higher than that of copper material; there was a mechanical wear area and arc erosion area on the wear surface of the composites, with the increase in graphite content, the adherence and the tear of the mechanical wear area weakened, the rolling, plastic deformation increased, and the surface roughness decreased obviously. The surface roughness of the wear surface of copper–copper-coated graphite composites with graphite content of 10 wt.% was 3.17 μm. The forms of arc erosion included melting and splashing, and were mainly distributed in the friction exit area.

Good influence of organosilicon dopant to the brush materials is stated in work [4]. The brush materials modified with organosilicon were prepared by the powder metallurgy method, and their current-carrying friction and wear properties were compared with those of brush materials modified with SiO_2. The materials were characterized by SEM, XRD, XPS, deep etching, and roughness. The results showed that, compared with the SiO_2, organosilicon can significantly reduce the wear rate of brush materials by 67–88%, because the SiOC fiber produced by pyrolysis of organosilicon could control the graphite content on the friction surface by reducing abrasive wear. In the aspect of wear mechanism, organosilicon could greatly reduce the abrasive wear of the materials and the mated materials, but aggravated the adhesive wear of the materials.

In research [5] copper-graphite sintered materials were prepared by powder metallurgy technology. The relationship of the graphite content to the third body topography and the impact of the graphite content on frictional properties of the materials were investigated on a constant speed friction test machine. The results showed that, when less than 15%, the graphite had a significant influence to the material porosity and the friction temperature. The results demonstrated clearly the friction and wear property of the material was closely related to the graphite content and this was due to the effect of the third body containing graphite particles formed on the frictional surface under dry friction condition. The third body derived from low graphite content sintered materials had a high level of metal composition. Plowing effect of the hard metal led to higher friction coefficient and wear rate. With the increase of graphite content, the density and adhesion of the third body reduced because of the increase level of graphite in the third body. The low compactness and easy flow of the third body alleviated the surface plowing, lowered and stabilized the friction coefficient and, therefore, reduced wear rate.

The following was comprehensively studied in paper [6]. Resin-coated graphite/copper composites and copper-plated graphite/copper composites were prepared by cold pressing-pressure sintering process using phenolic resin powder, graphite powder, copper-plated graphite powder and electrolytic copper powder as raw materials, respectively, the friction and wear properties of two kinds of graphite/copper composites at room temperature, high temperature and current-carrying were studied, and compared with overseas Roland grounding brush; the effects of resin decomposition on the conductivity, mechanical and friction and wear properties of the composites were analyzed based on the crystal structure of copper matrix and the variation of composite conductivity and mechanical properties at high temperature (200-600 °C). The results show that the mechanical properties of resin-coated graphite/copper composites at high temperature are better than that of copper-plated graphite/copper composites. When the ambient temperature reaches 600 °C, the shear strength of resin-coated graphite/copper composites decreases by only 6%, while that of copper-plated graphite/copper composites decreases by 24%. The high temperature (250 °C) wear resistance and friction stability of resin-coated graphite/copper composites are much better than those of copper-plated graphite/copper composites and Roland brush, the current-carrying friction factor of the resin-coated graphite/copper composites is lower than that of Roland brush. The resin coating of graphite can improve the friction and wear properties of copper matrix composites at high temperature and current-carrying, due to the protection of the resin layer, a continuous and stable graphite lubricating film can be formed even under the conditions of high temperature oxygen and current-carrying, thus reducing the friction contact micro-gap; the carbonized resin breaks into fine hard particles during the friction, which hinder the adhesion and wear between composite and disc; the Cu matrix softening at high temperature is not obvious, so the occurrence of arc decreases.

Copper-graphite composites were investigated in research [7]. Copper-graphite composites were prepared by spark plasma sintering (SPS) with copper powder and copper-coated graphite powder. The effect of particle size of raw material powder on the current-carrying friction properties of copper-graphite composites was studied. The results show that the friction coefficient of the composites decreased with the decrease of the particle size of copper-coated graphite powder, the friction coefficient of the composites increased with the decrease of the particle size of the copper powder, the wear rate of the composites increased with the decrease of the particle size of the copper-coated graphite powder, and the wear rate of the composites increased significantly with the decrease of the particle size of the copper-coated graphite powder. The current carrying properties of composites with different particle size ratios and QCr0.5 pairs are good and fluctuate little. The current-carrying friction properties of 150 μm copper powder and 75 μm copper-coated graphite powder were found to be the best. The wear surface could be divided into mechanical wear area and arc erosion area. The main area of arc erosion was less than 15% of the

total area, and it was mainly distributed in the friction outlet area. The main forms of mechanical wear included furrow, rolling deformation, cold welding, and tearing, among other forms. Graphite film was formed on the surface. The surface quality of the composite prepared by 150 μm copper powder and 75 μm copper-coated graphite powder was the best, the Sa was 3.22 μm, rolling deformation was the most adequate, no large tear pit and furrow appeared, and the carbon content on the worn surface was much higher than that in the composite. The behavior of arc erosion was mainly melting and splashing, and the particle size of the original powder had little effect on it.

As stated in scientific work [8], during the train operation, the pantograph/catenary system is subjected to an extremely harsh service environment. Relative humidity has a great influence on the current-carrying tribological behaviors of carbon strips. The identification and understanding of the wear mechanism are extremely important in wet and dry conditions. This study was carried out to investigate the humidity effect on the service properties of carbon sample rubbing against copper (Cu) with and without electric current using a home-made wear tester, and the humidity ranging from 10% RH to 80% RH. The results indicate that the sliding wear behavior of the friction interface is drastically affected by the intervention of water vapor and electric current. The coefficient of friction (COF) without current is obviously lower than current-carrying sliding when the humidity is constant. However, the increased humidity led to a decreasing trend. After the current increases to 10 A, all the COF values are closed to each other ultimately. These phenomena mainly result from the formation and destruction of water lubrication film. Furthermore, the tribo-pairs worn surface appears the most sensitive to the current effect under dry conditions. The reverse transfer of Cu and carbon is greater on account of the current agglomeration effect, and the oxidation degree is more severe. The wear mechanisms of carbon are mainly material transfer accompanying with oxidation erosion. However, the wear degradation is weakened under water lubrication and uniform current distribution which improves the conductive quality. This is the coupling effect of humidity environment, current and heat concentration. This experiment provides technical support for the operation of an electric locomotive under an extremely harsh service environment.

The purpose of thesis [9] is to propose a technique to improve electric brush properties in an effort to produce a more proficient electric motor by creating a new brush material with improved properties and performance. There are many applications for electric motors and each application would benefit from overall, increased proficiency. Understanding the role an electric brush plays within an electric motor is crucial to improving functionality. The proposed technique to create a novel graphite-copper material involves a two-step procedure that will intercalate $CuCl_2$ into the graphite structure, and then by chemical reduction, will reduce the $CuCl_2$ and result in the final products of copper and graphite. The proposed technique seeks to successfully increase the conductivity and wear properties of an electric brush by incorporating copper into graphite which will also enhance the properties of an electric motor. This thesis will detail the procedures of data collection and how to analyze results of the proposed technique. Expected results will also be discussed utilizing preliminary data collected utilizing XRD, SEM, TGA, and BET equipment. Finally, struggles and challenges of such a technique will also be discussed as well as plans for future work on the proposed technique.

Formerly some properties of aluminium electrospark coatings on copper substrate were researched is work [10]. The automotive electric equipment involves the electric machines (starter, alternator) incorporating the brush unit and hybrid drive vehicles as well. It is the friction joint of conducting copper and graphite brush. Work efficiency and lifetime of these machines strongly depend on the contact quality and general state of this friction joint. Thus preset objective of this study is research of friction joint of brush unit “copper-graphite” under working current flow and technique of its superficial improvement. For experimental purposes the samples of M1E electric conductive copper ГОСТ 859-2001 complying with ТУ 1276-003-38279335-2013 were fabricated in dimensions of hole disks 16×6×2,5 mm in order to provide the least friction contact area for experiment acceleration. As the friction couterbody the conventional alternator brush made of graphite ГЭ-1, ГОСТ 7478-75 was used. Copper samples were strengthened by electro-spark alloying on unit ALIER-52 on 6-7 modes by aluminum electrode made of rod aluminum ГОСТ 15176-89. The coated and uncoated samples were tested on the friction test bench M-22ПВ under “pin-on-shaft” layout. Friction speed was about 1,5-2 m/s that complies the test bench shaft rotation speed about 2000-2400 rpm. In order to simulate the brush unit work the 24 V DC voltage was applied to friction contact and linear wear rate was detected. So uncoated samples have demonstrated the wear rate of 345,5 micrometers per kilometer, unlike coated samples that have the wear rate 81,8 micrometers per kilometer what is about 4,26 times improvement of electro erosive wear resistance. Thus the technique researched is suitable and can be recommended for improvement of brush units of vehicle alternators and starters, DC engines collectors for electric power vehicles, hybrid vehicles and quadracopters as well.

This paper is devoted to investigation of wear results and friction surfaces of copper samples in ordinary atmisphere environment and in low vacuum condition modelling the the friction of contact unit of alternators and vehicle power starters.

Problem statement and objective

The objective of this study is friction testing of “ESA coated copper-graphite” under working current flow in amosphere pressure. Namely this paper is dedicated to research of coating wear resistance and wear mechanisms.

Methods

For experimental purposes the samples of M1E electric conductive copper (content: 99,96% Cu, 0,002 Ni, 0,005 Fe, 0,004 S, 0,002 Sn, 0,005 Pb, 0,004 Zn, 0,002 Sb) were fabricated in dimensions of hole disks 16×6×2,5 mm in order to provide the least friction contact area for experiment acceleration.

As the friction counterbody the conventional alternator brush made of graphite ГЭ-1, (contains 0.05% Cu, ash content 10-14 %) was used. Copper samples were strengthened by electro-spark alloying on unit ALIER-52 on 6-7 modes by aluminum electrode made of rod aluminum (АД31Е (1310Е, 6101) containing 97.68% Al, 0,5 % Fe, 0,7% Si, 0,03% Mn, 0,03% Cr, 0,1% Cu, 0,06% B, 0,8% Mg, 0,1% Zn. The 6 mode of ALIER-52 installation provides the following electrospark alloying descriptions: impulse duration was 700 microseconds, amplitude value of current impulse was 200 A; the impulse energy was 2,52 Joiles; coating thickness was 0,3 mm.

The coated and uncoated samples were tested on the friction test bench М-22ПВ under “pin-on-shaft” layout. Friction speed was about 1,5-2 m/s that complies the test bench shaft rotation speed about 2000-2400 rpm. In order to simulate the brush unit work the 24 V DC voltage was applied to friction contact and linear wear rate was detected. Using the rheostat the current strength has been changed from 1 to 5 A (fig. 1.).

a) b) c)

Fig. 1. Samples for wear testing: a) uncoated (deeply worn) copper samples; b) coated copper samples; c) real alternator graphite brush (couterbody) with the worn place shown.

So uncoated samples have demonstrated the wear rate of 345,5 micrometers per kilometer, unlike coated samples that have the wear rate 81,8 micrometers per kilometer what is about 4,26 times improvement of electro erosive wear resistance.

In order to detect the wear mechanisms for improvement the strengthening technique the wear surfaces were investigated instantly after testing on the electronic microscope РЭМ-106И and specific areas were additionally analyzed by X-ray element analyzer. SEM images and analysis results are on fig. 3.

Main research results

The wear testing results are represented on fig. 2.

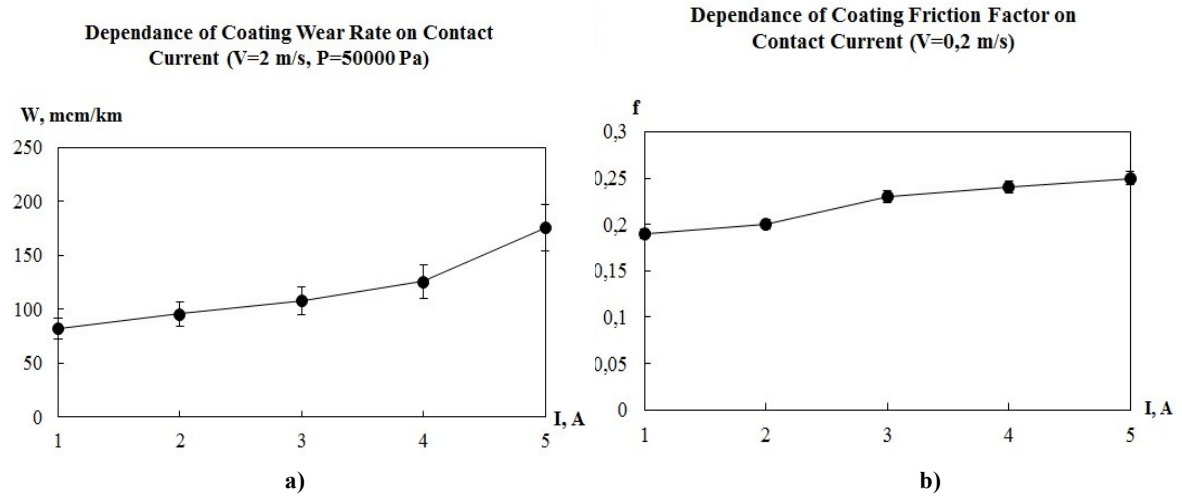

a) b)

Fig. 2. Dependance of wear rate and friction factor of aluminium electrospark coating on (a,b) current strength

The coating friction properties depending on current strength and atmospheric pressure are on fig. 3. So, the coating wear rate depending on the current strength increase (from 1 to 5 A) allowing prediction the brush unit lifetime on boosted modes is about increasing from 81,8 to 175,6 μm per km (fig. 2., a) and friction factor was kept in the antifriction limits 0,19-0,25 (fig. 2., b) that means it will not create the big resistanse to alternator rotor rotation.

In order to explain the acqured results the friction surfaces (right after experiment for better elements storage coverred by clean vacuum film while delivering to microscope) were invetigated on scanning electronic microscope REM-106I. Acquired results are on fig. 3.

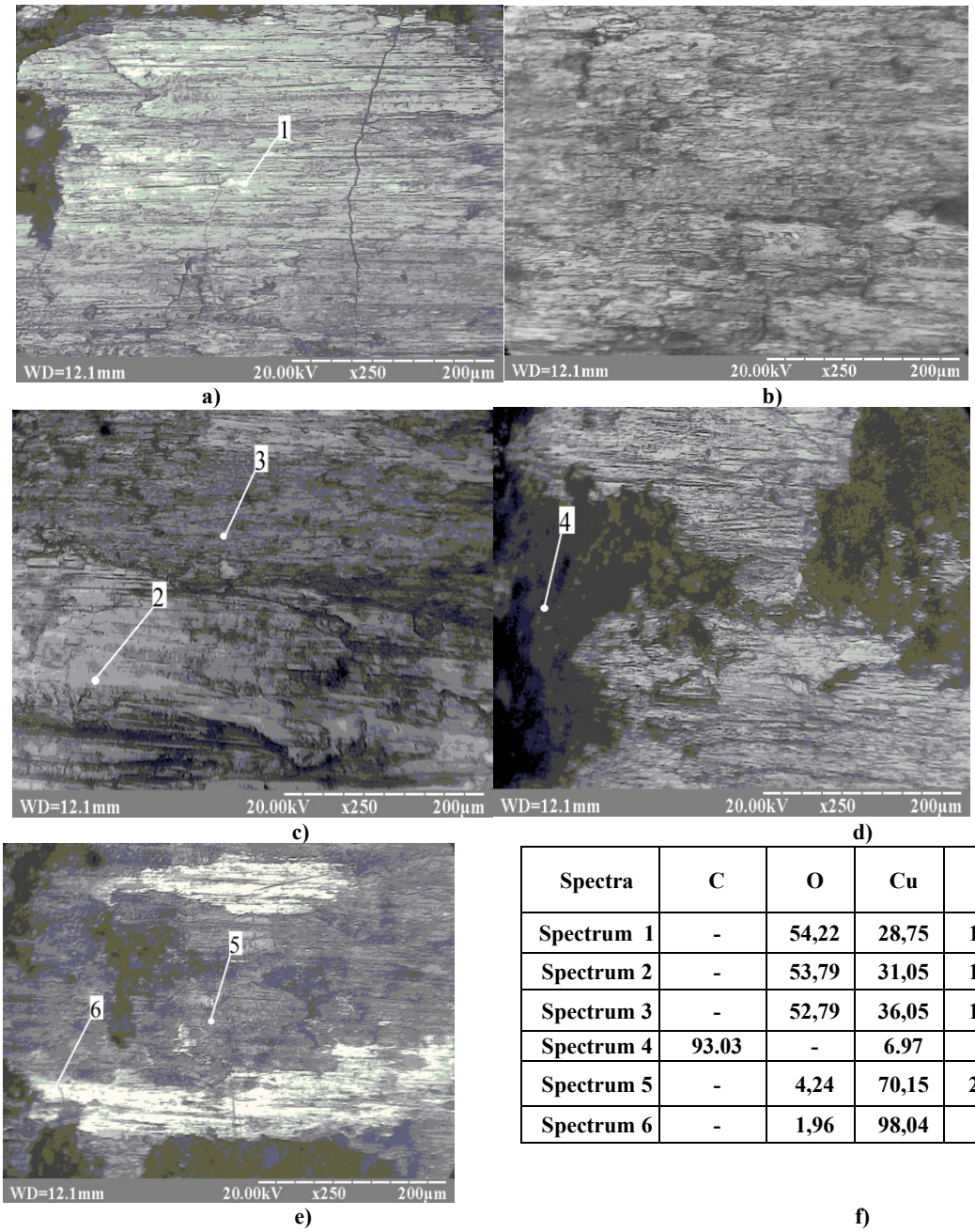

Spectra	C	O	Cu	Al
Spectrum 1	-	54,22	28,75	16,99
Spectrum 2	-	53,79	31,05	15,16
Spectrum 3	-	52,79	36,05	11,15
Spectrum 4	93.03	-	6.97	-
Spectrum 5	-	4,24	70,15	25,61
Spectrum 6	-	1,96	98,04	-

f)

Fig. 3. SEM images of friction surfaces of ESA coating of aluminium on copper M1E in 250 electronic zoom under 12 V conducting different DC in coated copper-grphite contact under atmospheric pressure (101 325 Pa): a) 1 A; b) 2 A; c) 3 A;d) 4 A; e) 5 A; f) elements content in specified areas

As it can be seen from fig. 3. a, under low current strength surface is covered by oxides of copper and aluminium and pure areas of hard solution of aluminium in copper. It can be stated according to spectra 1, 2, 3 and 5 elements content. Thin films of oxides and pure hard solution have good conductivity for power transfer purposes. Overheating of surfaces causes the superficial coating cracks. However increasing the current strength burns through spots appear in coatin surfaces and they are immediately covered by graphite particles spectrum 4 fig. 3. d. Overloading the coating by big current strength leads to coating destruction by burn out and naked substrate of pure copper comes to friction surface (see spectrum 6 fig. 3. e).

Natural testing of simple copper-graphite contact brush unit of vehicle alternator (under 14,5 V DC voltage amd no more than 5 A load current) has demonstrated the two and half longer unit lifetime comparing with uncoated copper rings of this unit. But more intensive wear rate of graphite brushes (double times bigger) was detected. But, it is obviously, replacement of graphite brushes (with new better voltage regulator built in) is much easier in operational conditions of vehicles duirng the next maintenance check procedure, than replacement of

copper rings of alternator (or starter commutator). That's why the findings of this paper can be considered as satisfactory and feasible in vehicles operation and maintenance process.

Conclusions

So the electrospark alloying coating of aluminium on copper has demonstrated satifactory wear resistance in power transferring contact under 24 V and current strength from 1 to 5 A. Wear mechanism with in atmospheric pressure is oxidative with sparking burn out. It is the area for future research. Thus alluminium electrospark coating can be applied for superficial strenthening of copper element of copper-graphite contact brush unit, which works under voltage up to 24 V and current load up to 5 A with satisfactory wear rate and friction factor.

Thus the ESA coating researched is suitable and can be recommended for improvement of brush units of vehicle alternators and starters, DC engines collectors for electric power vehicles, hybrid vehicles.

References

1. X.-C. Ma, G.-Q. He, Dahai He, C.-S. Chen, Zhengfei Hu, W.-H. Zhang Friction and wear behavior of copper-graphite material under electrical current, Mocaxue Xuebao. Tribology, 40 (March 2008) 167-172. https://www.researchgate.net/publication/288808411_Friction_and_wear_behavior_of_copper-graphite_material_under_electrical_current

2. Benfoughal Abdeldjalil, Ali Bouchoucha, Youcef Mouadji Effect of electrical current on friction and wear behavior of copper against graphite for low sliding speeds. UPB Scientific Bulletin, Series D: Mechanical Engineering No. 80(3) (January 2018) 117-130. https://www.researchgate.net/publication/327047120_Effect_of_electrical_current_on_friction_and_wear_behavior_of_copper_against_graphite_for_low_sliding_speeds

3. Zhenghai Yang,Yuexin Ge, Xu Zhang, Bao Shangguan,Yongzhen Zhang, Junwei Zhang Effect of Carbon Content on Friction and Wear Properties of Copper Matrix Composites at High Speed Current-Carrying, Materials, No. 12(18) (2019) 2881; https://doi.org/10.3390/ma12182881

4. Xueyang Lin, Rutie Liu, Jie Chen, Xiang Xiong, Ning Liao Study on current-carrying friction and wear properties of copper-graphite brush material reinforced by organosilicon, Journal of Materials Research and Technology, Volume 12, (May–June 2021) 365-375. https://www.sciencedirect.com/science/article/pii/S2238785421002209

5. Fu Rong, Gao Fei, Song Bao-yun, Wang Yan-hui Tribological Behavior of Copper-Graphite Friction Materials, Tribology, 30(5), (2010) 479-484. https://www.researchgate.net/publication/283581159_Tribological_Behavior_of_Copper-Graphite_Powder_Third_Body_on_Copper-Based_Friction_Materials

6. Fang Huachan, Sun Zhen, Xu Yongxiang, Zhang Zhuo, Wang Jiayu, Zhu Jiamin, Chen Zhuo High temperature and current-carrying friction and wear properties of resin-coated graphite/copper composites. Materials Science and Engineering of Powder Metallurgy, Vol. 28, Issue (4), (2023) 315-328 https://doi.org/10.19976/j.cnki.43-1448/TF.2023025

7. Zhenghai Yang, Yuexin Ge, Xu Zhang, Bao Shangguan,Yongzhen Zhang, Yao Wang Effect of Particle Size on Current-Carrying Friction and Wear Properties of Copper-Graphite Composites by Spark Plasma Sintering, Materials 2019, 12(17), 2825; https://doi.org/10.3390/ma12172825

8. Ming-jie Hu, Xin-long Liu, Chao-wei Zhou, Dong-yun Wang, Qian Xiao, Xin Guan, Song Zhang, Zhi-biao Xu Comparative study of the current-carrying tribological properties of carbon graphite composites with different hardnesses. International Journal of Mechanical Sciences, Volume 245, 1 May 2023, 108133 https://doi.org/10.1016/j.ijmecsci.2023.108133x

9. Kalbus, Kyle, "Copper Intercalation into Graphite" (2012). University of Wisconsin-Milwaukee. Theses and Dissertations. 34 p. https://minds.wisconsin.edu/handle/1793/93446

10. Andrii Dovhal Lifetime Improvement of Contact Brush Units of Automotive Power Machines. Book of Abstracts of 8th International Materials Science Conference HighMatTech-2023, October 2-6, 2023 Kyiv, Ukraine. p. 83. https://umrs.org.ua/activities/conferences/highmattech-2023/boa/

Довгаль А.Г., Білякович О.М., Приймак Л.Б. Поліпшення ресурсу контактно-щіткових вузлів автомобільних електромашин. Ч. 2.

Проведено випробування довговічності контактно-щіткового вузла автомобільних електромашин. Було модельовано фрикційний контакт міді та графіту на машині тертя за робочої напруги та струму у звичайному середовищі атмосфери. Було визначеного зносостійкість та фрикційні втрати такого вузла. Було досліджено поверхні тертя та механізми зношування за допомогою скануючого електронного мікроскопу. Це дослідження дозволяє рекомендувати оптимальну поверхневу обробку мідних деталей контактно-щіткового вузла генераторів та колекторних вузлів електричних стратерів.

Ключові слова: електрмашини змінного струму, автомобільний генератор, автостартер, контактно-щітковий вузол.

ISSN 2079-1372 Problems of Tribology, V. 31, No 1/119-2026, 23-32

Problems of Tribology
Website: http://tribology.khnu.km.ua/index.php/ProbTrib
E-mail: tribosenator@gmail.com

DOI: https://doi.org/10.31891/2079-1372-2026-119-1-23-32

Lubricating effect of oils by controlling the concentration of chemical components of the additives

O.A. Milanenko* 0000-0002-8197-5277, **A.M. Bobro** 0009-0002-1193-117X

National Transport University, Kyiv, Ukraine
milanmasla@gmail.com

Received: 15 December 2025: Revised 18 December 2025: Accept: 20 January 2026

Abstract

A proposed and substantiated multifactorial approach to assessing the lubricating effect of oils, considering the influence of physicochemical factors and rheological characteristics on the evolution of the creation and adaptation of chemically modified boundary layers (CMBLs) to real operating conditions in conditions of the partial EHD lubrication mode. Comparing the results of the anti-wear and anti-friction properties of the studied oil samples, while complying with the additive manufacturer's conditions for the mass fraction of sulfur, which is 1.488–1.9662%, a necessary condition for the best results in terms of the combined action of the anti-wear and anti-friction properties of the oils is to establish a total additive concentration of 3.9–4.9% with a phosphorus mass fraction of 0.046–0.057%. In the series of samples studied, *sample 4* with a concentration of 4.9% additive shows the best universal properties, especially for the operation of units with combined engine and transmission systems (universal STOU oils for agricultural machinery).

Key words: the lubricating effect of oils, physicochemical factors and rheological characteristics, chemically modified boundary layers (CMBLs), the partial EHD lubrication mode, the anti-wear and anti-friction properties, the concentration of chemical components of the additives, chemically active substances (CAS), manganese-iron-phosphate coating (MIP).

Introduction. Analysis of recent research and publications

Improving the reliability and energy efficiency of machines and vehicles is directly related to the intensity of friction and wear processes in friction units. According to international tribological reviews [1-3], up to 25-30% of energy losses in technical systems are due to friction processes, and more than 40% of equipment failures are tribological in nature. In this context, the improvement of lubricants (oils) as one of the most cost-effective means of reducing energy consumption due to friction and wear in machines is of particular importance.

Modern oils for various technical purposes are produced on the basis of compounding base stocks and multi-component additive packages that provide the main operational properties: anti-friction, anti-wear, anti-seize, antioxidant, anti-corrosion properties, etc. At the same time, research results from leading global additive manufacturers such as Afton Chemical (USA), Lubrizol (USA), BASF (Germany), indicate that the effectiveness of the respective additive packages is determined not only by their qualitative properties, but primarily by the quantitative properties (concentration) of active chemical components or chemically active substances (CAS), which are often in the range of hundredths and thousandths of a percent. The technical regulations of these companies indicate that exceeding or underestimating the concentration of anti-wear and anti-friction CAR at the level of 0.01–0.05% of the mass fraction may lead to a significant reduction in the protective properties of the modified layer, which are formed as a result of chemical modification of contact surfaces during friction, an increase in the intensity of wear up to the rupture of the lubricating layer [1–3].

Recent experimental studies published in renowned international journals included in the Scopus and Web of Science scient metric databases indicate that the concentration of active chemical components in additives plays a critical role in the formation of strong and stable chemically modified boundary layers (CMBLs).

In particular, study [4] found that adding titanium oxide (TiO_2) nanoparticles to motor oil at a concentration of 0.01–0.075% by mass reduces the friction coefficient from 0.112 to 0.05, i.e., by more than 55%, and at the optimal value of 0.075% — to a level of about 0.01, which corresponds to a reduction in friction of almost 90%

relative to the base oil without additives. With a further increase in the concentration of the additive, the reduction in the friction coefficient stabilizes or even increases, indicating the presence of a narrow optimal range. Similar patterns were also obtained for copper and iron oxides.

Studies [5] have shown that the use of copper oxide (CuO) nanoparticles at a concentration of 0.25% by mass reduces the friction coefficient by 11–54% and the wear intensity by 30–45% compared to the base oil without additives. At the same time, at concentrations above 1.0–1.3%, the reduction in the friction coefficient and wear intensity not only does not increase, but in some cases is accompanied by a deterioration in colloidal stability and an increase in contact wear due to particle agglomeration. Similar results were obtained for hybrid nanodispersed systems ($CuO–TiO_2$), where the optimal concentration range was within 0.05–0.15% by mass to ensure a 35–60% reduction in the friction coefficient and a 40–55% reduction in linear wear.

These results are consistent with the technical regulations of Afton Chemical and Lubrizol [1,2], which state that the optimal concentration of phosphorus- and sulfur-containing anti-wear additives within ±0.01–0.02% allows for a simultaneous reduction in wear by 20–35% in internal combustion engines (ICE).

Outline of unresolved issues

From an economic point of view, the problem of optimal additive formulation is no less significant. According to industry reviews, the cost of functional additive packages can be up to 40–60% of the cost of commercial oil, while their mass fraction exceeds 3–7%. At the same time, even a 0.1% reduction in the concentration of active components without loss of performance properties can reduce the cost of lubricant production by 5–8%, which, on a mass production scale, corresponds to a significant economic effect. In addition, a 30–50% reduction in friction wear, as reported in [4, 5], correlates with a 15–25% increase in machine maintenance intervals, thereby significantly improving the technical and economic efficiency of vehicle and industrial system operation.

Thus, an analysis of current scientific publications and technical regulations of leading additive manufacturers convincingly demonstrates that the lubricating effect of oils is determined not by the absolute amount of additives introduced, but by the precision of controlling the concentration of active chemical components, with a narrow range of hundredths and thousandths of a percent.

At the same time, most modern studies devoted to optimizing the qualitative and quantitative composition of chemical components of additives are carried out empirically without taking into account the mechanism of evolution of CMBLs formation under real friction conditions, thus limiting the possibilities of scientifically based forecasting of the resource and lubricating efficiency of oils. In this regard, it is important to develop a method for controlling the concentration of active chemical components of additives based on experimentally established patterns of the evolution of modified layers and changes in the friction coefficient in the contact zone under real operating conditions.

In addition, by solving the problem of increasing the lubricating effect of oils by controlling the concentration of active chemical components of additives, both from a scientific and applied point of view, the results obtained create the prerequisites for the development of energy-saving lubricating compositions with specified tribological properties that ensure a simultaneous reduction in friction losses, increased machine life, and optimized costs for expensive functional additives, which must correspond to current trends in sustainable development, energy conservation, and increased competitiveness of automotive and machine-building products.

Taking into account the multifactorial nature of the task of improving the lubricating effect of oils, it was necessary to use a comprehensive approach to assess the main tribological patterns and changes in tribotechnical characteristics—the evolution of the thickness of the modified layer and changes in the friction coefficient at all stages of real-time friction and wear processes depending on the mileage (friction path) according to the physicochemical factor.

Problem statement

An important role in the experimental study is the analysis of the qualitative and quantitative composition of active chemical components in the lubricant to improve the lubricating effect of oils by adapting the modified layers to the real operating conditions. Chemically active substances (CAS) create strong and stable CMBLs under high temperature conditions through chemical interaction and exchange of valence electrons of metal surface atoms with lubricant components in the form of metal salts: sulfides, phosphides, chlorides, and other compounds to increase anti-wear, anti-scuffing, and anti-friction characteristics.

Therefore, when analyzing the beneficial effect of CAS, it became necessary to study the analysis of CAS concentration and develop scientific and applied methods for improving the lubricating effect of oils for conditions as close as possible to the actual operating conditions of non-conforming friction units.

To conduct the relevant comprehensive experimental studies, it was necessary to use modern, specialized, and high precision tribotechnical equipment with simulation of the operation of bearing friction units of various classes in real operating conditions in two stages:

1) The first stage involved determining the presence of active chemical elements and measuring the concentration of the additives under study in neutral base oil using an energy-dispersive X-ray fluorescence spectrometer (EDXRF);

2) The second stage involved determining the best sample from the list of additives studied in neutral base oil by measuring the thickness of the formed modified layer or linear wear by the depth of the wear impression of the counterbody (anti-wear properties) and the friction coefficient (anti-friction properties) for a specified mileage on a CSM tribometer.

Method for determining the concentration of active chemical components of additives in EDXRF

A mixture of BS150 hydrocracked base oil and SN500 petroleum-based base oil (hereinafter referred to as "base oil") was used as a neutral oil. Subsequently, using the compounding method based on base oil, five samples of mixtures were produced containing the studied tribo-package of additives, which contains active chemical elements of sulfur and phosphorus in various concentrations, which are used in modern transmission oils for lubricating transmission components and universal (engine-transmission) oils for lubricating combined engine and transmission systems of military and agricultural equipment.

Neutral base oil was used as a sample in its pure form without additives to compare its results with other mixtures under study.

The sample preparation method was as follows:

– in the first stage, a tribo-package of additives was added in various concentrations to neutral base oil;

– the finished mixture was kept at a temperature of 70ºC with constant stirring using a laboratory vibrating mixer, after which a sample of the appropriate concentration was obtained (see Fig. 1).

The program of comprehensive laboratory studies included:

1) conducting a series of measurements:

– the presence of active chemical elements and the concentration of test samples on EDXRF (mass fraction of sulfur and phosphorus in percent);

– conducting a physicochemical analysis to measure kinematic viscosity at 40ºC and 100ºC, viscosity index, and density at 20ºC;

– thickness of the modified layer (depth of linear wear mark) from the mileage of test samples on a tribometer.

– coefficient of friction from the mileage of test samples on a tribometer.

2) establishing the following dependencies:

– changes in the thickness of the modified layer (depth of linear wear impression) from the mileage of test samples at different concentrations.

– changes in the friction coefficient from the mileage of test samples at different concentrations.

Fig. 1. General view of the laboratory vibration mixer

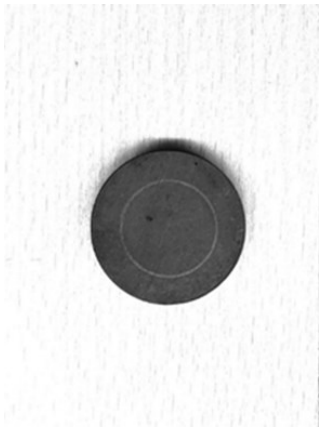

Fig. 2. Friction pair indenter with manganese-iron-phosphate coating

To simulate the operating conditions of friction bearing assemblies of various classes, the following tribotechnical pairs were proposed: as a counterbody — a 6 mm diameter ball made of SHX-15 steel (AISI E 52100, HRC 67, roughness class 10b); as an indenter — 25 mm diameter disc made of SHKH-15 steel coated with manganese-iron-phosphate salt (roughness class 10a), see Fig. 2. The test was conducted at a temperature of 70ºC, humidity of 75%, linear speed of 8.5 cm/s, maximum load of 50N, with a total mileage of up to 2,000 m.

Manganese-iron-phosphate coating (MIP) belongs to the class of conversion chemical coatings, which are formed directly on the metal surface as a result of chemical interaction with phosphate solutions. The resulting phosphate layer is a complex microcrystalline structure containing manganese and iron phosphates and characterized by high adhesion to the base material. Such coatings are widely used in mechanical engineering as a tribomodifying material that improves the running-in of contact friction surfaces and in tribology as a means of improving the modification of the surface of hard alloys in the composition of the additives under study.

In tribological laboratory studies, MIP coatings are used as a model surface that allows reproducing the operating conditions of real friction units, in particular in bearing friction units or in non-conforming units of the

cylinder-piston group of an ICE. The use of such a coating as a sample for a tribometer ensures the reproducibility of test results and the stability of the initial surface condition, which is of fundamental importance in the comparative analysis of the studied samples of additives dispersed in neutral base oils and in the study of the influence of the chemical composition of oils on the tribological characteristics of contact.

The use of MIP coating on the inner walls of internal combustion engine cylinders is associated with the need to improve the tribological conditions of the cylinder-piston group, especially during engine start-up and running-in. Under these conditions, boundary and mixed (partial the EHD) lubrication modes are mainly implemented, in which the efficiency of the unit is largely determined by the condition of the surface and its ability to interact with oils. The phosphate MIP coating formed on the inner surfaces of the cylinders creates a microcrystalline layer with a developed porous structure, which helps to retain oil and stabilize friction processes between the cylinder surface and compression piston rings.

From the point of view of interpreting the experimental results, the use of MIP coating reduces the influence of random factors associated with the microstructural heterogeneity of the metal surface. Thus, the main focus is on studying the lubricating properties of oils, taking into account the physicochemical factor influencing the creation of CMBLs, rather than on the random characteristics of the sample material. This is especially important when conducting serial experiments and statistical processing of the obtained data. EDXRF is one of the widely used methods of physical and chemical analysis of materials, based on the registration of characteristic X-ray radiation of atoms of the substance under study. The method allows determining the elemental composition of materials in a wide range of concentrations without significant destruction of the sample, which makes it particularly suitable for analyzing surface layers, coatings, and wear products [6]. In tribological studies, XRF is used for qualitative and quantitative assessment of the elemental composition of modified surfaces, protective films, friction and wear products, as well as for analyzing the distribution of active chemical components in the surface layers of materials. This allows establishing a connection between friction conditions, lubricant composition, and structural and chemical changes in the surface.

A typical energy-dispersive X-ray fluorescence spectrometer design includes a primary X-ray source, a beam shaping and collimation system, a sample chamber, a characteristic radiation detector, and a signal processing system. An X-ray tube with an anode made of molybdenum, rhodium, or silver is usually used as the primary radiation source, the choice of which is determined by the range of elements being analyzed [6]. The detector in modern XRF spectrometers is a semiconductor detector (Si-PIN or SDD), which provides high energy resolution and allows spectra to be recorded with sufficient accuracy even for elements with close energy lines. Signals from the detector are transmitted to a multichannel analyzer, where the energy spectrum of X-ray radiation is formed.

EDXRF method is particularly valuable when analyzing surfaces that have been subjected to tribological influences. During friction, secondary structures, modified tribochemical layers, and wear products can form on surfaces, the composition of which directly affects the thickness of the modified layer, the intensity of wear, and the friction coefficient. The use of EDXRF allows the identification of the elements that make up such films and the evaluation of their relative quantitative composition (concentration) [7]. The method is particularly effective for analyzing CAS added to lubricants in the form of additives, such as zinc, phosphorus, sulfur, calcium, or molybdenum. The detection and quantitative assessment of these elements in the surface layers after friction tests allows conclusions to be drawn about the mechanisms of formation of protective modified layers and the effectiveness of controlling the concentration of active components.

To perform elemental analysis of surfaces after tribological tests, this work uses an ElvaX Light energy-dispersive X-ray fluorescence spectrometer (see Fig. 3), which belongs to the class of universal laboratory EDXRF systems. The device is designed for qualitative and quantitative determination of the elemental composition of solid, powdery, and liquid materials, as well as surface deposits and modified layers. A distinctive feature of ElvaX Light is the combination of a compact design with sufficiently high sensitivity to elements of a wide periodic range. This makes it suitable for use in materials science and tribological research, where it is necessary to analyze both the main elements of the sample material and the active components of lubricant additives involved in the formation of tribochemical films.

Fig. 3. General view of the Elvax Light EDXRF spectrometer

Methodology for determining the anti-wear and anti-friction properties of oils from mileage on the CSM tribometer

Determining anti-wear properties (modified layer thickness and linear wear) is one of the key stages in a comprehensive assessment of the physical and chemical factors influencing the formation/wear of modified layers and their wear resistance. In laboratory conditions, such studies are carried out using high precision tribometric devices, in particular CSM tribometers, which provide controlled friction conditions and the ability to continuously record process parameters [8].

The CSM tribometer (see Fig. 4) is used in this study and is designed to perform tests in rolling with slippage, sliding, and reciprocating motion modes according to the “ball-disc” or “pin-disc” schemes. The device allows you to set the normal load, sliding speed, displacement amplitude, and total mileage, which ensures the reproducibility of experimental conditions. The high rigidity of the structure and the accuracy of the measuring sensors ensure the correct recording of both force and geometric wear parameters [9].

The reciprocating motion module (see Fig. 5) is used to simulate model tests close to real operating conditions, where it is necessary to reproduce rolling friction with slippage or sliding according to kinematic characteristics, which are typical for bearing friction assemblies of various classes.

Main characteristics of the module:

– Maximum torque: 450 N·mm;

– Maximum load 50 N;

– Frequency: from 0.005 to 1.6 Hz (1.6 Hz over the entire stroke length, up to 10 Hz possible with limited stroke length);

– Linear speed range: from 0.3 to 100 mm/sec;

– Working stroke: up to 60 mm;

– Test time: up to 40 days with 10 Hz data acquisition sampling.

Main characteristics of the module:

– Heating up to 120°C

– Indenter sample size, diameter - 25 mm;

– The heating module uses liquid to heat the sample when testing in the presence of oil;

– The external electronic unit guarantees temperature control accuracy of 0.1°C.

The heating module (see Fig. 6) allows you to select a convenient intermediate solution for the temperature factor (selected temperatures - up to 120°C, which are characteristic of the maximum temperatures of bearing friction units and non-conforming internal combustion engine units). The typical configuration of the CSM tribometer (see Fig. 7) includes a movable plate or sample (indenter) that performs linear or rotational movement relative to another contacting element of the counterbody (ball or pin). The system is equipped with high-precision force sensors that allow recording changes in friction force during testing, as well as recording the thickness or wear parameters of both contacting surfaces. In configurations with linear movement, the device measures the formation of a modified layer in terms of thickness or linear wear in terms of depth of contact surfaces under load and movement, simulating conditions of prolonged friction in real time at specified parameters of high loads and shear rates up to $10^6 \cdot s^{-1}$ for the studied oil samples with different viscosity stability (rheology) and physicochemical properties [10]. During measurement on a tribometer (see Fig. 8), the counterbody (ball) is fixed in the holder and immersed in a steel bowl filled with the oil sample under test, pressing down on the movable indenter (a disc coated with MIP) with a specified contact load. The indenter is fixed on a spring lever and connected to an LVDT inductive sensor. During the rotation of the indenter, a frictional force arises between it and the counterbody, which is measured by the minimum deflection of the spring lever in the vertical and tangential directions by the LVDT sensor.

Fig. 4. The CSM tribometer diagram: 1- Tribometer; 2 - Reciprocating motion module; 3 - Protective cover; 4 - Heating module

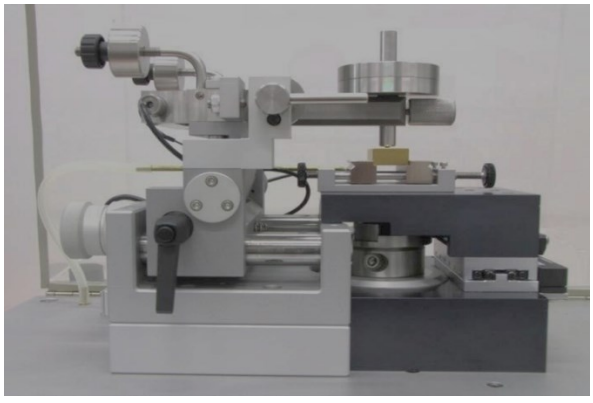

Fig. 5. Reciprocating motion module of the CSM tribometer

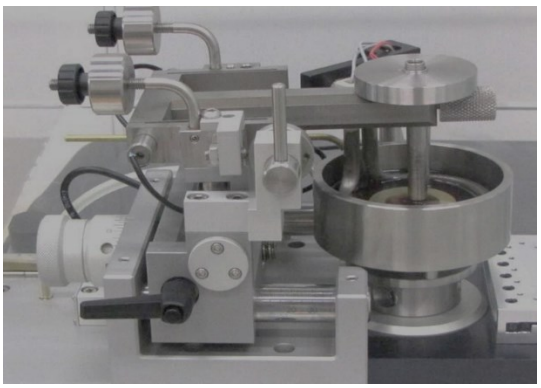

Fig. 6. The CSM tribometer heating module

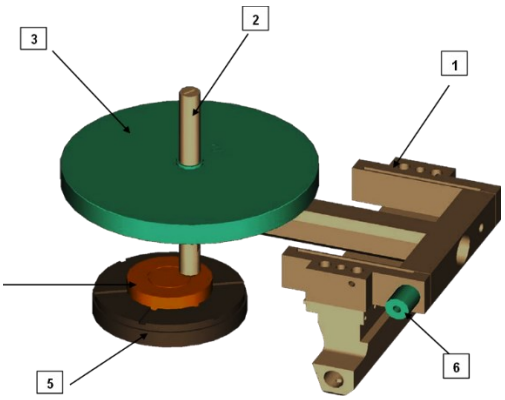

Fig. 7. Typical measurement diagram on the reciprocating motion module of the CSM tribometer: 1 - Elastic lever; 2 - Counterbody holder (ball or pin); 3 - Load; 4 - Indenter (disc with MIP coating); 5 - Indenter mounting chuck; 6 - LVDT micro-displacement sensor

As the mileage of the contacting surfaces increases, material is gradually formed/removed, accompanied by a change in the position of the contact pair depending on whether a modified layer is being formed, whether the corresponding modified layers are wearing out, or whether the surface layers of the metal are wearing out. These changes are recorded by a highly sensitive LVDT displacement sensor, which allows the total amount of modified layer thickness formation or linear wear to be determined with high accuracy depending on the mileage, which in our study is L = 2000 m. The obtained dependence of the thickness of the modified layer/linear wear on the mileage, taken from the vertical displacements of the LVDT sensor, allows us to evaluate the anti-wear properties of the studied oil samples, taking into account the physicochemical factor for the conditions of partial EHD contact in real-time testing. At the initial stages of the test, the modified layer is modified and adapted if the wear curve increases and stabilizes, and linear wear occurs if the wear curve decreases relative to the initial position, indicating a transition to wear of the base material. Thus, the nature of the change in thickness/linear wear from mileage allows determining the effective thickness of the modified layer, taking into account the rheological properties and physicochemical factors of the studied oil samples [10].

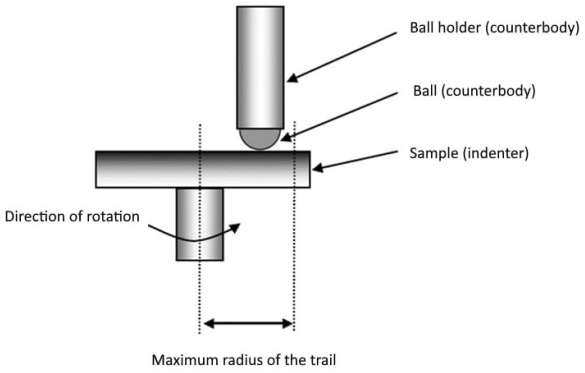

Fig. 8. Diagram of the position of the tribo-pair (indenter + counterbody) when taking measurements on the CSM tribometer

The anti-friction properties (friction force or coefficient) of the oil samples studied are one of the main tribological parameters characterizing the interaction of contacting surfaces during relative motion in the tangential direction. In tribological systems, the friction coefficient is defined as the ratio of friction force to applied normal load and allows quantitative assessment of the strength of the lubricating film, anti-friction properties of oils, and lubrication conditions. Determining the dependence of the friction coefficient on mileage is an important step in analyzing the behavior of a contact pair during running-in, wear-in, and subsequent stable operation.

On the CSM tribometer, the friction coefficient is determined in real-time friction force recording mode during testing. The design of the device includes an LVDT inductive sensor that records the tangential component of the force, including in the tangential direction, which characterizes the friction force. The normal load is set separately and maintained at a constant level throughout the test cycle. The ratio of the measured friction force to the normal load is used to calculate the instantaneous value of the friction coefficient. The dependence of the friction coefficient on mileage is usually analyzed in the form of a graphical curve μ(L), where L is the friction path or mileage of the contact pair. At the initial stage of the test, which corresponds to the run-in period, unstable

behavior of the friction coefficient is observed, which is due to the adaptation of the modified layers, smoothing of micro-irregularities, and the formation of the contact friction zone. During this period, both increased and decreased friction coefficient values are possible, depending on the surface condition and the presence of modified layers. A further increase in mileage is usually accompanied by the transition of the system to a steady-state friction mode, which is characterized by a relative stabilization of the friction coefficient values. In this mode, changes in the friction coefficient from mileage are insignificant and reflect the stable nature of the tribological system. The friction coefficient value in the steady state is often used for comparative evaluation of different olive samples under study, taking into account rheological properties and physicochemical factors, as it is less sensitive to random factors and the initial surface condition.

Analysis of the dependence of the friction coefficient on mileage on the CSM tribometer also allows identifying possible changes in the lubrication regime during the test, which is especially important for the partial EHD lubrication regime, which is a borderline lubrication regime from EHD to the limit in mixed friction and proceeds spontaneously. An increase or sharp fluctuation in the friction coefficient values may indicate the destruction of protective or modified layers, a change in lubrication conditions, or the appearance of lubricant layer breaks. At the same time, a decrease in the friction coefficient may be associated with the formation of strong and stabilized CMBLs in the sensitive zone of partial EHD contact.

The experimental data obtained on the friction coefficient are analyzed simultaneously with the results of measuring the thickness of the modified layer/linear wear. This approach allows for a comprehensive assessment of the tribological behavior of the contact pair, since the friction coefficient reflects the energy characteristics of the friction process, while the thickness/linear wear characterizes the geometric consequences of the tribological system's operation. A joint analysis of these parameters provides a more complete picture of the lubricating mechanisms of oils and wear processes under the influence of modification by CAS and the rheology of the samples under study.

Thus, the use of the CSM tribometer to determine anti-wear properties (modified layer thickness and linear wear) and anti-friction properties (friction coefficient) ensures high reliability and accuracy of experimental studies and allows for a comprehensive assessment of the lubricating effect of oils, taking into account the rheological properties and physicochemical factors of the studied oil samples in sensitive areas of partial EHD contact.

Results of the assessment of the anti-wear properties of the studied oil samples

The graphical interpretation of the results of the anti-wear properties of the studied oil samples was compiled into a single graph (see Fig. 9).

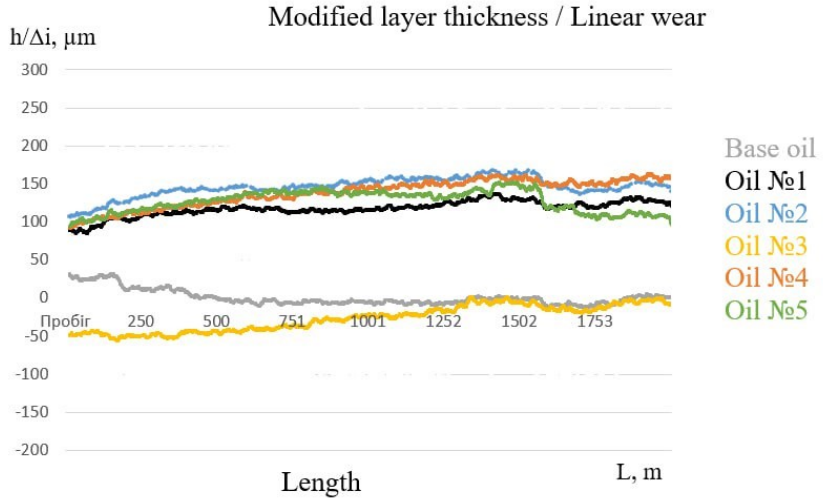

Fig. 9. Anti-wear properties for all samples studied

The results of the combined analysis of the anti-wear properties (see Fig. 9) of the oil samples studied showed the following:

– base oil sample is characterized by the destruction of the lubricating layer until cracks appear, which is reflected as linear wear, where the depth of the wear mark h reaches negative values below zero throughout the entire run L;

– sample 3 is characterized by the slow formation of modified layers with a predominance of intensifying wear friction processes, starting from negative values of linear wear. This is explained by the unexpressed anti-wear properties associated with an insufficient percentage (0.04%) of phosphorus mass fraction to ensure optimal anti-wear properties;

– unlike samples of base oil and 3, samples 1, 2, 4, and 5 are characterized by the formation and adaptation of modified layers with an average thickness of up to 30 μm at a maximum load of 50 N. Moreover, instantaneous

formation and adaptation of modified layers is observed during the running-in period, followed by an increase in the thickness of the modified layer, which lasts for approximately 1600 km of length;

– after 1600 m of length, for samples 1, 2, 4, 5, some stabilization is observed in the formation of the modified layer thickness, but with different thickness values. Samples 2 and 4 create thicker modified layers during the corresponding period.

Thus, after two periods: formation (running-in) and stabilization (adaptation) of the modified layer thickness, two best samples can be selected in terms of anti-wear properties: samples 2 and 4. Moreover, sample 2 adapts better in running-in conditions, forming and building up thicker modified layers during this period. Sample 4 is slightly inferior to sample 2 in terms of thickness during the running-in period, but during the stabilization period it retains the most negative value of the modified layer thickness, which indicates the ultra-high strength of the film during this period under all equal test conditions.

Based on the above analysis of the research results, to ensure optimal anti-wear properties, transmission and universal oils should contain a concentration of 0.046–0.057% by mass of phosphorus, which will allow the creation of strong CMBLs, quickly adapting to high loads during the running-in and stabilization period in the process of forming, building up, and wearing down modified layers.

Results of the evaluation of the anti-friction properties of the oil samples studied

A graphical interpretation of the results of the anti-friction properties of the studied oil samples was compiled into a single graph (see Fig. 10).

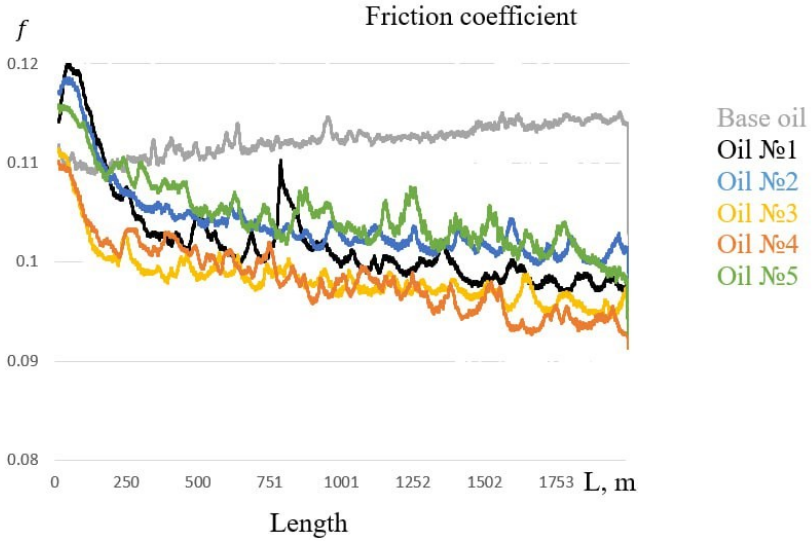

Fig. 10. Anti-friction properties for all samples studied

The results of the combined analysis of the anti-friction properties (see Fig. 10) of the oil samples studied showed the following:

– the base oil sample is characterized by an increase in the friction coefficient throughout the entire run, since the lubricating layers do not provide anti-friction properties in the absence of CMBLs;

– unlike the base oil sample, samples 1, 2, 3, 4, and 5 are characterized by an initial significant reduction in friction to 200 m of the test run by an average of 30%, and then after 200 m throughout the entire test run, by a gradual reduction in friction by an average of 10%;

– for the initial friction coefficient value during the running-in period and the stabilization period, samples 3 and 4 have the minimum value, which indicates pronounced anti-friction properties with a sulfur mass fraction in the range of 1.488-1.9662%, i.e., across the entire range of selected samples studied.

Thus, it can be stated that to ensure high anti-wear and anti-friction properties, it is not so much the mass fraction of sulfur, which must be within a certain range guaranteed by the manufacturer, that is important, but rather the mass fraction of phosphorus, which requires additional tribotechnical research.

Comparing the results of anti-wear (see Fig. 9) and anti-friction (see Fig. 10) properties of the studied oil samples, while complying with the additive manufacturer's conditions for the mass fraction of sulfur, which is: 1.488 - 1.9662%, a necessary condition for the best results in terms of the combined action of anti-wear and anti-friction properties of oils is to establish a total additive concentration of 3.9-4.9% with a mass fraction of phosphorus of 0.046-0.057%. In the series of samples studied, sample 4 with a concentration of 4.9% additive shows the best universal properties, especially for the operation of units with combined engine and transmission systems (universal STOU oils for agricultural machinery). The corresponding universal properties make it possible to modify friction surfaces with durable CMBLs for high load conditions and to adapt more quickly to extreme friction conditions when operating temperature and load conditions change significantly, for example, when

operating in the engine and transmission simultaneously.

Conclusion

A multifactorial approach to assessing the lubricating effect of oils has been proposed and justified, taking into account the influence of physicochemical factors and rheological characteristics on the evolution of the creation and adaptation of CMBLs to real operating conditions in conditions of partial EHD lubrication mode. The substantiated choice of modern spectral and tribometric equipment made it possible to comprehensively evaluate the tribological behavior of the contact pair, since the friction coefficient reflects the energy characteristics of the friction process, while thickness/linear wear characterizes the geometric consequences of the tribological system's operation. Thus, a joint analysis of these parameters provides a more complete understanding of the mechanisms of the lubricating action of oils and the wear processes under the influence of modification by CAS and the rheology of the studied samples.

References

1. Afton Chemical. Engine Oil Additive Technology: Performance Optimization Through Precise Additive Treat Rates. Technical Bulletin. Richmond, VA, 2020. https://www.aftonchemical.com/products/engine-oil-additives/

2. Lubrizol Corporation. Additive Systems for Modern Lubricants: Concentration Sensitivity and Performance Balance. Technical White Paper. Wickliffe, OH, 2019. https://lubrizol.com/Lubricant-Additives/Products-Applications

3. BASF SE (2021). Lubricant Additives: Structure–Performance Relationships and Optimization Strategies (Technical Report). Fuel & Lubricant Solutions, BASF SE, Ludwigshafen, Germany. https://automotive-transportation.basf.com/global/en/fuel-and-lubricants/portfolio

4. Waqas M., Zahid R., Khan A., et al. A review of friction performance of lubricants with nano additives // Materials. 2021. Vol. 14, No. 21. Art. 6310. https://doi.org/10.3390/ma14216310

5. Muhammad Waqas, Rehan Zahid, Muhammad Usman Bhutta, Zulfiqar Ahmad Khan, Adil Saeed//A Review of Friction Performance of Lubricants with Nano Additives, 2021. - 14(21), - 6310 https://doi.org/10.3390/ma14216310.

6. Mang T., Dresel W. Lubricants and Lubrication. — Wiley-VCH, 2017. Chapter 6: Additives, P. 117–152. https://doi.org/10.1002/9783527645565

7. Daniel Merk, Thomas Koenig, Janine Fritz, Joerg W. H. Franke //Tribological Behavior of Hydrocarbons in Rolling Contact, 2024. - 12(6), 201. https://doi.org/10.3390/lubricants12060201

8. CSM Instruments. Tribometer User Manual. — Switzerland. Sections 2–4. https://www.csm-instruments.com/en/products/tribometers.

9. Hutchings I. M., Shipway P. Tribology: Friction and Wear of Engineering Materials. — Elsevier, 2017. P. 145–158.
https://www.educate.elsevier.com/book/details/9780081009109.

10. ASTM G133–05 (Reapproved 2016). Standard Test Method for Linearly Reciprocating Ball-on-Flat Sliding Wear. https://doi.org/10.1520/G0133-05R16.

Міланенко О., Бобро А. Мастильна дія олив шляхом керування концентрації хімічних компонентів присадок.

Запропоновано та обґрунтовано багатофакторний підхід щодо оцінки мастильної дії олив з урахуванням впливу фізико-хімічного фактору та реологічної ознаки на еволюцію створення та адаптації хімічно модифікованих граничних шарів (ХМГШ) до реальних умов експлуатації в умовах часткового ЕГД режиму мащення. Порівнюючи результати протизношувальних і антифрикційних властивостей досліджуваних зразків олив, при дотриманні умов виробника присадок щодо масової частки сірки, яка становить 1,488–1,9662%, необхідною умовою для досягнення найкращих результатів з точки зору комбінованої дії протизношувальних і антифрикційних властивостей олив є встановлення загальної концентрації присадок в діапазоні 3,9–4,9% з масовою часткою фосфору 0,046–0,057%. Для досліджуваного ряду зразків, зразок 4 з концентрацією присадки 4,9% показує універсальні властивості, які особливо важливі при експлуатації в суміщених системах двигуна і трансмісії (універсальні оливи STOU для сільськогосподарської техніки).

Ключові слова: мастильна дія олив, фізико-хімічний фактор та реологічна ознака, хімічно модифіковані граничні шари (ХМГШ), частковий ЕГД режим мащення, протизношувальні й антифрикційні властивості, концентрація хімічних компонентів присадок, хімічно активні речовини (ХАР), марганцево-залізо-фосфатне покриття (МЗФ).

*ISSN 2079-1372 **Problems of Tribology**, V. 31, No 1/119-2026, 33-40*

Problems of Tribology
Website: http://tribology.khnu.km.ua/index.php/ProbTrib
E-mail: tribosenator@gmail.com

DOI: https://doi.org/10.31891/2079-1372-2026-119-1-33-40

Justification of the microcutting scheme in the friction-mechanical method of applying anti-friction coatings

I.V. Shepelenko[1] 0000-0003-1251-1687, **Ya.B. Nemyrovskyi**[2] 0000-0001-8005-8584, **M.I. Chernovol**[1] 0000-0003-3048-6833, **M.V. Krasota**[1] 0000-0001-8791-3264, **I.F. Vasylenko**[1] 0000-0003-0973-0053

[1]*Central Ukrainian National Technical University, Kropyvnytsky, Ukraine*
[2]*Zhytomyr Polytechnic State University, Ukraine*
E-mail: kntucpfzk@gmail.com

Received: 25 December 2025: Revised 15 January 2026: Accept: 30 January 2026

Abstract

A review of modern approaches to substantiating the patterns of anti-friction coating formation during friction-mechanical application has made it possible to establish the importance of ensuring favourable conditions for microcutting of anti-friction material. Creating these conditions requires studying the interaction scheme of microirregularities in the contact zone between the tool and the part. From the point of view of cutting mechanics, a scheme of interaction of a single micro-irregularity, which is a model – a cutter made of 200 gray cast iron, with a contact surface made of anti-friction material – brass L63, was constructed, which made it possible to establish physical changes in the tool and machined surface system. The value of the front cutting angle has been theoretically established to ensure maximum efficiency of the microcutting process and filling of microcavities between microirregularities. The use of a model experiment, the method of similarity and dimensions made it possible to confirm the main theoretical regularities obtained using characteristic microcutting diagrams. It has been shown that the process of changing the geometry of the micro-irregularity vertex occurs in accordance with the principle of adaptability of the entire 'tool-part' system, according to which the minimum micro-cutting energy is realised. The results obtained are an important reserve for improving the quality of anti-friction coating application by the friction-mechanical method.

Keywords: anti-friction coating, final anti-friction non-abrasive treatment, microcutting, micro-irregularity interaction diagram, cutting angle, microchips, microcutter

Introduction

Numerous studies have shown that in order to increase reliability and service life, it is necessary to ensure that the working surface of a part has a protective coating in accordance with its intended use and operating conditions [1, 2, etc.].

Among the simplest, most effective and environmentally friendly methods of obtaining coatings, it is worth highlighting a group of technologies for finishing anti-friction non-abrasive treatment (FANT), which is implemented through the frictional interaction of the processing tool with the surface of the part being processed [3]. It has been proven that the use of FANT technology improves the characteristics of the working surface: it reduces the running-in time and friction coefficient and increases the load-bearing capacity of the part and connection [4].

The quality of FANT antifriction coating formation is determined by the conditions of contact between the tool and the machined surface and depends on the completeness of physical contact and activation of contact surfaces [5]. Among the main channels of activation, in the performance of which depends on the formation of quality antifriction coating, should be highlighted as follows: mechanical, chemical, thermal and channel associated with plastic deformation. These channels are closely connected with each other and are simultaneously involved in the formation of antifriction coating during friction-mechanical contact.

A number of factors affecting the final results of FANT should also be considered [6]:

- the adhesive tendency between the applied material and the surface to be treated;

- structural and phase composition of the treated surface;
- initial quality of the treated surface;
- friction and wear conditions.

However, in our opinion, a number of processes accompanying FANT require clarification and deeper study.

In particular, there is no consensus on the values of the initial roughness of the treated surface, which determines the conditions of contact with the antifriction material. At the same time, the surface roughness obtained by FANT is one of the main criteria of coating quality [6, 7, etc.].

Thus, studies of the contact interaction of surfaces and the processes occurring during FANT seem to be very relevant. Establishment of the basic regularities of the processes at this process will allow to increase the quality of the coating, and hence the operational properties of the part.

Literature review

There are a number of approaches that allow us to understand the mechanism of formation of antifriction coating at the friction-mechanical method of FANT implementation [8, 9, etc.]. The authors of the presented works agree that it is necessary to create a number of conditions and achieve certain criteria to obtain a high-quality antifriction coating. Such mandatory conditions and criteria should include: the conditions of micro-cutting and plastic contact; the criterion of seizure and achievement of optimal modes of coating application.

Considering the stages of the process of frictional transfer of antifriction material the authors of works [8, 9] note the presence of:

- plastic pushing away of the initial material, carried out by the microroughnesses of the surface, on which the coating is applied, passing to destruction by micro-cutting;
- adhesion of the particles formed as a result of micro-cutting with the surface to which the transfer takes place.

Microscopic analysis of the particles contained in the contact zone 'friction rod - machined surface' showed the presence of chip microparticles, which indicates that the process of micro-cutting [8].

Realisation of the specified conditions of micro-cutting is associated with certain requirements to the microroughness of the contacting surfaces, which can be described by the following dependence [9]:

$$\frac{2h_i}{r} = 1 - \frac{2\tau_n}{\sigma_T} \le 0{,}02\ , \tag{1}$$

where h_i – is the height of a single microroughness;

r – is the radius of rounding of the top of a single microroughness;

τ_n – is the tangential component of the adhesive bond strength;

σ_T – is the yield strength of the brass rod.

The model of applying FANT anti-friction coating is discussed in detail in the works of German researchers [10], where it is stated that at the initial moment of tribointeraction, the process of microcutting of copper alloy prevails. The authors note the following processes occurring on contact surfaces:

- the Rebinder effect with adsorption plasticisation and an increase in the positive strength gradient during shear in the friction zone;
- transfer of more plastic metal to a harder substrate due to microadhesion;
- the Kirkendall effect (diffusive) with selective dissolution of alloying elements due to the potential difference;
- deposition of copper particles and ions by an electrochemical process activated tribochemically;
- formation of organometallic compounds with a surface-active environment and catalytic effect of copper.

Analysis of experimental data and theoretical description of the coating formation process has revealed tool wear and material transfer, which is characteristic of microcutting with surface roughness of the workpiece. However, there is no consensus on the optimal value of this roughness parameter. Thus, the authors of works [11, 12] indicate the formation of a high-quality anti-friction coating at an initial surface roughness value of Ra from 0.08 μm to 3.4 μm, and in some cases significantly higher [13].

In our opinion, the process of coating formation by the FANT friction-mechanical method is quite complex and requires in-depth research. Analysis of the literature on this issue reveals different approaches to explaining the mechanism of coating formation. At the same time, despite different approaches and views, the authors agree on the importance of ensuring the necessary conditions for microcutting of anti-friction material. Creating these conditions requires research into the interaction of micro-irregularities to better ensure microcutting of anti-friction material.

Purpose

The aim of the work is to clarify the scheme of interaction of micro-irregularities at the micro-cutting stage using the friction-mechanical method of applying anti-friction coatings.

Research Methodology

The theoretical and experimental studies of micro-cutting are based on the method of the theory of similarity and dimensionality [14], in accordance with which the miro cutters made of 200 gray cast iron (Fig. 1), the geometry of the cutting part of which modelled a separate microroughness of the surface of the processed workpiece, were manufactured.

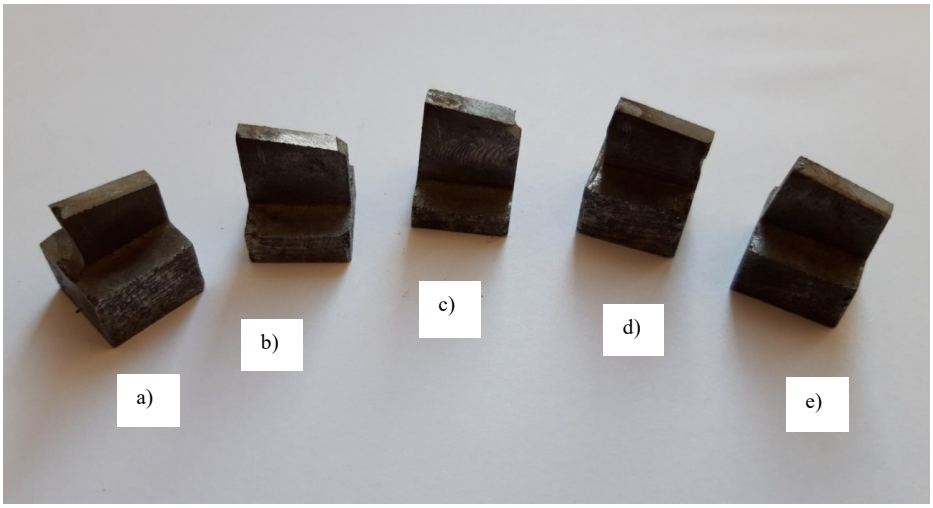

Fig. 1. Micro-cutters from the value of the front cutting angle γ: a) +5°; b) 0°; c) -5°; d) -10°; e) -15°

The interaction scheme of contacting surfaces during the model experiment is shown in Fig. 2.

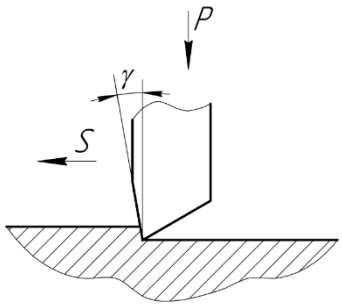

Fig. 2. Surface contact diagram in microcutting modelling: *P* – micro-cutter force; *S* – microcutter feed

Simulation of the microcutting process during the application of anti-friction coatings using a friction-mechanical method was performed using the proposed device (Fig. 3).

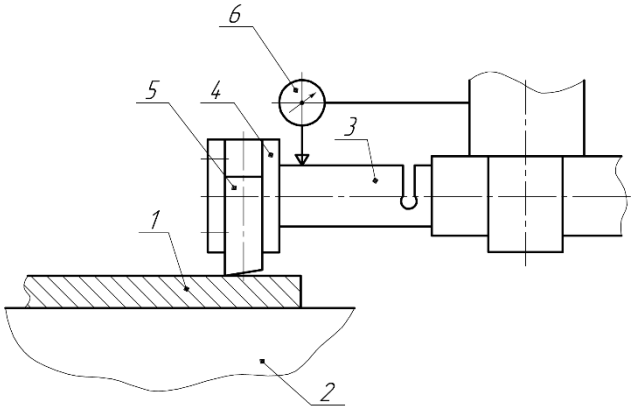

Fig. 3. Microcutting research setup: 1 – sample made of anti-friction material; 2 – machine table; 3 – microcutter mounting device; 4 – mounting head; 5 – replaceable microcutter; 6 – indicator head

In accordance with the diagram presented (see Fig. 3), the test sample 1 made of anti-friction material was rigidly fixed on the work table 2 of the milling machine. Device 3 with head 4, to which a replaceable micro-cutter 5 made of 200 gray cast iron is attached. A magnetic stand with indicator head 6 is provided to fix the pressure of the anti-friction sample against the surface being machined on the machine. Microcutter 5, which simulates a separate micro-irregularity, was pressed against the outer edge of sample 1. The load on microcutter 5 was provided

by the vertical feed mechanism of the machine table, which was controlled by indicator head 6. The simulated microcutter, moving under load, cuts off a layer of the sample made of anti-friction metal (brass), thereby imitating the microcutting process in the friction-mechanical method of applying anti-friction coatings.

Results

To clarify the main patterns that occur when a single micro-irregularity interacts, let us consider in detail the interaction scheme of a 200 gray cast iron with the surface of a sample made of anti-friction material (Fig. 4).

The cutting wedge contour consists of the following parts:

AB – a straight part of the front surface contour, sharpened with a front angle $\gamma > 0$;

BC – a rounded part of the front surface, in which $\gamma < 0$;

CD – a rounded part of the rear surface contour, in which the rear angle $\alpha < 0$;

DE – part of the contour of the rear surface, formed as a result of its wear;

EF – part of the straight contour of the rear surface, in which the rear angle $\alpha > 0$. The length of this section is practically determined by the process of plastic restoration, since the value of elastic restoration of the processed material $d_{el} << d_{pl}$.

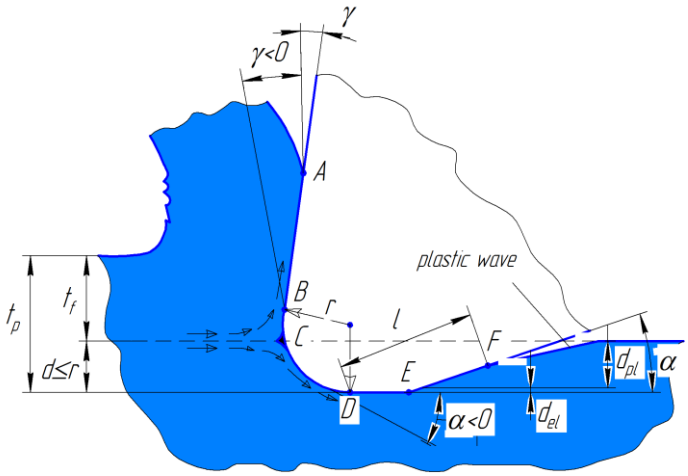

Fig. 4. Schematic representation of the interaction between a single micro-irregularity and the machined surface during micro-cutting

Thus, the front surface of the cutting wedge consists of two parts $L = AB + BC$, and its rear surface with a length of L_1 consists of the following parts $L_1 = CD + DE + EF$. Point *C* corresponds to the section of contact between the material being processed and the front and rear surfaces of the wedge.

The workpiece material flowing onto the cutting wedge at point *C* is divided into two streams, one of which moves along the front surface of the tool, and the second layer, with a thickness of *d*, is deformed by the rear surface of the cutting wedge. In this case, the actual cutting surface passes through point *C*, and the actual cutting depth t_f does not coincide with the nominal thickness t_p of the surface cut. Thus, point *C* will be the dividing point of the entire removed layer with a thickness t_p, namely: the layer of material that goes into microchips, with an actual cutting depth t_f, and the layer that is processed by surface plastic deformation by the radial section of the rear surface. Its value is $d \le r$, i.e. $t_p \sim t_f + r$, where r is the radius of the tool tip blunting, which changes during operation, especially in the initial period of operation.

In the chip formation zone, plastic deformation of the material occurs, preceded by elastic deformation. It leads to the lowering of the layer of material located below the surface cut. After the micro-cutter passes, the load is removed, and this layer elastically recovers, returning to its original state, which leads to its interaction with the rear surface of the micro-cutter. The value of elastic recovery d_{pl} determines the length of elastic contact along the rear surface of the cutting wedge.

Modeling the FANT process using microcutters (Fig. 5, a-e), each of which should be considered as a separate micro-irregularity, allowed us to establish the following.

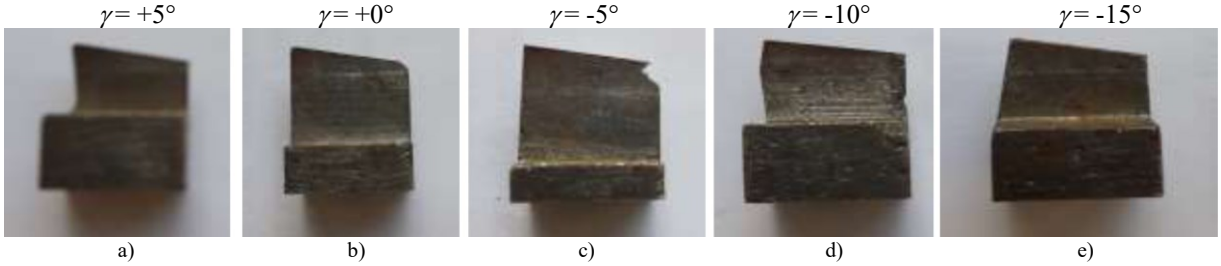

a) b) c) d) e)

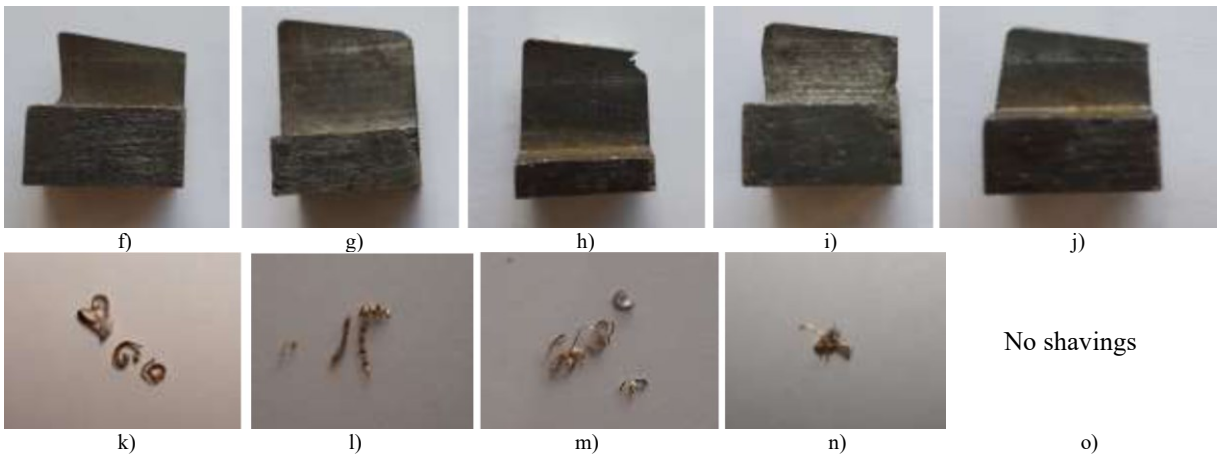

Fig. 5. View of the cutting part of a micro cutter before processing (a-e) and after processing (f-j), as well as chip formation by different micro cutters (k-o)

The cutting blade of a cast iron micro-cutter wears out intensively during interaction with a brass surface, and this occurs at the very beginning of its operation. The process of changing the geometry of the cutter tip occurs in accordance with the principle of adaptability of the entire "cutter-part" system [7], according to which the minimum energy of microcutting is realized. A detailed examination of microcutters after processing shows the formation of a blunt cutting edge (Fig. 5, f-j). It is also worth noting the patterns of chip formation when using micro-cutters with different cutting angles (Fig. 5, k-n). Moreover, at a front cutting angle of γ = -15°, there are no chips at all (Fig. 5, o).

Photographs of the roots of the chips (Fig. 6, a) also confirm the statement that the greatest thickness of the cut layer is observed at an angle of γ= +5°. At γ = 0°, the thickness of the cut layer decreases significantly (Fig. 6, b), and the smallest thickness of the cut layer is observed at an angle of γ = -5° (Fig. 6, c).

Fig. 6. Micro-chips obtained during micro-cutting at different front cutting angles γ: a) –γ= +5°; b) – γ= 0°; c) –γ= -5°, increase × 50

To quantitatively assess the effectiveness of microcutting in FANT, the term "volumetric efficiency of microcutting" η, is used, which is determined by the following relationship:

$$\eta = \frac{t_f}{t_p} = \frac{t_f}{t_f + r}. \tag{2}$$

The proposed dependence allows determining the volumetric efficiency of microcutting η (Fig. 7) and proving the effectiveness of microcutting at positive angles γ.

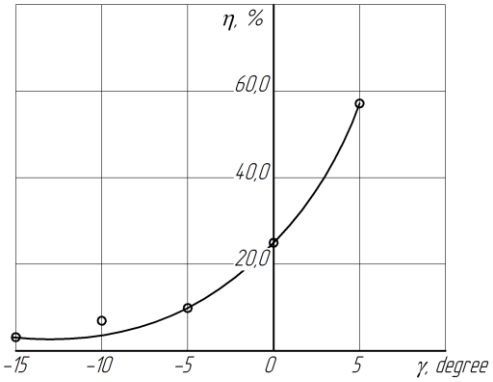

Fig. 7. Dependence of the volumetric efficiency of microcutting η on the angle γ

The experimental data obtained made it possible to present diagrams of the interaction between the tool and the machined surface at different angles γ (Fig. 8).

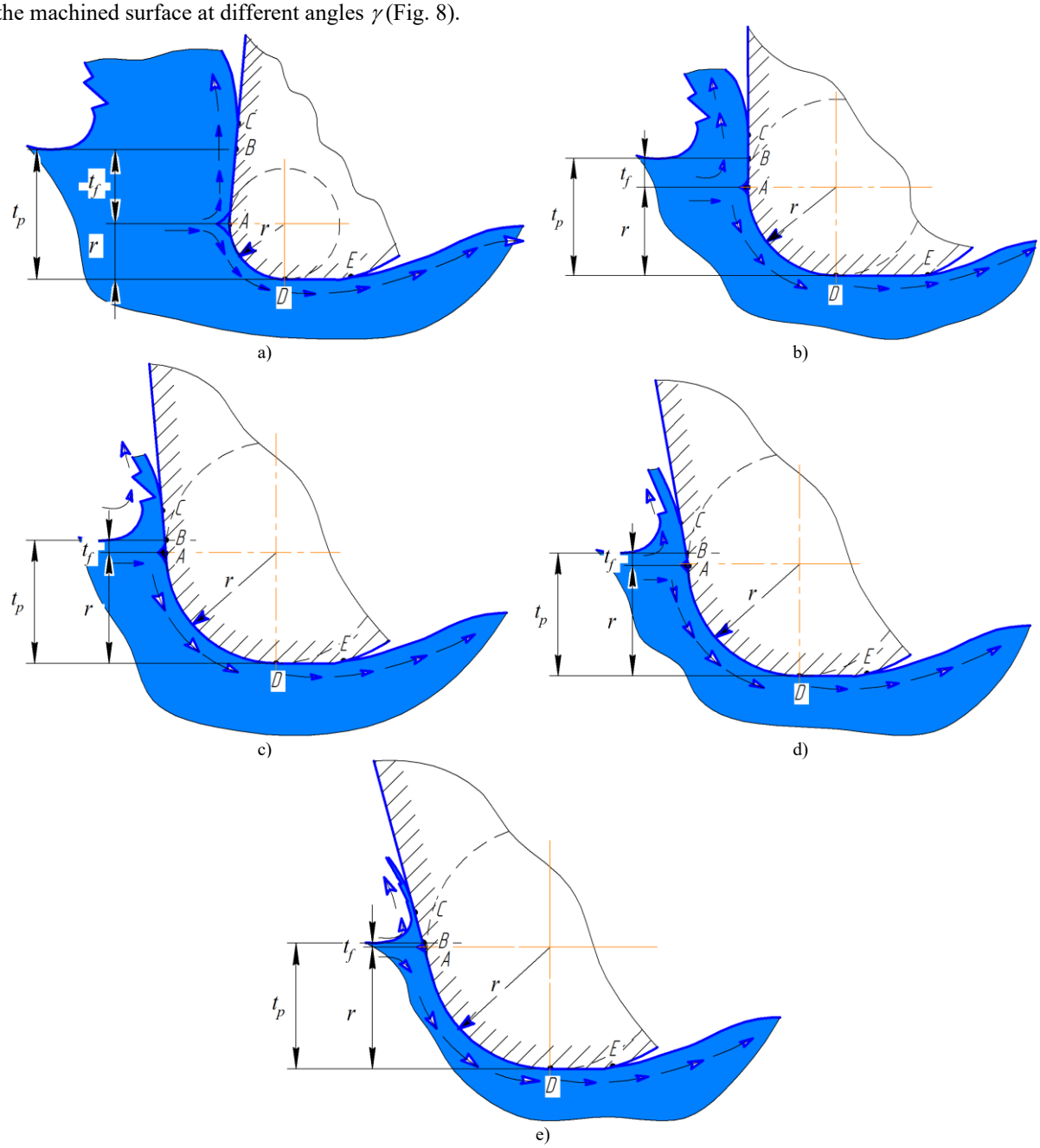

Fig. 8. Characteristic microcutting patterns for FANT at different angles γ: a) –γ= +5°; b) – γ= 0°; c) –γ= -5°; d) –γ = -10°; e) –γ= -15°

Analysis of the proposed microcutting schemes at different front cutting angles (Fig. 8) allowed us to establish the following patterns.

At γ= +5° (Fig. 8, a), the following relationship between the thickness of the anti-friction material cut is observed:

$$t_f = 0,57t_p\ ;\ r = 0,43t_p\ . \tag{3}$$

For an angle γ= 0° (Fig. 8, b), the following is characteristic:

$$t_f = 0,25t_p\ ;\ r = 0,75t_p\ . \tag{4}$$

For angle γ = -5° (Fig. 8, c), the following is determined:

$$t_f = 0,1t_p\ ;\ r = 0,9t_p\ . \tag{5}$$

For an angle γ= -10° (Fig. 8, d), it has been established that:

$$t_f = 0,083t_p\ ;\ r = 0,917t_p\ . \tag{6}$$

For angle γ= -15° (Fig. 8, e):

$$t_f = 0,032t_p\,;\ r = 0,968t_p\,. \tag{7}$$

Thus, a series of theoretical and experimental studies has made it possible to establish a scheme of interaction between micro-irregularities at the micro-cutting stage during FANT and to recommend a value for the front angle γ to ensure maximum efficiency of the micro-cutting process and filling of micro-pits between micro-irregularities.

Conclusions

On the basis of theoretical and experimental studies of the micro-cutting process, which is considered as the first stage of FANT, the following conclusions are formulated:

1. Schemes of interaction between the tool and the machined surface at FANT at the micro-cutting stage at different cutting angles have been obtained, which made it possible to study the main regularities of chip formation.

2. Theoretically proved and experimentally confirmed the feasibility of obtaining microrelief with the value of the cutting angle $\gamma \geq 0°$. The most efficient micro-cutting process is carried out at $\gamma = +5°$.

3. It has been established that when micro-irregularities interact with a brass tool, a blunt micro-irregularity tip with a rounding radius is formed almost immediately, which subsequently remains virtually unchanged.

References

1. Sun, T., Jin, K., Wang, T. *et al.* Synergistic effect of graphene oxide and cathodic protection to enhance the long-term protective performance of organic coatings. *J Mater Sci* **58**, 10853–10869 (2023). https://doi.org/10.1007/s10853-023-08701-2.

2. Shepelenko, I. (2021). Technological factors influence on the antifriction coatings quality. *Problems of Tribology*, *26*(2/100), 50–57. https://doi.org/10.31891/2079-1372-2021-100-2-50-57.

3. Tiškevičius K., Padgurskas J., Prosyčevas I. Investigation of Non-abrasive Antifrictional Surface Finishing. Medžiagotyra 9, 1 (2003) 62 – 67.

4. Kosiuk, M.M., Kostiuk, S.A., Kostiuk, M.A. (2018). Technological support for the application of antifriction coating on incomplete spherical surfaces by friction-mechanical method. *Bulletin of Khmelnytsky National University*. Technical sciences. No. 4. 38-42.

5. Shepelenko, I., Posviatenko, E., Cherkun, V. (2019). The mechanism of formation of anti-friction coatings by employing friction-mechanical method. *Problems of Tribology*, *24*(1/91), 35-39. https://doi.org/10.31891/2079-1372-2019-91-1-35-39.

6. Shepelenko, I. (2020). The study of surface roughness in the process of finishing anti-friction non-abrasive treatment. *Problems of Tribology*, *25*(1/95), 34–40. https://doi.org/10.31891/2079-1372-2020-95-1-34-40.

7. Shepelenko, I., Tsekhanov, Y., Nemyrovskyi, Y., Posviatenko, E. (2020). Improving the Efficiency of Antifriction Coatings by Means of Finishing the Antifriction Non-abrasive Treatment. In: Tonkonogyi, V., *et al.* Advanced Manufacturing Processes. InterPartner 2019. Lecture Notes in Mechanical Engineering. Springer, Cham. https://doi.org/10.1007/978-3-030-40724-7_30.

8. Shepelenko, I., Nemyrovskyi, Y., Tsekhanov, Y., Posviatenko, E., Sardak, S. (2020). Power Parameters of Micro-cutting During Finishing Anti-friction Non-abrasive Treatment. In: Karabegović, I. (eds) New Technologies, Development and Application III. NT 2020. Lecture Notes in Networks and Systems, vol 128. Springer, Cham. https://doi.org/10.1007/978-3-030-46817-0_22.

9. Shepelenko, I., Nemyrovskyi, Y., Tsekhanov, Y., Mahopets, S., Bevz, O. (2020). Peculiarities of interaction of micro-roughnesses of contacting surfaces at FANT. In: Ivanov, V., Trojanowska, J., Pavlenko, I., Zajac, J., Peraković, D. (eds.) DSMIE 2020. LNME, 452-461. https://doi.org/10.1007/978-3-030-50794-7_44.

10. Gottlieb Polzer (1981). Erhöhung der Verschleißfestigkeit auf der Grundlage der selektiven Übertragung. 192 p.

11. Abdullah Rasheed A, Ihor Shepelenko, Eduard Posviatyenko (2020). Experimental quality improvement of the application of antifriction coating. First International Conference on Advances in Physical Sciences and Materials 13-14 August 2020, Coimbatore, India. Journal of Physics: Conference Series, Vol. 1706. 1-11. https://iopscience.iop.org/article/10.1088/1742-6596/1706/1/012187.

12. Shepelenko I.V., Kirichenko A.M., Magopets S.O., Krasota M.V., Vasilenko I.F. (2022). Change in surface roughness when applying anti-friction coatings. *National interdepartmental scientific and technical collection*. Design, manufacture and operation of agricultural machinery. 52, C.156-165. https://doi.org/10.32515/2414-3820.2022.52.156-165.

13. Cherkun V.V. Increasing the wear resistance of hydraulic pump gear trunnions by finishing antifriction non-abrasive vibration treatment [Abstracts dys. ... kand. tekhn. nauk: 05.02.04]. 2011. 16 p.

14. Shepelenko I.V., Nemyrovskyi Y.B., Posviatenko E.K. (2020). Intensification of the process of applying anti-friction coatings. *Materials of the XXI International Scientific and Technical Conference*. Progressive Technology, Technology and Engineering Education. 94-96.

Шепеленко І.В., Немировський Я.Б., Черновол М.І., Красота М.В., Василенко І.Ф. Обґрунтування схеми мікрорізання при фрикційно-механічному методі нанесення антифрикційних покриттів

Огляд сучасних підходів до обґрунтування закономірностей формування антифрикційного покриття при фрикційно-механічному їх нанесення дозволив встановити важливість забезпечення сприятливих умов для мікрорізання антифрикційного матеріалу. Створення цих умов вимагає дослідження схеми взаємодіїї мікроонерівностей в зоні контакту «інструмент – деталь». З позиції механіки різання побудована схема взаємодії одиничної мікронерівності, що являє собою модель – різець із чавуну СЧ20, з контактуючою поверхнею з антифрикційного матеріалу – латуні Л63, що дозволило встановити фізичні зміни в системі інструмент і оброблювана поверхня. Теоретично встановлено значення переднього кута різання для забезпечення максимальної ефективності процесу мікрорізання і заповнення мікровпадин між мікронерівностями. Використання модельного експерименту, методу теорії подібності та розмірності дозволило підтвердити основні теоретичні закономірності, отримані за допомогою характерних схем мікрорізання. Показано, що процес зміни геометрії вершини мікронерівності відбувається відповідно до принципу пристосовності всієї системи «інструмент – деталь», відповідно до якого реалізується мінімум енергії мікрорізання. Отримані результати є важливим резервом для підвищення якості нанесення антифрикційного покриття фрикційно-механічним методом.

Ключові слова: антифрикційне покриття, фінішна антифрикційна безабразивна обробка, мікрорізання, схема взаємодії мікронерівностей, кут різання, мікростружка, мікрорізець

ISSN 2079-1372 Problems of Tribology, V. 31, No 1/119-2026, 41-47

Problems of Tribology
Website: http://tribology.khnu.km.ua/index.php/ProbTrib
E-mail: tribosenator@gmail.com

DOI: https://doi.org/10.31891/2079-1372-2026-119-1-41-47

Correlation between sliding bearing wear rate and material characteristics of friction surfaces in heavily loaded construction and road machinery

O. Shchukin[*1] 0000-0001-6332-1811, **O. Orel**[1] 0000-0003-0265-7527, **A. Kholodov**[1] 0000-0002-4120-4654, **A. Kravets**[2] 0000-0002-3251-6576, **S. Fedoriachenko**[3] 0000-0002-8512-3493

[1]*Kharkiv national automobile and highway university, Ukraine*
[2]*O.M. Beketov National University of Urban Economy in Kharkiv, Ukraine*
[3]*Dnipro University of Technology, Ukraine*
[*]*E-mail: alexhome88@gmail.com*

Received: 30 December 2025: Revised 18 January 2026: Accept: 30 January 2026

Abstract

Based on an investigation of how entropy generation depends on material and tribological characteristics, it was found that the wear rate of a sliding bearing operating under elastic and elastoplastic contact conditions exhibits a nonmonotonic relationship with the surface dislocation density. Specifically, at relatively low dislocation densities, wear intensifies as this parameter increases, whereas in the high-density regime, further growth leads to a reduction in wear. A mathematical model describing entropy generation arising from the interaction between lubricant molecular dipoles and dipoles induced by fluctuations in surface dislocation density has been derived. The results demonstrate that the component of wear associated with this mechanism of entropy production decreases as the dipole moment of the lubricant molecules increases.

An additional analysis focusing on the influence of material parameters on entropy generation shows that bearing wear intensity rises with increasing surface dislocation density. An analytical expression for entropy production due to fluctuations in surface dislocation density has been obtained.

It is also established that, for the crankshaft sliding bearing of the DZk-250 motor grader operating under elastoplastic contact conditions, the wear intensity follows a similar trend: it increases with growing surface dislocation density in the low-value range and decreases when this parameter reaches higher values. Furthermore, an equation describing entropy generation during the interaction between lubricant molecular dipoles and dipoles associated with dislocation density fluctuations has been formulated.

Key words: sliding bearing, entropy, dislocation, oil, contact, wear intensity

Introduction

It is known that friction is a dissipative process that causes destruction and structural changes in the layers of rubbing bodies. The study of these processes is complicated by the lack of information about the physical and chemical properties of the surface layers, which are directly exposed to high deformation rates, significant temperature gradients, and force effects, so creating an adequate model of friction and wear is a challenging task. Studying friction and wear processes for specific systems operating under varying mechanical and thermal conditions is even more difficult.

Let us consider a plain bearing installed in the engine of a motor grader DZk-250 as such a system.

Literature review

In [1], it is shown that the value of the wear intensity of a sliding bearing in elastic and elastoplastic contact is determined by the expression

$$I = C_1 \cdot \alpha_{\Gamma e} \cdot p_a \cdot \tau_0^{\frac{t'}{2}} \cdot \theta^{1-\frac{t'}{2}} \cdot \left(\frac{K' \cdot f}{\sigma_0'} \right), \quad (1)$$

where $C_1 = 0{,}1216^{\frac{2t'}{5}} 2{,}6^{\frac{5}{5}-t'}$ p_a – nominal pressure; τ_0 – shear resistance; $\theta = \frac{1-\mu^2}{E}$ – Kirchhoff elastic constant; μ – Poisson's ratio; K' – coefficient close to three; f – friction coefficient; t' – friction fatigue curve indicator; σ_0' – fatigue fracture stress; $\alpha_{\Gamma e}$ – hysteresis loss coefficient.

The latter value is determined by the ratio of energy loss (dissipation) per unit volume per cycle (period) ΔW_σ to the maximum elastic energy density of the system [2].

$$\alpha_\Gamma = \frac{\Delta W_\sigma}{2\pi W_0}. \quad (2)$$

During plastic deformation, energy dissipation is described by the dissipative function [2]

$$D = \sigma_{ij}^D e_{ij}, \quad (3)$$

where σ_{ij}^D – dissipative stress tensor; e_{ij} – plastic strain rate tensor.

It is evident that the integral value of the dissipative function over a period τ is equal to the energy loss over this period, i.e.

$$\Delta W_\sigma = \int_0^\tau D dt. \quad (4)$$

The value of the maximum elastic energy density is [3]

$$W_0 = \frac{\sigma_0 \cdot e_0}{2}, \quad (5)$$

where σ_0 – maximum stress; e_0 – maximum relative strain.

Then, according to expressions (2), (4) and (5)

$$\alpha_\Gamma = \frac{\int_0^\tau D dt}{\pi \cdot e_0 \cdot \sigma_0}. \quad (6)$$

Since the dissipative function D and entropy production p_s are related by the relation $D = p_s T$ (where T – тis the temperature), we obtain the expression of the hysteresis loss coefficient through entropy production:

$$\alpha_\Gamma = \frac{\int_0^\tau p_s \cdot T \cdot dt}{\pi \cdot e_0 \cdot \sigma_0}. \quad (7)$$

Purpose

The purpose of the study is to establish the relationship between the values that determine the entropy production in the surface layer of the crankshaft sliding bearing of the DZk-250 motor grader and its wear resistance.

Summary of the primary material

Let's consider the role of entropy production in the friction and wear processes of a sliding bearing.

As shown in [3], during the movement of dislocations, plastic deformations are created in the surface layer, which causes entropy production

$$p_{s1} = \frac{10 \cdot \gamma \cdot b^4 \cdot \sigma_\tau^2}{3 \cdot k \cdot T^2}, \tag{8}$$

where σ_τ – tangential stress; b – value of the Burgers vector; γ – surface density of dislocations; k – Boltzmann's constant.

According to [4], the second reason for entropy production in the friction layer is the attenuation of surface acoustic waves (Rayleigh waves) on the dislocations of the surface layer. As shown in [4], the Rayleigh wave flux density at a distance z from the surface is determined by the equation

$$J_{vz} = 2\pi \cdot \sigma_s \cdot \sigma_\tau \cdot u_R \cdot n_s \cdot \exp(-2\alpha \cdot z) \tag{9}$$

where α – absorption coefficient; U_R – Rayleigh wave velocity; σ_s – wave scattering cross-section; n_s – concentration of surface inhomogeneities.

In the resulting equation, the surface tangential stress σ_τ depends on the coordinate z, which corresponds to numerous experimental data summarised in [1] and can be represented as

$$\sigma_\tau = \sigma_{\tau 0} + \frac{d\sigma_\tau}{dz}\lambda_R \tag{10}$$

where $\sigma_{\tau 0}$ – is the tangential stress on the friction surface; λ_R – is the length of the Rayleigh wave, which is the interval of localisation of the wave field along the axis z.

Substituting (10) into (9) and taking into account that at large obstacles compared to the wavelength of the wave, the cross-section of the wave scattering σ_s is proportional to the fourth power of its frequency, we can represent (9) in the form

$$j_{Vz} = 2\pi\varsigma\omega^4 u_R n_s \sigma_{\tau 0}\lambda_R \left(\frac{1}{\lambda_R} + \frac{1}{\sigma_{\tau 0}}\frac{d\sigma_\tau}{dz}\right)\exp(-2\alpha z), \tag{11}$$

where ς – is the proportionality coefficient between σ_s and ω^4.

The expression shows that the energy flux density of a bulk wave arising during the scattering of surface Rayleigh waves is proportional to the gradient of the tangential stress value $\frac{d\sigma_\tau}{dz}$, with which it is natural to associate the thermodynamic force. Let us define the thermodynamic force corresponding to the volume wave flux density X_v, corresponding to the volume wave flux density, using the relation

$$X_{Vz} = \frac{1}{\sigma_{\tau 0}}\frac{d\sigma_\tau}{dz} \tag{12}$$

Then, taking into account that the entropy production is equal to the product of the flow density and the corresponding thermodynamic coordinate, we find the entropy production caused by the absorption of elastic waves by dislocations (taking into account the smallness of the second term in the brackets of Equation (11) compared to the first):

$$p_{s2} = 2\pi\varsigma\frac{\omega^4 u_R n_s}{T}\exp(-2\alpha z)\frac{d\sigma_\tau}{dz} \tag{13}$$

We will assume that the average value of entropy production in the wave field localization layer is close to its value at the point $z = \lambda_R / 2$, i.e.

$$\langle p_{s2}\rangle = 2\pi\varsigma\frac{\omega^4 u_R n_s}{T}\exp(-\alpha\lambda_R)\frac{d\sigma_\tau}{dz} \tag{14}$$

The absorption coefficient α in the latter equation is mainly due to dislocations and, according to the Granato-Lücke-Koehler dislocation string model [5], is

$$\alpha = \frac{d_0 \gamma \Delta_0 \eta^2}{2\pi C_\tau \left[\left(\frac{\omega_0^2 - \omega^2}{\omega} \right)^2 + d_0^2 \right]}. \tag{15}$$

where ω_0 – is the natural frequency of oscillations of the dislocation strings; Δ_0 – is a constant of the order of unity; d_0 – is the attenuation coefficient of the dislocation strings; G – is the shear modulus; C_τ – is the shear modulus; - is the propagation speed of transverse acoustic waves (transverse sound velocity); $\eta^2 \approx 2C_\tau^2$.

Substituting this expression into (14), taking into account the value of η^2, and the fact that the Rayleigh wave length $\lambda_R = \frac{2\pi u_R}{\omega}$ and velocity u_R are not much different from the longitudinal wave velocity, $C_t \left(u_R \approx 0{,}9 C_t \right)$, we obtain

$$\left\langle p_{s2} \right\rangle = 2\pi\varsigma \frac{\omega^4 u_R n_s}{T} \exp\left\{ -\frac{2 d_0 \gamma \Delta_0 C_\tau C_t}{\left[\left(\frac{\omega_0^2 - \omega^2}{\omega} \right) + d_0^2 \right] \omega} \right\} \frac{d\sigma_\tau}{dz} \tag{16}$$

Substituting expressions (8) and (16) for entropy production into equations (1) and (7) and taking into account that in the stationary mode, none of the values under the sign of the integral is time-dependent, and $\int_0^\tau dt = \frac{2\pi}{\omega}$, we obtain the following equation for the wear rate of a plain bearing under elastic contact:

$$I = \frac{2 C_1 p_\alpha \tau_0^{\frac{t'}{2}} \Theta^{1-\frac{t'}{2}}}{e_0 \sigma_0} \left(\frac{k' f}{\sigma'_0} \right)^{t'} \left[\frac{10 \gamma b^4 \sigma_\tau^2 C_t}{3kT\omega} + 2\pi\varsigma\omega^3 u_R n_s \exp\left\{ -\frac{2 d_0 \gamma \Delta_0 C_\tau C_t}{\left[\left(\frac{\omega_0^2 - \omega^2}{\omega} \right)^2 + d_0^2 \right] \omega} \right\} \frac{d\sigma_\tau}{dz} \right] \tag{17}$$

The equation shows that under conditions of elastoplastic contact, the wear rate of a sliding bearing increases with an increase in the surface density of dislocations γ at low values and decreases in the region of large values γ. It should be borne in mind that the first term in equation (17) is due to the movement of dislocations, which is possible at their low density, which is possible only at the initial stages of running-in, while the steady-state mode is characterized by higher values of γ and the consolidation of dislocations, and therefore this term in the equation turns to zero.

However, elastic deformation is not the only and by no means the dominant factor that determines the wear process in a plain bearing. According to [6] and [7], the intensity of wear depends to a large extent on the interaction of lubricant molecules with the friction surface. The molecular dipoles that make up such lubricants and are located in the sliding bearing gap are exposed to the electric field created by dislocation fluctuations and interact with the friction surface using electrostatic image forces.

$$\left\langle p_{s3} \right\rangle = \sqrt{\frac{2}{3}} K^{3/2} \frac{n_p p_0^{7/6}}{T^{2/3} \ell_0^{6/5} \sqrt{m_p}} \left[\frac{p_0 + 7{,}7 e L^2 \sqrt{\gamma(\xi - 1)}}{1 + \frac{n_p p_0^2}{3\varepsilon_0 kT}} \right]^{7/6} \tag{18}$$

Within the framework of the model of interaction of molecular dipoles with fluctuating dislocation moments, the physical mechanism of the anti-wear effect of lubricants and additives is the adsorption of lubricant molecules by the surface of the friction unit and blocking of dislocation nuclei by lubricant molecules, which leads to a decrease in the electric fields they create, at least to the quadrupole approximation and a reduction in the interaction between friction surfaces. Based on the analysis of the data presented in [6] and [7], the following expression can be obtained for the average value of entropy production caused by the interaction of molecular dipoles with dislocations in the volume of the friction surface layer:

Now let us determine the total entropy production in the surface friction layer containing the deformed

layer and the adsorbed layer by summing the terms p_{s1} ,$\langle p_{s2}\rangle$,$\langle p_{s3}\rangle$, defined by equations (8), (14), and (18), and taking into account the small weight of the term p_{s1} at large values of γ

$$p_s = 2\pi\varsigma\frac{\omega^4 u_R n_s}{T}\exp\left\{-\frac{2d_0\gamma\Delta_0 C_\tau C_t}{\left[\left(\frac{\omega_0^2-\omega^2}{\omega}\right)^2+d_0^2\right]}\right\}\frac{d\sigma_\tau}{dz}+\frac{n_p}{T^{2/3}\sqrt{m_p}}\left[\frac{p_0+7,7eL^2\sqrt{\gamma(\xi-1)}}{1+\frac{n_p p_0^2}{3\varepsilon_0 kT}}\right]^{7/6} \tag{19}$$

In [8], it was shown that entropy production p_s is related to the specific friction force σ_{fr} by the ratio

$$p_s = \frac{\sigma_{fr}u}{hT} \tag{20}$$

where u – relative speed of movement of the tribological surfaces; h – thickness of the surface friction layer.

Although there is no unambiguous relationship between the friction force and the wear rate, a correlation was established in [9], which, taking into account Equation (20), can be used to obtain the following equation for the wear rate:

$$I = n_s R_\delta\sqrt{\Delta A_\tau}\left[I+\left[\left[2\pi\varsigma\frac{\omega^4 C_1 n_s}{T}\exp\left\{-\frac{2d_0\gamma\Delta_0 C_\tau C_t}{\left[\left(\frac{\omega_0^2-\omega^2}{\omega}\right)^2+d_0^2\right]\omega}\right\}\frac{d\sigma_\tau}{dz}+\right.\right.\right.$$
$$\left.\left.\left.+\frac{n_p}{T^{2/3}\sqrt{m_p}}\left[\frac{7,7eL^2\sqrt{\gamma(\xi-1)}}{1+\frac{n_p p_0^2}{3\varepsilon kT}}\right]^{7/6}\right]\frac{2\pi h}{\langle\sigma_\tau\rangle\Lambda\omega}-\frac{\sigma_R}{\langle\sigma_\tau\rangle}\right], \tag{21}$$

where n_s – is the surface density of contact spots; R_δ – is the average profile deviation; ΔA_r – is the area of a single contact; σ_R – is the real tensile strength; $\langle\sigma_\tau\rangle$ – is the average value of tangential stresses; m_p – is the mass of the molecular dipole.

Let us analyze the results obtained. First of all, it should be noted that the conclusions drawn from the analysis of the above models are fully relevant to the operating conditions of sliding bearings, i.e., they relate to the transitional between hydrodynamic and boundary friction regimes, when the thickness of the lubricating layer is large enough to allow for the movement of molecular dipoles of the lubricant in it. As can be seen from Equation (21), the wear rate depends most strongly on the surface concentration of material inhomogeneities whose dimensions exceed the Rayleigh wavelength (they do not include dislocations whose line lengths are usually less than the wavelength), the area of contact spots, and the surface density of dislocations. The effect of the dislocation density on the wear rate is manifested in a decrease in the wear rate with increasing dislocation density, since the exponential decline is much greater than the increase according to the law of $\gamma^{7/12}$. A similar dependence is observed in the wear model described by equation (18). The physical reason for this increase is associated with crystal hardening and increasing dislocation density. The dependence of the wear intensity on the tangential stress gradient σ_τ corresponds to the gradient rule of I.V. Kragelsky [1], according to which the condition must be met in the tribunal $grad\ \ \sigma_\tau > 0$. This condition follows from equation (16), which is part of the structure of equation (21), as a consequence of the non-negative value of entropy production. Equation (21) implies a decrease in the wear intensity with an increase in the dipole moment of the lubricant molecules, which is inherently associated with blocking fluctuating dislocation dipoles by molecular dipoles.

Conclusions

1. Entropy production in friction contact is caused by the movement of dislocations (at their relatively small concentration of the order of $10^{14}-10^{15}\,м^{-2}$) and the attenuation of elastic waves on dislocations, the latter mechanism playing a more significant role in the steady-state friction regime. The non-negativity of entropy

production caused by the latter factor implies the necessity of a positive tangential stress gradient in the friction layer, which coincides with the well-known 'gradient rule' of I.V. Kragelsky.

2. Based on the analysis of the dependence of entropy production on material and tribotechnical parameters, it was found that the intensity of sliding bearing wear in elastic and elastic-plastic contact increases with the increase in the surface density of dislocations γ at low values (of the order of $10^{14} - 10^{15} м^{-2}$) and decreases with an increase γ in the region of large values of this value.

3. The equation for the entropy production in the process of interaction of molecular dipoles of the lubricant with dipoles caused by fluctuations in the surface density of dislocations is obtained. It is shown that the wear intensity caused by this component of entropy production decreases with an increase in the dipole moment of the lubricant molecules.

Further studies of the wear intensity of sliding bearings are advisable to determine other entropy production components that affect the friction and wear processes of crankshaft sliding bearings of a motor grader DZk-250.

References

1. Kragelsky I. V. Friction and Wear. Butterworths, London, 1965. DOI: 10.1016/C2013-0-07722-6

2. Chunliang Kuo, Jhihjie Liu, Mengkun Liu, Chiachun Chung Exploring electrical metrics for tribology measures in oil films: System design, analysis principle and physical effects. Tribology International. 2024. Volume 192. Pp. 112–115. https://doi.org/10.1016/j.triboint.2023.109233

3. Ventsel, Ye., Shchukin, O., Orel, O., Saienko, N. The equation of the entropy production in a tribounit. Problems of Tribology. 2020. Vol. 25, No. 2/96. Pp. 12–18. https://doi.org/10.31891/2079-1372-2020-96-2-12-18

4. Nosonovsky M., Bhushan B. Thermodynamics of surface degradation, self-organization and self-healing for friction, wear and lubrication. Philosophical Transactions of the Royal Society A, 2009, 367, 1607–1627. https://doi.org/10.1098/rsta.2008.0300

5. Shchukin, O. Technical Research and Development: Collective Monograph. International Science Group. Boston: Primedia eLaunch, 2021. 616 p. https://doi.org/10.46299/ISG.2021.MONO.TECH.I

6. Nosonovsky M. Entropy in tribology: In the search for wear law. Entropy, 2010, 12(6), 1345–1360. https://doi.org/10.3390/e12061345

7. Ventsel, Ye., Orel, O., Shchukin, O., Saienko, N., Kravets', A. Dependence of wear intensity on parameters of tribo units. Tribology in Industry. 2018. Vol. 40, No. 2. Pp. 195–202. https://doi.org/10.31891/2079-1372-2021-102-4

8. Granato A.V., Lücke K. Theory of mechanical damping due to dislocations. Journal of Applied Physics, 1956, Vol. 27, pp. 583–593. https://doi.org/10.1063/1.1722436

9. Bowden F. P., Tabor D. The Friction and Lubrication of Solids. Oxford University Press, 2001. https://doi.org/10.1093/oso/9780198507772.001.0001

Щукін О.В., Орел О.В., Холодов А.П., Кравець А.М., Федоряченко С.О. Взаємозв'язок між інтенсивністю зношування підшипника ковзання та матеріальними характеристиками поверхонь тертя у важконавантажених механізмах будівельних і дорожніх машин.

Запропоновано рівняння для опису процесу утворення ентропії під час взаємодії молекулярних диполів мастильного матеріалу з диполями, викликаними флуктуаціями поверхневої густини дислокацій. Встановлено, що збільшення дипольного моменту молекул мастила сприяє зниженню інтенсивності зношування, пов'язаної з цією складовою ентропійного виробництва.

Досліджено, що інтенсивність зношування підшипника ковзання колінчастого валу автогрейдера ДЗк-250 у режимі пружно-пластичного контакту залежить від поверхневої густини дислокацій: вона зростає за низьких значень густини та зменшується у разі її високих значень.

Ключові слова: підшипник ковзання, ентропія, дислокація, мастило, контакт, інтенсивність зношування

ISSN 2079-1372 Problems of Tribology, V. 31, No 1/119-2026, 48-55

Problems of Tribology
Website: http://tribology.khnu.km.ua/index.php/ProbTrib
E-mail: tribosenator@gmail.com

DOI: https://doi.org/10.31891/2079-1372-2026-119-1-48-55

Experimental and Analytical Study of Acid Number Variation in Engine Oils Under Operational Contamination

M.O. Dykha 0000-0002-6075-1549, **M.V. Hetman** 0000-0002-8835-7172, **V.O. Dytyniuk** 0000-0001-6377-524X, **O.M. Makovkin** 0000-0003-4487-7448

Khmelnytskyi national University, Ukraine
**E-mail: marrix117@gmail.com*

Received: 05 January 2026: Revised 20 January 2026: Accept: 02 February 2026

Abstract

This paper presents an experimental and analytical study of the variation of the total acid number (TAN) in engine oils under operational contamination. The research is aimed at assessing the correlation between the acidity growth of lubricants and their wear behavior in the four-ball test configuration. Theoretical modeling and experimental testing were performed to identify the parameters of a wear law that incorporates contact pressure, oil viscosity, hardness, and TAN as key variables. The obtained results confirm that the acid number increases significantly during oil operation: from 0.9 to 2.9 mg KOH/g—which leads to an intensified wear rate of the contact surfaces. The proposed model quantitatively describes the relationship between the acidity level and wear intensity and enables prediction of oil performance based on its physicochemical degradation. The developed approach allows for improved evaluation of the residual life of lubricants and optimization of maintenance intervals for internal combustion engines.

Keywords: engine oil degradation; total acid number (TAN); operational contamination; wear model; four-ball test; physicochemical properties; lubrication; tribology; predictive maintenance

Introduction

The efficiency of an internal combustion engine is largely determined by the stability of the physicochemical properties of the engine oil, which performs the functions of lubrication, cooling, cleaning, and protecting parts from corrosion. During operation, the oil is exposed to the combined effects of high temperature, pressure, combustion products, and mechanical impurities, leading to gradual degradation of its composition. One of the most informative indicators of lubricant condition is the acid number (TAN), which characterizes the amount of acidic compounds formed as a result of oxidation of the base oil and decomposition of additives. An increase in the acid number indicates the accumulation of organic and inorganic acids, which in turn enhances the corrosive activity of the medium and reduces the service life of friction components.

Research conducted for different types of engines confirms that the acid number of engine oils increases consistently with longer operating time or vehicle mileage. In the initial stages of operation, a relatively slow increase in acidity is observed due to the consumption of neutralizing additives and stabilization of the chemical composition. Subsequently, as oxidation processes intensify and contamination by combustion products grows, the rise in TAN becomes accelerated. Experimental studies show that in used oils, the acid number can increase by 170–280% compared with the fresh oil, as a result of the accumulation of resinous and oxygen-containing compounds. It has been established that the moment when the acid number reaches or exceeds the base number (TBN) is critical, indicating the depletion of the oil's alkaline reserve and the need for replacement. For gasoline engines, this typically corresponds to a mileage of about 10–13 thousand km, while for diesel engines: 14–16 thousand km.

Thus, the dynamics of acid number variation serve as a sensitive diagnostic parameter that reflects the degree of lubricant aging and contamination level. It enables timely assessment of the remaining service life of the oil, optimization of replacement intervals, and prevention of premature engine wear. The analysis of the influence of engine oil contamination on changes in acidity is therefore an important step toward improving the reliability

and durability of internal combustion engines, as well as developing efficient systems for monitoring their technical condition.

Literature Review

The variation of the total acid number (TAN) in engine oils during operation is a key factor in assessing their technical condition and predicting service life. A synthesis of modern studies indicates that the acid number is an integral indicator of oil degradation, reflecting the accumulation of organic and inorganic acids formed as a result of base oil oxidation, additive decomposition, and contamination by combustion products [1]. It has been established that with increasing temperature, operating time, and levels of fuel or soot contamination, the acid number rises consistently, leading to greater corrosive activity and reduced protective properties of the lubricating film [2].

Analytical and experimental investigations show that the dynamics of TAN changes are closely related to degradation processes such as oxidation, nitration, and the formation of varnishes and deposits [3,4]. At the early stages of oil operation, the TAN increase is minor due to the effective action of neutralizing additives; however, after the depletion of the alkaline reserve, a sharp rise in acidity is observed. This point is considered critical for deciding when to replace the oil [5].

The change in the acid number is accompanied by a decrease in the base number (TBN) and variations in viscosity, which allows these parameters to be used together for comprehensive assessment of oil condition [6]. Practical studies demonstrate that as engine mileage increases, TAN steadily grows, particularly under urban driving conditions characterized by frequent start–stop cycles that accelerate oxidation [7]. Analysis of used oil samples also revealed that in different viscosity grades, the rate of TAN increase may vary significantly, reflecting the distinct resistance of oils to thermal and oxidative aging [2, 5].

Recent research increasingly treats TAN as a fundamental parameter for real-time oil condition monitoring systems. The use of electrochemical and dielectric sensors enables continuous tracking of acidity changes during engine operation, forming the basis for adaptive maintenance strategies [8]. In addition, statistical and intelligent models are being developed to predict oil degradation by integrating TAN data with oxidation parameters, viscosity, wear-metal content, and temperature profiles [9].

Special attention has also been given to identifying the chemical nature of the acidic components formed during oil aging. It has been shown that the main degradation products are organic acids—predominantly carboxylic and phenolic—which catalyze further oxidation and sludge formation [8]. These compounds deteriorate antifriction properties and increase temperatures in friction zones, thereby accelerating wear.

In summary, the reviewed studies [1–10] confirm that the acid number is one of the most sensitive diagnostic indicators of engine oil condition. Its growth with increasing operating time signifies the intensification of oxidation processes, depletion of the alkaline reserve, and loss of lubricant stability. Monitoring TAN dynamics, in combination with other physicochemical properties, makes it possible not only to determine the remaining oil life but also to optimize replacement intervals—directly enhancing the reliability and durability of internal combustion engines.

Geometric parameters of the four-ball test scheme

The structural scheme consists of four identical balls of radius R. Three lower balls 1-3 are motionlessly located on the plane and touch each other according to the scheme in Fig. 1.

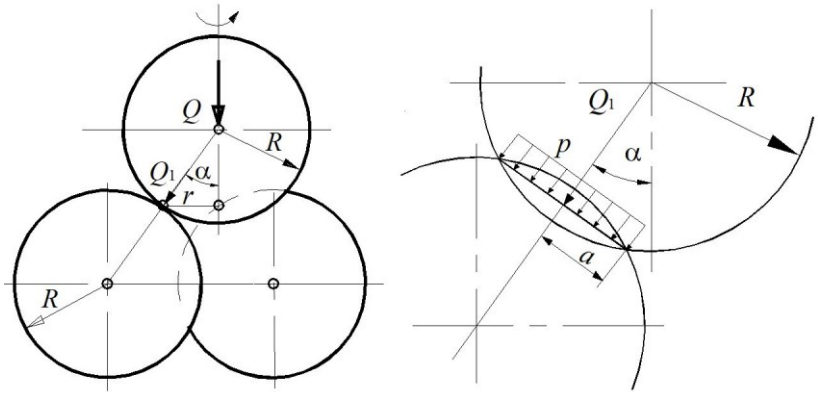

Fig.1. The geometry of the four-ball test scheme.

The upper ball 4 rotates and is pressed in the center to the lower balls with a force Q. In the process of friction of the upper ball on the lower ones, wear areas of a circular shape are formed on them. To determine the normal component of the force Q1 on the lower balls, it is necessary to determine the angle α:

$$Q_1 = \frac{Q}{3\cos\alpha}. \tag{1}$$

From the geometry of the contact (Fig. 1), the angle α is determined:

$$\alpha = \arcsin\frac{r}{R} = \frac{R/\sqrt{3}}{R} = \frac{1}{\sqrt{3}} = 35.26^{\circ}. \tag{2}$$

Taking into account (2), we obtain an expression for the normal force on the lower balls:

$$Q_1 = 0.4082Q. \tag{3}$$

Friction path for the friction pads of the lower balls:

$$L = 2\pi rnt = \frac{2\sqrt{3}}{3}\pi Rnt, \tag{4}$$

where n is the number of revolutions of the upper ball per unit of time; t is the test duration.

Wear model.

Traditionally, the wear model (law) is understood as the functional dependence of the wear rate (intensity) on the determining factors of the wear process: contact pressure, properties of structural and lubricant materials, sliding speed, temperature and other factors in the form:

$$\frac{dW}{dL} = F(p, HB, \mu, \nu, \alpha...).$$

The number of determining factors and their form of presentation depend on the physical formulation of the wear problem with respect to the design of the friction pair and the conditions of testing and operation in practice. It is convenient to represent the level of influence of determining factors on wear in the form of power dependences. In this case, the values of the parameters determine both the quantitative and qualitative effect on wear. For practical calculations based on the wear model, it is rational to represent the determining factors in the form of dimensionless complexes. In our case, to predict the wear of non-conformal joints in the presence of a lubricant and tests using a four-ball scheme, the following form of the wear model (law) is proposed:

$$\frac{dW}{dL} = k_W\left(\frac{\mu p}{HB}\right)^m\left(\frac{\alpha}{\nu}TAN\right)^n, \tag{5}$$

where dW/dL is the were rate;
k_W is the were coefficient;
μ is the friction coefficient;
p is the contact pressure, N/mm^2;
HB is brinell hardness, N/mm^2;
α is the oil temperature conductivity coefficient, m^2/s;
ν is the kinematic oil viscosity, m^2/s;
TAN is the total acidity number, *mg KOH/g*;
m, n are the parametres.

The model is proposed in the form of two dimensionless complexes that determine the influence of contact pressures, properties of structural and lubricant materials. The principle of similarity and dimensions was used as the basis for constructing the model.

The geometric relationship between normal wear and the half-width of the circular area a will be written in the form (Fig. 1):

$$W(L) = \frac{a^2(L)}{2R}. \tag{6}$$

Let us assume that the pressure is uniformly distributed over the contact area. Then the contact pressure through the load and the contact area is determined by the formula:

$$p = \frac{Q_1}{\pi a^2(L)}. \tag{7}$$

Based on the results of wear tests, an approximating power function of the size of the wear area a from the friction path L is determined in the form:

$$a(L) = cL^{\beta}, \tag{8}$$

where c, β are the parameters of the approximating function.

After substituting (3, 6-8) into the wear model (5), we get:

$$\frac{d(\frac{(cL^{\beta})^2}{2R})}{dL} = k_W \left(\frac{0.4082Q\mu}{\pi(cL^{\beta})^2 HB}\right)^m \left(\frac{\alpha}{\nu}TAN\right)^n, \tag{9}$$

After integrating and transforming equation (9), we have:

$$c^2 L^{2\beta} = 2RK_W \left(\frac{0.4082Q\mu}{c^2\pi HB}\right)^m \left(\frac{\alpha}{\nu}TAN\right)^n \frac{L^{1-2\beta m}}{1-2\beta m}. \tag{10}$$

From the condition of satisfaction of equation (10) for any L it follows:

$$m = \frac{1-2\beta}{2\beta}. \tag{11}$$

To determine the parameter n, a series of tests is carried out at different values of the acidity number. In this case, the corresponding approximating functions of the type (8) are obtained.

Here, the tasks of determining the wear parameters based on the test results of samples with a variable contact area are considered. The exponent m in expression (5) characterizes the rate of change in contact pressures during wear and is related to the exponent β of the experimental function according to (11). The acid number of the oil does not depend on the size of the wear area and therefore does not affect the parameters m and β. The acid number will only affect the dimensional coefficient c, which is confirmed experimentally.

Let two approximating functions be obtained from the test results at two values of the acid number:

$$a = c_1 L^{\beta}, a = c_2 L^{\beta}. \tag{12}$$

Thus, we get a system of two equations:

$$\left.\begin{aligned} \beta c_1^{\,2m+2} &= RK_W \left(\frac{0.4082Q\mu}{\pi HB}\right)^m \left(\frac{\alpha}{\nu}(TAN)_1\right)^n \\ \beta c_2^{\,2m+2} &= RK_W \left(\frac{0.4082Q\mu}{\pi HB}\right)^m \left(\frac{\alpha}{\nu}(TAN)_2\right)^n \end{aligned}\right\}. \tag{13}$$

Dividing the first equation by the second after taking the logarithm and transformations, we obtain the formula for the parameter n:

$$n = (2m+2)\frac{\ln(c_1/c_2)}{\ln\left[(TAN)_1/(TAN)_2\right]}. \tag{14}$$

The coefficient K_W is determined from one of the equations of system (13):

$$K_W = \frac{\beta c_1^{\,2m+2}}{R}\left(\frac{\pi HB}{0.4082Q\mu}\right)^m \left(\frac{\nu}{\alpha(TAN)_1}\right)^n. \tag{15}$$

An example of identifying the parameters of the wear model (5).

The results of wear tests with a lubricant according to the four-ball scheme are shown in Table 1. The friction path was calculated using the formula (4) at n=1420 rpm.

Table 1

Wear test results

Test oil	TAN, mg KOH/g	Load, N	Test duration, h	WSD/2 (a), mm	L, mm·10^6
New oil 10W40 Test 1	0.91	150	60	0.140	3.919
			180	0.165	11.758
		300	60	0.220	3.919
			180	0.260	11.758
After 5000 km Test 2	1.7	150	60	0.150	3.919
			180	0.170	11.758
		300	60	0.320	3.919
			180	0.440	11.758
After 10000 km Test 2	2.9	150	60	0.190	3.919
			180	0.335	11.758
		300	60	0.425	3.919
			180	0.680	11.758

Shown below are approximations (Excel) of the dependence of the wear area on the friction path at different loads and values of the acid number of the lubricant.

Test 1

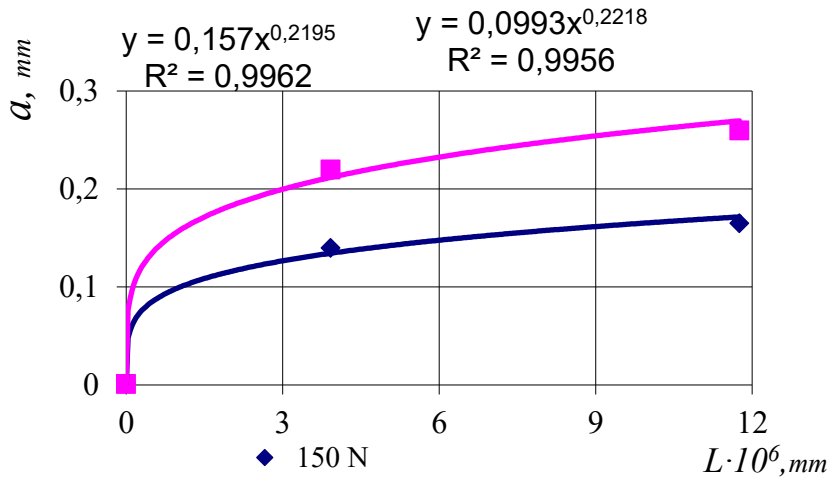

Test 2

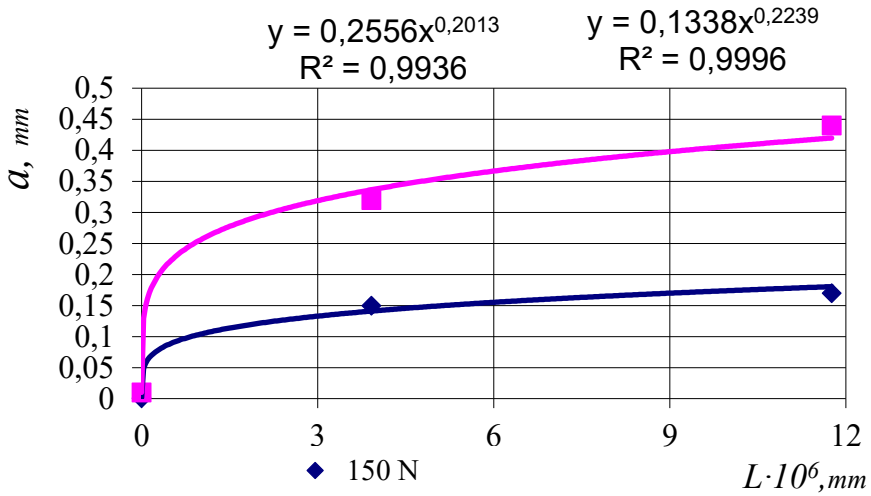

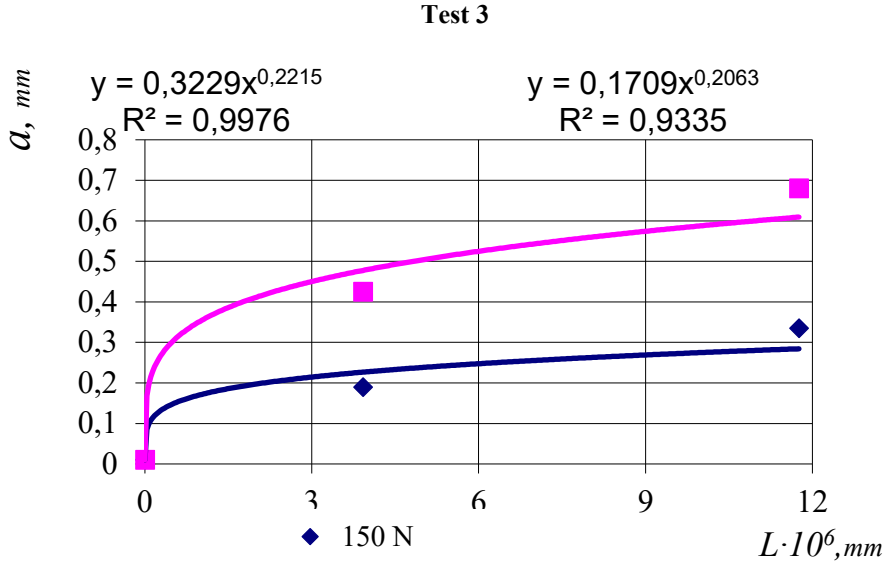

Fig. 2. Determination of the parameters of the approximation function $a(L) = cL^{\beta}$

The parameters of the approximation function (4) are summarized in Table 2.

Table 2

Approximation function parameters (4)

Load		Q=150 N	Q=300 N
Test 1	c	0.0953	0.157
	β	0.2218	0.2195
Test 2	c	0.1338	0.2556
	β	0.2013	0.2239
Test 3	c	0.1709	0.3229
	β	0.2063	0.2215

As expected, the values of the β parameter for a given lubricant are approximately the same. In accordance with the data in Table 2, we take the average value of the β parameter equal to 0.2157.

Then, according to formula (11), the parameter m=1.32. The determination of the parameter n was carried out for tests 2 and 3 according to the formula (14):

$$n(150N) = (2\cdot 1.32 + 2)\frac{\ln(0.1338/0.1709)}{\ln(1.7/2.9)} = 2.1;$$

$$n(300N) = (2\cdot 1.32 + 2)\frac{\ln(0.2556/0.3229)}{\ln(1.7/2.9)} = 2.05.$$

Accepted n=2.075. The coefficient K_W was determined by the formula (15) for the following test parameters: HB=200 MPa, μ=0.05, ν=13.6 N/mm^2, α=6.9 N/mm^2, TAN=1.7 mg KOH/g, R=12.7 mm.

$$K_W = \frac{0.2157\cdot 0.1338^{2\cdot 1.32+2}}{12.7}\left(\frac{\pi\cdot 200}{0.4082\cdot 150\cdot 0.05}\right)^{1.32}\left(\frac{13.6}{6.9\cdot 1.7}\right)^{2.075} = 2.3\cdot 10^{-3}.$$

Thus, the law of wear (5) after identifying the parameters takes the form:

$$\frac{dW}{dL} = 2.3\cdot 10^{-3}\left(\frac{\mu p}{HB}\right)^{1.32}\left(\frac{\alpha}{\nu}TAN\right)^{2.075}.$$

The dimensionless complex for the wear rate allows one to quantitatively take into account the effect of contact pressures, mechanical and frictional properties of materials, and lubrication parameters on wear. This

model makes it possible to predict the wear resistance of lubricated friction units of the type: gear drives, rolling bearings, cam mechanisms and others.

Conclusions

1. The study confirms that the total acid number (TAN) of engine oils increases progressively with operating time and contamination, reflecting the accumulation of oxidation and degradation products.
2. The proposed mathematical wear model, which integrates TAN as a parameter along with contact pressure, viscosity, hardness, and friction coefficient, accurately describes the wear behavior of lubricated contacts.
3. Experimental results demonstrate that with an increase of TAN from 0.9 to 2.9 mg KOH/g, the wear scar diameter and wear rate rise proportionally, indicating the strong influence of acidification on surface damage.
4. The model parameters identified from the four-ball test ($m = 1.32$, $n = 2.075$) characterize the dependence of wear on contact pressure and acidity, providing a reliable basis for quantitative wear prediction.
5. The inclusion of TAN in the wear equation allows the use of acidity as a diagnostic indicator for lubricant condition and residual life assessment.
6. The obtained results can be applied to optimize oil change intervals, reduce maintenance costs, and enhance the reliability and durability of friction units in internal combustion engines.

References

1. De Rivas, B. L., Vivancos, J. L., Ordieres-Meré, J., & Capuz-Rizo, S. F. (2017). Determination of the total acid number (TAN) of used motor oils by IR and chemometrics applying a combined strategy for variable selection. Chemometrics and Intelligent Laboratory Systems, 160, 32–39. https://doi.org/10.1016/j.chemolab.2016.02.008
2. Wolak, A. (2018). Changes in lubricant properties of used synthetic oils based on the total acid number. Measurement and Control, 51(3–4), 65–72. https://doi.org/10.1177/0020294018770916
3. Wei, L., Duan, H., Jin, Y., & Li, J. (2021). Motor oil degradation during urban cycle road tests. Friction, 9(5), 1002–1011. https://doi.org/10.1007/s40544-020-0386-z
4. Shinde, H. M., & Bewoor, A. K. (2020). Evaluating petrol engine oil deterioration through oxidation and nitration parameters by low-cost IR sensor. Applied Petrochemical Research, 10(1), 83–94. https://doi.org/10.1007/s13203-020-00248-6
5. Tomita, M. (1995). Study on deterioration of engine oil and its sensing. Wear, 186–187, 286–293. https://doi.org/10.1016/0389-4304(95)00019-4
6. Ramírez Camba, R., García García, C., García Tobar, M., & Fajardo Merchán, J. (2025). An integrated methodological approach for interpreting used oil analysis in diesel engines. Lubricants, 13(4), 169. https://doi.org/10.3390/lubricants13040169
7. Wakiru, J. M., Pintelon, L., Muchiri, P. N., & Chemweno, P. (2019). A review on lubricant condition monitoring information analysis for maintenance decision support. Mechanical Systems and Signal Processing, 118, 108–132. https://doi.org/10.1016/j.ymssp.2018.06.050
8. Harvath, P. V., & Walzer, M. (2016). Identification of organic acids in used engine oil residues. SAE Technical Paper. https://doi.org/10.4271/2016-01-2274
9. Bastiampillai, N. (2023). Statistical analysis and modelling of engine oil degradation. DIVA-Portal Dissertation, 1–150. https://doi.org/10.1017/CBO9781107415324.004
10. Gołębiowski, W., Zając, G., & Wolak, A. (2018). Definition of oil change intervals based on the analysis of selected physicochemical properties of used engine oils. Combustion Engines, 172(1), 44–50. https://doi.org/10.19206/CE-2018-105

Диха М.О., Гетьман М.В., Дитинюк В.О., Маковкін О.М. Експериментальне та аналітичне дослідження зміни кислотного числа моторних олив за умов експлуатаційного забруднення

У цій статті представлено експериментальне та аналітичне дослідження зміни загального кислотного числа (ЗКЧ) моторних олив за умов експлуатаційного забруднення. Метою дослідження є оцінка кореляції між зростанням кислотності мастильних матеріалів та їхньою поведінкою при зносі в конфігурації чотирикулькового випробування. Було проведено теоретичне моделювання та експериментальні випробування для визначення параметрів закону зносу, який включає контактний тиск, в'язкість оливи, твердість та ЗКЧ як ключові змінні. Отримані результати підтверджують, що кислотне число значно зростає під час експлуатації оливи: від 0,9 до 2,9 мг KOH/г, що призводить до посиленої швидкості зносу контактних поверхонь. Запропонована модель кількісно описує зв'язок між рівнем кислотності та інтенсивністю зносу та дозволяє прогнозувати характеристики оливи на основі її фізико-хімічної деградації. Розроблений підхід дозволяє покращити оцінку залишкового ресурсу мастильних матеріалів та оптимізувати інтервали технічного обслуговування двигунів внутрішнього згоряння.

Ключові слова: деградація моторної оливи; загальне кислотне число; експлуатаційне забруднення; модель зносу; чотирикульковий прилад; фізико-хімічні властивості; змащування; трибологія; прогнозне обслуговуванн

ISSN 2079-1372 ***Problems of Tribology****, V. 31, No 1/119-2026, 56-61*

Problems of Tribology
Website: http://tribology.khnu.km.ua/index.php/ProbTrib
E-mail: tribosenator@gmail.com

DOI: https://doi.org/10.31891/2079-1372-2026-119-1-56-61

Investigation of the effect of tribological loading parameters on the linea wear rate of a polytetrafluoroethylene-based composite reinforced with polyimide fiber

Ye.A. Yeriomina[1] 0000-0001-8595-5735, **K.R. Voloshina**[1] 0009-0007-8929-2191, **Predrag Dašić**[2] 0000-0002-9242-274X

[1]*Dniprovsk State Technical University, Kamyanske, Ukraine*
[2]*Academy of Professional Studies Šumadija – Department in Trstenik, Trstenik, Serbia*
E-mail: voloshina.k25.06@gmail.com

Received: 15 January 2026: Revised 05 February 2026: Accept: 20 February 2026

Abstract

The article presents the results of a comprehensive experimental and theoretical study of the tribotechnical characteristics of a composite material based on polytetrafluoroethylene reinforced with polyimide fiber. The main objective of the study was to determine the quantitative regularities governing changes in the intensity of linear wear as a function of external tribological loading parameters, as well as to establish optimal operating modes for the material. A mathematical modeling approach based on a full factorial design was employed to plan and conduct the experiments. During the study, the effects of sliding velocity and normal load on the linear wear intensity of the composite were analyzed. The experimental results enabled the derivation of a first-order regression equation describing the dependence of wear on the variable parameters. Statistical analysis of the model included an assessment of its adequacy and the significance of the regression coefficients. By constructing response surfaces, zones of minimum wear intensity were identified, and optimal operating conditions for the material under dry friction were determined. The study confirms the significant influence of both individual factors and their interaction on the wear resistance of the composite material. It was established that deviations of tribological loading parameters from their optimal values lead to a substantial increase in linear wear intensity. The combined use of statistical analysis methods and tribological testing allowed for a deeper evaluation of the material behavior and a significant reduction in the scope of experimental work through the development of a mathematical model. The proposed approach can be effectively applied to optimize the operating modes of composite materials based on polytetrafluoroethylene and polyimide fiber in friction units of machines and mechanisms operating under high loads and requiring enhanced wear resistance.

Keywords: polytetrafluoroethylene, polyimide fiber, composite material, tribological properties, experimental design, linear wear intensity, regression model

Introduction

Increasing the wear resistance of friction units is one of the key challenges of modern industry, especially under operating conditions involving high sliding speeds, significant mechanical loads, and limited lubrication. Under such conditions, traditional structural materials often rapidly lose their functional performance, which has led to increased interest in polymer composite materials [1]. These materials are capable of providing stable tribotechnical characteristics under severe operating conditions. Composites based on polytetrafluoroethylene (PTFE) are considered among the most promising representatives of this class of materials. PTFE exhibits a low coefficient of friction and high physicochemical stability; however, in its pure form it is characterized by insufficient wear resistance. The tribotechnical properties of PTFE can be improved by introducing fibrous fillers. Among them, polyimide (PI) fibers are particularly promising due to their high thermal stability, mechanical strength, and chemical inertness. Previous studies of PTFE–PI composite materials have shown that the optimal filler content is 7.5 vol.% of PI fibers [2]. At this filler concentration, the highest level of structural uniformity and wear resistance is achieved. Tribological tests conducted on this composite confirmed the dependence of linear

wear intensity on sliding velocity and applied load. An increase in these parameters intensifies thermomechanical processes in the contact zone, which leads to a reduction in wear resistance. Considering the need to obtain accurate experimental data while minimizing experimental costs, the application of mathematical methods for experimental design is of particular importance. Methods of experimental design are among the most effective tools for identifying regularities in complex multifactorial processes [3]. They significantly reduce the number of experiments required compared to direct empirical approaches while ensuring high accuracy of the obtained results.

The purpose of the work

Determining the quantitative relationships governing the linear wear of a polytetrafluoroethylene–polyimide composite under varying tribological loading conditions and to identify its optimal operating modes.

Objects and methods of research

To optimize the developed polymer composite material with an effective filler content of 7.5 vol.%, linear wear intensity was selected as the key performance parameter. The description of the investigated process was carried out in accordance with established mathematical relationships:

$$y(I_h) = f(x_1, x_2).$$

In this case, the sliding velocity (x_1) and the applied load (x_2) were selected as independent factors. To simplify the calculation procedure, the values of the independent factors were normalized to a dimensionless scale with corresponding levels of −1, 0, and +1. For this purpose, the following normalization formula was used, which allowed the experimental data to be converted into a standard form for further analysis:

$$x_i = \frac{X_i - X_{i0}}{n},$$

where x_i is the coded value of the factor, X_i and X_{i0} are the upper and central levels of factor variation, respectively and n is the step of factor variation (Table 1) [4]. The calculated values of the initial levels of the studied factors are presented in Table 1.

Table 1

Independent factors and their variation levels

Factor	Symbol	Designation	Variation step (n)	Variation levels		
				-1	0	+1
Slip speed	v, m/s	x_1	0.25	1.5	1.75	2
Load	P, MPa	x_2	0.5	1	1.5	2

According to the mathematical experimental design (Table 2), four experiments (N) were carried out, each of which was repeated twice ($k = 2$) in a random order in order to completely eliminate systematic errors.

Table 2

Planning matrix with calculated interaction columns of factors

Experiment No.	Values of variables on a coded scale				Values of variables on a natural scale	
	x_0	x_1	x_2	x_1x_2	v, m/s	P, MPa
1	+1	+1	+1	+1	2	2
2	+1	-1	+1	-1	1.5	2
3	+1	+1	-1	-1	2	1
4	+1	-1	-1	+1	1.5	1

Mathematical modeling of the dependence of the linear wear intensity of the PTFE–PI composite on the selected variable factors was proposed to be carried out in the form of a regression equation represented by a first-order polynomial:

$$y = b_0 + b_1x_1 + b_2x_2 + b_{12}x_{12},$$

where y is the calculated value of the optimization parameter; b_i and b_{ij} are the regression coefficients in the equation. Based on the experimental data presented in Table 3, the average values of the response functions were determined:

$$\widetilde{y_j} = \frac{1}{k}\sum_{i=1}^{k} y_{ji}, \qquad j = 1,2,\dots,N. \tag{1}$$

Table 3 presents both the experimental values (y_j) and the averaged results (y_j^C) obtained in the study of the influence of sliding speed and applied load on the linear wear intensity of the developed composite material.

Table 3

Experimental and Calculated Values of Linear Wear Intensity

Experiment No.	y_1	y_2	Average Value	Calculated Value
			$\widetilde{y_j}$	y_j^C
1	$3.66\cdot10^{-8}$	$3.56\cdot10^{-8}$	$3.61\cdot10^{-8}$	$3.31\cdot10^{-8}$
2	$4.4\cdot10^{-8}$	$1.61\cdot10^{-8}$	$3.01\cdot10^{-8}$	$3.31\cdot10^{-8}$
3	$1.71\cdot10^{-8}$	$0.84\cdot10^{-8}$	$1.27\cdot10^{-8}$	$1.21\cdot10^{-8}$
4	$0.87\cdot10^{-8}$	$1.43\cdot10^{-8}$	$1.15\cdot10^{-8}$	$1.21\cdot10^{-8}$

The reproducibility variance was calculated according to formula (2), and the variance of parallel measurements was calculated according to formula (3):

$$S_y^2 = \frac{1}{N}\sum_{j=1}^{N} S_j^2, \tag{2}$$

$$S_j^2 = \frac{\sum_{j=1}^{N}(y_i - \widetilde{y_j})}{k-1}. \tag{3}$$

The homogeneity of the variances obtained in parallel experiments was evaluated using Cochran's test:

$$G = \frac{max S_j^2}{\sum_{i=1}^{k} S_j^2}. \tag{4}$$

The calculated and tabulated values of the criterion were compared for degrees of freedom $f_1 = k - 1 = 1$ and N=4 at a confidence probability of P=0.95. The calculated value of Cochran's test was G_C = 0.881 which is lower than the tabulated value G_{table} = 0.91. Therefore, the obtained variances can be considered homogeneous. The coefficients of the regression equation have the same error, which is determined using the following formula:

$$S_{bi} = \frac{S_y}{\sqrt{N\cdot k}}. \tag{5}$$

Based on the analytical expressions obtained in the course of a full factorial experiment, the coefficients of the regression equation were calculated:

$$b_0 = \sum_{i=1}^{N} \frac{\widetilde{y_j} x_0}{N}, \tag{6}$$

$$b_i = \sum_{i=1}^{N} \frac{\widetilde{y_j} x_i}{N}, \tag{7}$$

$$b_{ij} = \sum_{i=1}^{N} \frac{\widetilde{y_j} x_{ij}}{N}. \tag{8}$$

Based on the calculations performed according to formulas (1)–(7), a first-order regression equation was obtained, describing the dependence of the response function on the experimental factors:

$$y(I_h) = 2.26 \cdot 10^{-8} + 0.18 \cdot 10^{-8} x_1 + 1.05 \cdot 10^{-8} x_2 + 0.12 \cdot 10^{-8} x_{12}.$$

The statistical significance of the regression coefficients b_0, b_1, b_2, b_{12}, was estimated by calculating confidence intervals. These intervals take into account the variance arising from errors in the determination of the coefficients. Confidence intervals were calculated using Student's t-test, considering the specified degrees of freedom (f_1, f_2) and a confidence probability of 0.95. The formula for calculating the confidence interval is as follows:

$$|b_{cr}| = t_{cr} \cdot S_{bi}. \tag{9}$$

The critical value of Student's t-criterion (t_{cr}) was determined based on the degrees of freedom $N(k-1)=4$ and the chosen significance level of 0.95. A regression coefficient was considered statistically significant if the inequality $t<t_{cr}$ was satisfied. After testing the statistical significance of the coefficients using Student's t-test according to formula (9), it was found that two of the obtained coefficients could be neglected. As a result, the structure of the regression equation was modified, and it was established that, within the studied range of sliding speeds, the applied load has the greatest influence on the linear wear intensity:

$$y(I_h) = 2.26 \cdot 10^{-8} + 1.05 \cdot 10^{-8} x_2. \tag{10}$$

The adequacy of the obtained regression equation was verified by comparing the theoretical values of the optimization parameter, calculated according to equation (10), with the corresponding experimental results for each performed experiment. This allowed the variance of the equation's adequacy to be calculated using the following formula:

$$S_{ad}^2 = \frac{1}{N-B} \sum_{j=1}^{N} (\widetilde{y_j} - y_j^C)^2. \tag{11}$$

In this case, B represents the number of statistically significant coefficients in the regression equation. Accordingly, the degrees of freedom for assessing the adequacy of the model were determined using the formula $f_{ad} = N - B = 2$. The calculated values of the optimization parameter are presented in Table 4.

Table 4

Calculated Data for Assessing the Adequacy of the Mathematical Model Using the Fisher Criterion

S_y^2	Regression Coefficients				S_{ad}^2
	b_0	b_1	b_2	b_{12}	
$1.1 \cdot 10^{-16}$	$2.26 \cdot 10^{-8}$	$0.18 \cdot 10^{-8}$	$1.05 \cdot 10^{-8}$	$0.12 \cdot 10^{-8}$	$0.09 \cdot 10^{-16}$

To assess how well the mathematical model (10) represents the actual relationship between the input and output parameters, Fisher's test [5] was used. This criterion is defined as the ratio of the adequacy variance to the reproducibility variance (see Table 4) and is calculated using the following formula:

$$F_C = \frac{S_{ad}^2}{S_y^2}. \tag{12}$$

At a confidence probability of 0.95 and degrees of freedom $f_1 = 4$ and $f_2 = 4$ the calculated value of Fisher's test, $F_C = 0.081$ was found to be lower than the tabulated value. This indicates that the constructed mathematical model is adequate for describing the studied process [6]. The relationship between the coded and natural values of the factor affecting the optimization parameters is described by the following equation:

$$x_2 = \frac{P-1.5}{0.5}. \tag{13}$$

Results analysis and discussion

Based on a properly selected regression equation, the response surface of the linear wear intensity of the PTFE–PI composite was modeled as a function of slip rate and applied load (Fig. 1). The response surface analysis results show that the minimum wear intensity is achieved at lower applied loads across the entire range of slip rates studied [7]. As the load increases, a noticeable rise in linear wear intensity is observed, confirming the findings of the regression analysis.

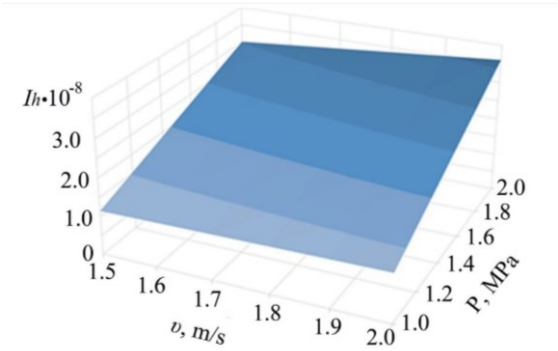

Fig. 1. Response surface of the linear wear intensity of the PTFE–PI composite as a function of slip rate and applied load

The transition from coded variables (x_1, x_2) to natural variables (υ, P) made it possible to develop a mathematical model describing the dependence of linear wear intensity on the applied load.

$$y(I_h) = 0.89 \cdot 10^{-8} + 2.1 \cdot 10^{-8} P. \quad (14)$$

Conclusions

The results of a comprehensive experimental and theoretical study of the tribotechnical characteristics of a polytetrafluoroethylene-based composite reinforced with 7.5 vol.% polyimide fibers showed that:

1. It was established that within the studied speed range, the linear wear intensity of the composite significantly depends on the applied normal load. As the load increases, the wear intensity increases, which is attributed to elevated contact stresses and the activation of thermomechanical processes in the friction zone.
2. Based on a full factorial experiment, a first-order regression model was developed to describe the dependence of linear wear intensity on the key influencing factors. The results of the statistical analysis showed that the applied normal load is the dominant factor, whereas the effects of slip rate and factor interactions within the investigated range are statistically insignificant.
3. The validity of the developed mathematical model was verified using Cochran's test for homogeneity of variances and Fisher's test to assess model adequacy. The results confirmed its reliability and consistency with the actual wear behaviour of the composite material under dry friction conditions.
4. The developed model made it possible to identify the regions in which the linear wear intensity is minimal, as well as to determine the optimal operating conditions of the composite. These conditions correspond to relatively lower levels of applied load within the investigated range.

Thus, the application of experimental design methods in combination with tribological testing significantly reduced the scope of experimental studies and enabled the derivation of accurate quantitative relationships describing the wear process. The proposed high-efficiency approach can be used to optimize the operating conditions of PTFE-based composite materials reinforced with polyimide fibers in friction units of machines and mechanisms operating under elevated loads and dry friction conditions.

References

1. Chang B. P., Md Akil H., Nasir R., Khan A. Optimization on wear performance of UHMWPE composites using response surface methodology. Tribology International. 2015. Vol. 88, P.158–167. https://doi.org/10.1016/j.triboint.2015.03.028

2. Tomina A.-M., Voloshina, K., Dašić, P., & Hranitskyi, Y. E. The effect of polyimide fibre on the tribological properties of polytetrafluoroethylene. Problems of Tribology. 2025. Vol. 30, No 3/117, P. 69–75. https://doi.org/10.31891/2079-1372-2025-117-3-69-75

3. Voitov A. V. Modeling the processes of friction and wear under dynamic influences on the tribosystem. Problems of Tribology. 2020. No 3/97(25). P. 45–49. https://doi.org/10.31891/2079-1372-2020-97-3-45-49

4. Yeromenko O., Yeriomina Y., Tomina A.-M., Dašić P. Optimization of the Processes of Operation of Basalt Plastic Friction Unit. Lecture Notes in Networks and Systems. 2024. Vol. 926 LNNS. P. 118–128. https://doi.org/10.1007/978-3-031-54664-8_12

5. Naberezhna O. O., Yeriomina K. A. Optimization of technological parameters of organoplastic pressing using experimental design. Metinvest Polytechnic Scientific Journal. Series: Technical Sciences. 2025. No 4, P. 167–173

6. Rula I. V., Dyachenko N. K. Study of the influence of molding regimes of carbon fiber products using mathematical planning. Interuniversity Collection «Scientific Notes». 2022. № 74. https://doi.org/10.36910/775.24153966.2022.74.21

7. Sagar P., Handa A. Prediction of wear resistance model for magnesium metal composite by response surface methodology using central composite design. World Journal of Engineering. 2021. №2(18). P. 316–327. https://doi.org/10.1108/WJE-08-2020-0379

Єрьоміна К.А., Волошина К.Р., Predrag Dašić Дослідження впливу трибологічних параметрів навантаження на лінійну інтенсивність зношування композиційного матеріалу на основі політетрафторетилену, армованого поліімідним волокном

У роботі наведено результати комплексного експериментально-теоретичного дослідження триботехнічних характеристик композиційного матеріалу на основі політетрафторетилену, армованого поліімідним волокном. Метою дослідження було визначення кількісних закономірностей зміни інтенсивності лінійного зношування як функції параметрів зовнішнього трибологічного навантаження та встановлення оптимальних режимів роботи матеріалу. Для планування та проведення експериментів застосовувався підхід математичного моделювання на основі повного факторного експерименту. Проаналізовано вплив швидкості ковзання та нормального навантаження на лінійну інтенсивність зношування композиту. Експериментальні результати дозволили побудувати рівняння регресії першого порядку, оцінити адекватність моделі та значущість її коефіцієнтів. На основі поверхонь відгуку визначено зони мінімальної інтенсивності зносу та оптимальні умови експлуатації при терті без змащення. Дослідження підтверджує значний вплив окремих факторів та їх взаємодії на зносостійкість композиту. Комбіноване використання статистичного аналізу та трибологічного тестування дозволяє глибше оцінити поведінку матеріалу та скоротити обсяг експериментальної роботи. Запропонований підхід може ефективно застосовуватися для оптимізації режимів роботи полімерних композицій у фрикційних агрегатах машин та механізмів, що працюють при високих навантаженнях і потребують підвищеної зносостійкості.

Ключові слова: політетрафторетилен, поліімідне волокно, композиційний матеріал, трибологічні властивості, математичне моделювання, інтенсивність лінійного зношування, рівняння регресії

ISSN 2079-1372 Problems of Tribology, V. 31, No 1/119-2026, 62-71

Problems of Tribology
Website: http://tribology.khnu.km.ua/index.php/ProbTrib
E-mail: tribosenator@gmail.com

DOI: https://doi.org/10.31891/2079-1372-2026-119-1-62-71

Improved algorithm for engineering calculations of the parameters of a container tipping mechanism in a garbage truck taking into account the wear of friction pairs

O.V. Bereziuk [1] 0000-0002-2747-2978, **V.I. Savulyak** [1] 0000-0002-4278-5155, **V.O. Kharzhevskyi** [2] 0000-0003-4816-2781, **S. Cv. Ivanov** [3] 0000-0002-7719-6086, **V.Ye. Yavorskyi**[1] 0009-0002-8724-3963

[1] *Vinnytsia National Technical University, Ukraine*
[2] *Khmelnytskyi National University, Ukraine*
[3] *Technical University Sofia, Branch Plovdiv, Bulgaria*
E-mail: berezyukoleg@i.ua

Received: 20 January 2026: Revised 07 February 2026: Accept: 20 February 2026

Abstract

The article is dedicated to the development of the scientifically grounded improved method, based on the analysis of scientific literature sources, for the design calculation of the parameters of a mechanism for tipping a container with municipal solid waste into a garbage truck, taking into account friction wear, in order to determine its main geometric, force, and speed parameters. The drive of the working parts of the mechanism for tipping a container with municipal solid waste into a garbage truck is hydraulic, with a power source from the garbage truck's pump station. The usage of the proposed improved methodology for the engineering calculation of the parameters of the mechanism for tipping a container with municipal solid waste into a garbage truck, taking into account the wear of friction pairs, allows significant reduction in design time and avoids unnecessary costs for labor-intensive experimental and theoretical research. Using the proposed scientifically based improved method of design calculation of the parameters of the mechanism for tipping a container with municipal solid waste into a garbage truck, taking into account the wear of friction pairs, its main geometric, force, and speed parameters have been determined. It has been established that the development of an improved methodology for the design calculation of the parameters of the mechanism for rotating the manipulator lever during the loading of municipal solid waste into a garbage truck, taking into account the wear of friction pairs, requires further research.

Keywords: algorithm, project calculation methodology, wear accounting, hydraulic drive, wear, friction units, container tipping mechanism, garbage truck, municipal solid waste.

Introduction

Among the main directions of development of modern municipal engineering in Ukraine, tasks related to the improvement of mobile manipulator-type machines, in particular garbage trucks, have an important role [1]. Within this area, issues related to improving the wear resistance, reliability, and durability of machine elements are of particular importance, since these indicators determine the efficiency of technical equipment operation, contribute to reducing repair and maintenance costs, and ensure an increase in the service life of equipment under conditions of intensive use [2, 3]. In Ukraine, the collection and transportation of municipal solid waste (MSW) to facilities for further processing or disposal is mainly carried out using body garbage trucks [4, 5]. The key functional element of such machines is loading devices [6-8], designed as manipulator mechanisms [9-13] with hydraulic drive [14, 15]. Currently, there are about 3,700 garbage trucks in operation, which, in addition to transporting solid waste, perform compaction operations. This significantly reduces transportation costs and the area of landfills required for solid waste disposal, which is of great economic and environmental importance. During the technological operation of loading MSW into the body of a garbage truck, friction units, primarily hinge joints and hydraulic cylinders of the manipulator mechanism, are subjected to significant mechanical loads. The increased wear and tear on these components is due to a combination of factors, including the significant

weight of waste containers, which can reach 500 kg, the operation of mechanisms in reverse mode with reciprocating movements, and the large number of work cycles performed during a single trip. In addition, operating conditions are complicated by operational factors, in particular significant fluctuations in relative humidity and temperature, as well as increased dusty environment, the combined effect of which causes intensified wear of working elements, which, in turn, negatively affects the reliability and durability of garbage trucks. The deterioration of the operational properties of the materials of the parts or an insufficient level of lubrication cause an increase in friction forces in the hinge joints of the manipulator mechanism, resulting in an increase in the level of vibrations in the system, which negatively affects its dynamic stability and reduces the ability of the mechanism to withstand significant loads under conditions of reversible friction. Intensive wear of friction components not only reduces the efficiency of the manipulator mechanism of the garbage truck, but also creates additional risks to the safe operation of the equipment. As a result, emergency operating modes may occur, posing a health hazard to service personnel and potentially causing negative environmental consequences in the event of uncontrolled spillage or leakage of solid waste. According to the provisions of Resolution No. 265 of the Cabinet of Ministers of Ukraine [16], one of the priority areas for the development of the public utilities sector is the introduction of modern, highly efficient garbage trucks, which are considered a key element of the system of technical means designed for the collection, transportation, and primary processing of solid waste. The usage of modern equipment not only optimizes logistics processes and reduces operating costs, but also contributes to the comprehensive solution of topical environmental problems related to the waste management system, and also ensures the reliability and effectiveness of public utility companies, which is of strategic importance for the sustainable development of populated areas. The planning of the renewal, maintenance, and repair of garbage trucks is facilitated by the development of an improved methodology for the design calculation of the parameters of the mechanism for tipping a container with municipal solid waste into a garbage truck, taking into account the wear of friction pairs.

Analysis of recent research and publications

Scientific paper [17] presents the results of structural analysis of garbage truck parts subject to intensive wear. The study described in article [18] proposes a method for diagnosing failures caused by wear of the sealing elements of the hydraulic cylinder and the presence of internal working fluid leaks, based on the usage of energy characteristic fusion. The study [19] developed the design of a robotic manipulator, created its 3D model in SOLIDWORKS, and performed a motion analysis. At the structural optimization design stage, key parameters, in particular the stresses and deformations of the manipulator, were evaluated comprehensively, and target functions and constraints for improving its design were determined. This approach reduces the probability of manipulator failure during prolonged heavy-duty operation and ensures more efficient interaction with other garbage truck systems, increasing the overall productivity of MSW collection and transportation processes.

A mathematical model that allows to determine the optimal geometric parameters of the manipulator's structural elements, taking into account the maximum boom reach, lifting capacity, and other kinematic characteristics of the machine, was developed in [20]. This model is an important tool for design engineers, as it ensures a rational choice of dimensional parameters of structural elements in order to improve the efficiency of the manipulator and ensure its reliability in operation. Particular attention is paid to the characteristics of hinge joints operating in a cyclic mode typical for manipulator-type machines. It has been established that under such conditions, the formation of a normal hydrodynamic friction regime is impossible, since the lubrication process occurs mainly in semi-dry or boundary friction modes. This leads to increased requirements for the properties of parts materials, the quality of surface treatment, and the efficiency of the lubrication system, since these factors determine the wear resistance and durability of hinge assemblies in real operating conditions. Contrary to the stable hydrodynamic friction regime, the operation of sliding bearings under semi-dry or boundary friction conditions is accompanied by more intense wear of contact surfaces, which leads to a gradual loss of kinematic accuracy, the occurrence of additional dynamic and shock loads and vibrations, which contribute to the development of fretting corrosion and premature failure of parts. To reduce friction forces, it is proposed to use special coatings for the contact elements of joints, in particular lead, phosphate, and indium coatings. It has been proven that the intensity of contact wear can be significantly reduced by using lubricants based on oils and fats, as well as consistent lubricants, which at a temperature of 25 °C acquire a thick, ointment-like consistency. In addition, the usage of phosphate and anodic metal coatings has been shown to be effective in improving grease retention on friction surfaces, increasing the efficiency and durability of components.

A method for optimizing the operation of a robotic workspace, which involves adjusting the position of the robot manipulator within the working area for programs with a fixed end-point motion trajectory, is proposed in the article [21]. The main aim of the study was to reduce the total wear of the manipulator joints and prevent their uneven loading when individual joints are subjected to greater mechanical stress than others. Wear was assessed by approximating the integral of the mechanical work of each joint along the entire trajectory, which was determined by the angular velocities and applied torques. The approach was based on dynamic modeling, which allows calculating the torques and rotational speeds of the joints in different positions of the robot. The results of the study showed that the optimal location of the manipulator base reduces the overall wear of its joints by 22-53%, depending on the configuration of the motion trajectory.

A detailed analysis of the main types of wear of hinge joints used in forestry manipulator designs is presented in [22]. The results of the study made it possible to identify promising areas for improving their wear resistance, which can be used by design engineers to extend the working life of components depending on specific operating conditions and technical requirements. Particular attention is paid to the fact that manipulator machines mostly operate in difficult climatic conditions with sharp fluctuations in ambient temperature, which significantly affects the stability of the properties of lubricants and the performance characteristics of structural materials of joints. At low temperatures, friction pair materials lose their plasticity, their brittleness increases, their yield strength decreases, and the stiffness of working surfaces increases, which complicates movement processes and the annihilation of dislocations in the crystal lattice, accompanied by exoelectron emission and accelerated wear. In addition, the properties of lubricants change: at low temperatures, they can lose their fluidity, transition to a solid state, or significantly increase their viscosity, which reduces their ability to form a protective film and increases the intensity of wear. During the summertime, when the ambient temperature is high, lubricants overheat, lose their viscosity, and can spontaneously leak from the friction zone, which negatively affects the lubrication and cooling of working surfaces, increases the risk of overheating of contacting elements, and accelerates the wear of hinge assemblies. To prevent these effects, it is recommended to use special sealing devices that can simultaneously protect the hinge joints from dust, moisture, and aggressive impurities, as well as retain the lubricant in the friction zone. Studies have confirmed the effectiveness of integrating contact and labyrinth sealing elements into the design of joints, which, thanks to their specific design, provide reliable protection of assemblies from negative factors of the operating environment and increase the service life of manipulators.

The study [23] demonstrates that when designing and creating new promising hinge joint designs, it is advisable to use a comprehensive approach to selecting scientific and engineering solutions. This is due to the fact that the performance of such assemblies is simultaneously influenced by a significant number of related factors, including design features, properties of friction pair materials, load conditions, lubrication modes, and the nature of the operating environment. Taking into account the combined effect of these parameters creates the prerequisites for the formation of fundamentally new design solutions capable of ensuring an increased level of reliability and durability of the hinge assemblies of forestry machine manipulators. The use of a comprehensive approach makes it possible to directly influence not only the mechanical properties of joints, such as strength and rigidity, but also their tribotechnical characteristics, in particular the coefficient of friction, wear intensity, and stability of operation under variable load conditions. In addition, the implementation of modern design solutions contributes to the optimization of the thermal regime of the joints, which is essential for reducing thermal deformations and preventing premature destruction of materials. As a result, this approach ensures increased efficiency of logging equipment operation, reduced maintenance costs, and increased service life of manipulator systems in difficult operating conditions.

In the paper [24], a method for synthesizing the motion trajectory of a manipulator robot is proposed, which takes into account its kinematic characteristics and the degrees of mobility of individual links. In particular, the influence of the rod deflection on the support reactions in the contact zone is considered, which in its physical essence resembles the work of a beam supported by two supports. This approach allows modeling the distribution of force influences on the robot's elements during its operation, including the contact areas of the hydraulic cylinder, rod, and ground bushing. Based on the determined values of contact pressure, it is possible to quantitatively assess the potential wear processes of friction surfaces, predicting their intensity and localization. It has been established that even in conditions where there is no danger of critical destruction of the rod under bending, contact stresses reaching approximately one third of the material's strength limit can significantly accelerate the wear of working surfaces. This is due to the fact that repeated load cycles lead to microdamage, increased local surface roughness, and the development of abrasive and contact wear processes. Additionally, it is taken into account that the specifics of contact pressure formation depend on the opening angle of the rod, its speed of movement, and the sequence of the manipulator's working cycles, which makes it possible to evaluate wear in different operating modes.

The results of the analysis of the design characteristics of the manipulator grippers of body garbage trucks and the assessment of their reliability are presented in scientific article [25]. Based on the research, a computational model of a garbage truck was developed, which is considered as an oscillatory system. The analysis revealed the peculiarities of the garbage truck frame vibrations during operation and the patterns of force formation in the interaction of the "gripper-tank-gripper" system elements. The research found that the greatest loads are on the thrust and rod of the hydraulic cylinder, and their magnitude increases with the increase in container weight. A change in the mass of the garbage truck itself does not affect the magnitude or amplitude of the loads, but changes their frequency characteristics. Operational observations have shown that the main causes of garbage truck failures are wear and corrosion of the working surfaces of equipment parts. In particular, 32% of all hydraulic drive failures occur in hydraulic cylinders. The failures of these units are caused by wear on the contact surfaces of the connections, deformation of the rod and cylinder under the action of operational loads, uneven loading of the body, and abrasive wear in difficult operating conditions. The main factor in hydraulic drive failures is the intensive wear of key components, in particular spools and hydraulic distributor housings, as well as hydraulic cylinder rods. Additional degradation is caused by hydroabrasive damage, which occurs due to delayed replacement of the working hydraulic fluid and the use of low-quality or worn sealing elements, such as hydraulic cylinder seals. This leads to the penetration of dust particles and wear products into the friction zone, which significantly accelerates

the destruction of working surfaces. To increase the service life and restore the performance of parts, it is recommended to use cold self-regulating electrolyte chromium plating technology, which provides the formation of chrome coatings with high deposit quality, increased wear resistance, and sufficient productivity. This makes this technology one of the most promising methods for restoring worn hydraulic drive components.

An analytical study of the mathematical model of the process of grinding polymer waste in the grinding chamber of a rotary crusher with continuous classification of the finished product, conducted in [26], provided a detailed understanding of the influence of various technological and design parameters on the performance of the installation. In particular, the study made it possible to determine with high accuracy the particle size distribution of the final product, evaluate the crusher's performance, and analyze energy consumption under variable operating conditions. It was found that the key factors affecting the quality of grinding and the efficiency of the process are the angular velocity of the rotor, the initial size and physical and mechanical properties of the waste, the design parameters of the crusher, in particular the geometry of the chamber and the size of the grid slots, as well as the chamber loading modes. The study showed that changing the angular velocity of the rotor allows optimizing the ratio of productivity and energy consumption, since an increase in speed leads to more intensive crushing of particles, but also increases the specific energy consumption of the process. At the same time, analysis of the influence of the initial size of the waste and the design characteristics of the crusher allows predicting the final particle distribution, determining the optimal parameters for achieving the desired product size, and avoiding overloads in the chamber. Complex evaluation of the loading modes and rotor rotation parameters makes it possible not only to increase the efficiency of the crusher, but also to optimize operating costs and energy consumption, which is an important aspect in the industrial scaling of the polymer waste grinding process.

The article [27] describes an algorithm for numerical and analytical research of dynamic processes in a planar six-bar linkage mechanism of a sewing machine threader. The proposed approach is based on the numerical solution of the differential equation of motion of the mechanism, taking into account its kinematic and dynamic parameters, which allows to describe details of the motion of individual links and determine the change in velocities and accelerations during the working cycle. In addition to analytical calculations, the authors performed computer modeling of the analyzed mechanism in Mathcad, which made it possible to visually reproduce its operation and verify the correctness of the obtained numerical results. The use of a combination of analytical methods and computer modeling made it possible to investigate the influence of design parameters and operating modes on the dynamic characteristics of the threader mechanism. During the simulation, changes in loads in hinge joints were analyzed, and regularities in the distribution of inertial forces arising during the operation of the mechanism were determined. The results of this study can be used to develop a design calculation methodology for optimizing the design of the threader, improving its reliability, and reducing dynamic loads.

In the scientific work [28], on the basis of a detailed analytical study of the mathematical model, the main regularities of the functioning of vibration and vibration-impact machines operating with the usage of a hydraulic pulse drive equipped with a single-stage pulsator valve were established. The developed model made it possible to describe the dynamic processes that occur in the hydraulic system and working parts of the machine, as well as to analyze the nature of pressure pulse formation and their influence on the kinematic and force parameters of vibrational motion. The study identified the relationships between the design parameters of the hydraulic pulse drive, its operating modes, and the dynamic characteristics of the machines, in particular the amplitude and frequency of vibrations, as well as the energy of shock pulses. The obtained results made it possible to establish the conditions for the stable operation of vibrating and vibro-impact machines, to evaluate the effectiveness of using a hydraulic pulse drive in various operating modes, and to formulate recommendations for optimizing the parameters of the pulsator valve in order to increase the productivity, reliability, and energy efficiency of such machines, necessary for creating a methodology for the design calculation of the parameters of these machines.

The article [29] proposes an improved nonlinear mathematical model of the operation of the hydraulic drive of the mechanism for loading MSW into a garbage truck during tipping of the container. A distinctive characteristic of the developed model is that it takes into account the wear of the friction pairs of the main elements of the hydraulic drive, which made it possible to describe the real conditions of its operation more accurately. Using numerical methods, the dynamic characteristics of the hydraulic drive at the start-up phase were studied, and the change in the main operating parameters of the system depending on the level of wear of its components was analyzed. The simulation results showed that taking into account the wear of friction pairs has a significant impact on the dynamics of the hydraulic drive for tipping the container during the loading of MSW into the garbage truck. In particular, significant changes in speed and power characteristics were found, as well as an increase in the time required to perform the technological operation. It was found that the duration of container tipping increases with the degree of wear of the hydraulic cylinder according to a power law, which indicates the nonlinear nature of the effect of wear on the efficiency of the mechanism. The obtained regularities can be used to predict the operating parameters of the hydraulic drive, establish maintenance intervals, and improve the reliability of MSW loading systems in garbage trucks.

The scientific work [30] is dedicated to the analytical study of an improved mathematical model of the hydraulic drive of the mechanism for tipping a container with municipal solid waste into a garbage truck, taking into account the wear of friction pairs. To perform design calculations for new garbage truck designs, it was obtained approximate analytical dependencies of pressure in the pressure line of the hydraulic cylinder, angular velocity, and container tipping angle as a function of time, based on the proposed linearized mathematical model

of the hydraulic drive of the container tipping mechanism during the technological operation of MSW loading into a garbage truck during the first phase— rotation of the container to the equilibrium position, taking into account the wear of friction pairs. The obtained regression equation allows to approximately determine the duration of the first phase – the rotation of the container to the equilibrium position during its overturning in the technological operation of MSW loading into a garbage truck, taking into account the wear of friction pairs. This can be used during design calculations for new garbage truck designs, taking into account the wear of the executive bodies without the need to study the nonlinear mathematical model of the drive of its working bodies, as well as during the optimization of the main parameters of the hydraulic drive.

In the article [31], using a first-order experimental design with first-order interaction effects using the Box-Wilson method, an appropriate regularity of wear of the friction nodes of the garbage truck loading mechanism was determined based on the properties of anti-friction materials, and in the work [32], an appropriate regularity of maximum impact dynamic stresses in the most loaded section of the garbage truck manipulator boom is determined based on the wear of the manipulator hinge and its load level.

However, during the analysis of known publications, the authors did not find a complete methodology for the design calculation of the parameters of the mechanism for tipping a container with municipal solid waste into a garbage truck, taking into account the wear of friction pairs.

Aims of the article

Development of a scientifically grounded, improved methodology for the design calculation of the parameters of a mechanism for tipping a container with municipal solid waste into a garbage truck, taking into account the wear of friction pairs in order to determine its main geometric, force, and speed parameters.

Methods

The following methods were used in the work: analysis of scientific literature sources; synthesis of mathematical interdependencies of the main geometric, force, and speed parameters of the equipment; a systematic approach to take into account the interaction of all machine subsystems.

Results

Fig. 1 shows a schematic diagram of the hydraulic drive of the mechanism for container tipping in the technological operation of loading MSW into a garbage truck, taking into account the wear of friction pairs when using the rear MSW loading scheme.

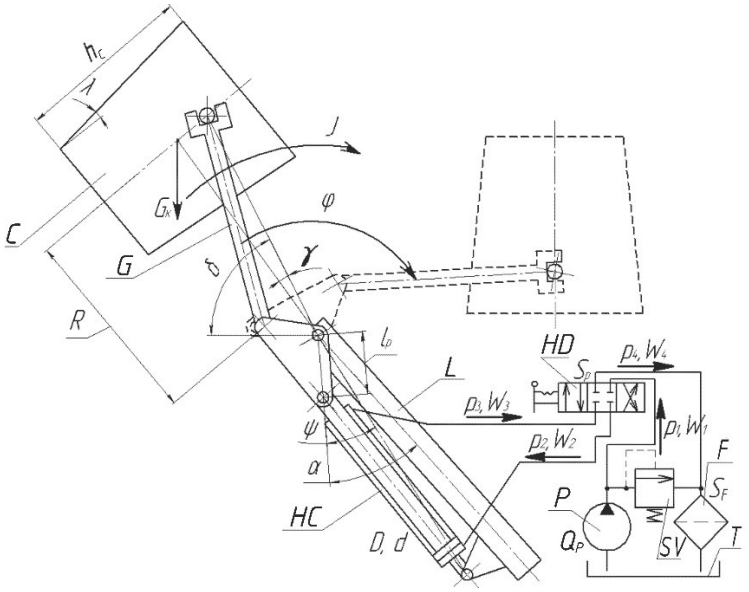

Fig. 1. Schematic diagram of the hydraulic drive of the container turning mechanism in the technological operation of MSW loading into a garbage truck, taking into account the wear of friction pairs

The diagram shows the following structural elements: C – container, G – gripper, L – lever, HC – hydraulic cylinder, HD – hydraulic distributor, P – hydraulic pump, SV – safety valve, F – filter, T – tank with working fluid, as well as the main geometric, kinematic and power parameters: p_1, p_2, p_3, p_4 – pressures at the pump outlet, at the hydraulic cylinder inlet, at the hydraulic cylinder outlet and at the filter inlet, respectively; W_1, W_2, W_3, W_4 – volumes of pipelines between the pump and the hydraulic distributor, the hydraulic distributor and the hydraulic

cylinder inlet, the hydraulic cylinder outlet and the hydraulic distributor, the hydraulic distributor and the filter; Q_P –actual pump flow rate; S_P – cross-sectional area of the distributor opening; S_f – surface area of the filter element; D , d – piston and rod diameters; J – moment of inertia of moving elements; G_C –container weight; R – radius of rotation of moving elements; l_P – distance between the centers of rotation of the gripper and the rod; h – the height of the container; α – angle between the axes of the lever and the cylinder arm, γ – angle that takes into account the deviation of the center of mass position; δ – angle between the gripping arm and the horizontal; λ – angle of inclination of the container wall; ψ – the angle between the axis of the cylinder arm and the axis passing between the centers of rotation of the gripper and the hydraulic cylinder; φ – grip rotation angle.

The area of the rod cavity of the hydraulic cylinder of the container tipping mechanism can be found by using the following formula [30]:

$$S_{C1} = \frac{\pi\left(D^2 - d^2\right)}{4} \text{ [m}^2\text{]}. \tag{1}$$

The speed of the rods of the paired hydraulic cylinders of the container tipping mechanism can be determined by the formula [30]:

$$v = \frac{Q_P}{2S_{C1}} \text{ [m/s]}. \tag{2}$$

The pressure of the working fluid in the rod cavity of the hydraulic cylinder of the container tipping mechanism during steady-state operation can be found using the formula [30]:

$$p \approx \frac{GR\cos\left(\delta - \gamma\right)}{S_{C1} l_p \sin\left(\phi + \alpha\right)} \text{ [Pa]}. \tag{3}$$

The wear of friction components in the garbage truck loading mechanism due to the properties of anti-friction materials is determined according to the following regularity [31]:

$$u = 458.2f + 0.1696HB + 4366v - 546.2p + 33782fv \text{ [μm]}, \tag{4}$$

where u – wear of the manipulator joint, μm; f – coefficient of friction between steel and anti-friction material; HB – hardness of anti-friction material according to Brinell, MPa; v – sliding speed, m/s; p – pressure in the friction zone, MPa.

The maximum dynamic stress in the most loaded section of the manipulator boom due to wear of the manipulator hinge and its load level is found according to the following regularity [32]:

$$\sigma_{\max} = 0.08552u + 89.58\frac{G}{G_n} + 0.06243u\frac{G}{G_n} - 2.99\cdot10^{-5}u^2 - 10.02\left(\frac{G}{G_n}\right)^2 \text{ [MPa]}, \tag{5}$$

where σ_{max} – maximum dynamic impact stresses in the most loaded section of the manipulator boom, MPa; G/G_n – manipulator load rate; G – weight of a container with municipal solid waste, N; G_n – nominal load capacity of the manipulator, N.

Based on the obtained value of σ_{max} according to DSTU EN 1993-1-1:2010 [33], the grade of the manipulator boom material can be determined.

The average value of the container tipping angle for the first phase – the phase of turning the container to the equilibrium position can be determined by the formula [30]:

$$\overline{\varphi}_1 = \frac{\pi/2 + \lambda - \delta}{2} \text{ [rad]}. \tag{6}$$

The duration of container overturning, taking into account the wear of friction pairs during the first phase, is calculated using a simplified equation that is obtained in the article [30]:

$$t_1 \approx \frac{2S_{C1}l_p\beta_\sigma\sigma_0 J\sin\left(\overline{\phi}_1 + \psi\right)}{\left(Q_P - \alpha_\sigma\right)\left\{\beta_\sigma\sigma_0 J + 2S_{C1}^2 l_p^2 \sin^2\left[\overline{\phi}_1 + (\alpha + \psi)/2\right]\right\}}\phi_1 \text{ [s]}, \tag{7}$$

where σ_0 – coefficient of working fluid loss due to flow from a high-pressure area to a low-pressure area, without taking into account friction wear, m^5/(N·s); α_σ, β_σ – approximation coefficients of the dependence of working fluid losses on the duration of the friction pair wear process ($\alpha_\sigma = 4.054 \cdot 10^{-4}$; $\beta_\sigma = 128.1$).

The average value of the container tilt angle for the second phase—the phase of emptying MSW from the container into the garbage truck body can be determined by the following formula [34]:

$$\overline{\varphi}_2 = 0{,}75\pi + 1{,}5\lambda - \delta \text{ [rad]}. \tag{8}$$

The coefficient of working fluid loss due to flow from a high-pressure area to a low-pressure area, taking into account the wear of friction pairs, can be found using the formula [30]:

$$\sigma = \frac{\pi D\left(\delta_0 + u \cdot 10^{-6}\right)^3}{12\nu\rho l} \text{ [m}^5\text{/(N·s)]}, \tag{9}$$

where δ_0 – nominal gap size, m; ν – kinematic viscosity of the working fluid, m^2/s; ρ – density of working fluid, kg/m^3; l – ring gap length, m.

The duration of container tipping during the second phase can be determined using a simplified equation that was obtained in [34]:

$$t_2 \approx \frac{2S_{C1}^2 l_p^2 \sin\left(\overline{\phi}_2 + \alpha\right)\sin\left(\overline{\phi}_2 + \psi\right)}{Q_P S_{C1} l_p \sin\left(\overline{\phi}_2 + \alpha\right) - \sigma GR\cos\left(\delta - \gamma\right)}\phi_2 - \frac{2l_p}{Rg} \times$$
$$\times \sqrt{\frac{-Q_P S_{C1} l_p^2 \sin\left(\overline{\phi}_2 + \alpha\right)\sin\left(\overline{\phi}_2 + \psi\right) h_K \phi_2}{\sigma V_K \rho_B \left(1 + 2\tan\lambda\right) R^2 g^2 \left[\cos\left(\delta - \lambda\right) + f_B \sin\left(\delta - \lambda\right)\right]\cos\left(\overline{\phi}_2 + \delta - \gamma\right)}} \text{ [s]}. \tag{10}$$

The total duration of container tipping can be determined using the formula:

$$t = t_1 + t_2 \text{ [s]}. \tag{11}$$

The parameters of the mechanism for tipping the container with MSW into the garbage truck, taking into account the wear of friction pairs, calculated according to the proposed methodology, are given in the Table 1.

Table 1

Basic parameters of the mechanism for tipping a container with MSW into a garbage truck, taking into account the wear of friction pairs

S_{C1}, m^2	v, m/s	p, MPa	u, μm	σ_{max}, MPa	material	$\overline{\varphi}_1$, rad	t_1, s	$\overline{\varphi}_2$, rad	σ, m^5/(N·s)	t_2, s	t, s
$5.027 \cdot 10^{-3}$	0.0912	1.43	13.5	247	40Kh steel	0.271	0.755	1.378	$1.228 \cdot 10^{-10}$	4.196	4.95

The parameters of the mechanism for tipping the container with MSW into the garbage truck, taking into account the wear of the friction pairs, were obtained based on the following initial data: D = 80 mm; d = 50 mm; Q_P = 55 l/min; G = 1742 N; R = 0.72 m; γ = 20°; δ = 65°; l_p = 150 mm; α = 40°; f = 0.1; HB = 250 MPa; G_n = 4900 N; λ = 6°; $\alpha_\sigma = 4.054 \cdot 10^{-4}$; β_σ = 128,1; $\sigma_0 = 9.24 \cdot 10^{-11}$ m^5/(N·s); J = 112.6 kg·m^2; ψ = 30°; δ_0 = 0.136 mm; $\nu = 1.83 \cdot 10^{-5}$ m^2/s; ρ = 890 kg/m^3; l = 35 mm; h_κ = 0.46 m; V_k = 1.1 m^3; ρ_B = 210 kg/m^3; f_B = 0,3.

The usage of the proposed improved method for engineering calculation of the parameters of the mechanism for tipping a container with MSW into a garbage truck, taking into account the wear of friction pairs, allows to significantly reduce the design time and avoid unreasonable costs for labor-intensive experimental and theoretical research.

The development of an improved method for project calculation of the parameters of the manipulation lever rotation mechanism during the loading of municipal solid waste into a garbage truck, taking into account the wear of friction pairs, requires further research.

Conclusions

A scientifically based improved algorithm for the design calculation of the parameters of the mechanism for turning a container with municipal solid waste into a garbage truck, taking into account the wear of friction pairs, is proposed, which allows to obtain its main geometric, force, and speed parameters. It has been established

that the development of an improved methodology for the design calculation of the parameters of the manipulator lever rotation mechanism during the loading of municipal solid waste into a garbage truck, taking into account the wear of friction pairs, requires further research.

References

1. Holenko K., Dykha O., Koda E., Kernytskyy I., Horbay O., Royko Y., Fornalchyk Y., Berezovetska O., Rys V., Humenuyk R., Berezovetskyi S., Żółtowski M., Baryłka A., Markiewicz A., Wierzbicki T., Bayat H. (2024) Structure and strength optimization of the Bogdan ERCV27 electric garbage truck spatial frame under static loading. Applied Sciences, 14(23), 11012, https://doi.org/10.3390/app142311012

2. Dykha A., Sorokatyi R., Pasichnyk O., Yaroshenko P., Skrypnyk T. (2020, December) Machine wear calculation module in computer-aided design systems. In IOP Conference Series: Materials Science and Engineering, 1001(1), 012040, https://doi.org/10.1088/1757-899X/1001/1/012040

3. Kindrachuk M.V., Kharchenko V.V., Marchuk V.Y., Humeniuk I.A., Leusenko D.V. (2024) Methodology for Selecting Compatible Metal Materials for Friction Pairs During Fretting-Corrosion Wear. Metallophysics & Advanced Technologies, 46(7), 637-648, https://doi.org/10.15407/mfint.46.07.0637

4. Giel R., Dąbrowska A. (2021) Estimating time spent at the waste collection point by a garbage truck with a multiple regression model. Sustainability, 13(8), 4272, https://doi.org/10.3390/su13084272

5. Hao Y., Zhang Y., Ma N., Li P., Liu Y. (2024) Developing driving cycles for garbage trucks to estimate fuel consumption. Transportation Research Part D: Transport and Environment, 136, 104469, https://doi.org/10.1016/j.trd.2024.104469

6. Chulkov A.S., Chaplygin M.E., Shaykhov M.M. (2024) Justifying the Operation Parameters of a Robotic Cassette Loading Device of the Carousel Type for a Selection Seeder. Engineering Technologies and Systems, 34(4), 549-562, https://doi.org/10.15507/2658-4123.034.202404.549-562

7. Zhu B., Wang L., Wu J. (2022) Optimal design of loading device based on a redundantly actuated parallel manipulator. Mechanism and Machine Theory, 178, 105084, https://doi.org/10.1016/j.mechmachtheory.2022.105084

8. Guo J., Wang D., Li T., Gao S., Chen W., Fan R. (2018) Triaxial loading device for reliability tests of three-axis machine tools. Robotics and computer-integrated manufacturing, 49, 398-407, https://doi.org/10.1016/j.rcim.2017.05.009

9. Tinoco V., Silva M.F., Santos F.N., Morais R., Magalhães S.A., Oliveira P.M. (2025) A review of advanced controller methodologies for robotic manipulators. International Journal of Dynamics and Control, 13(1), 36, https://doi.org/10.1007/s40435-024-01533-1

10. Kuang X., Zhou S. (2024) Robotic Manipulator in Dynamic Environment with SAC Combing Attention Mechanism and LSTM. Electronics, 13(10), 1969, https://doi.org/10.3390/electronics13101969

11. Bronnikov A., Bendeberia M. (2024) Development of a manipulator kinematic model using ABB RobotStudio. Innovative Technologies and Scientific Solutions for Industries, 4(30), 5-18, https://doi.org/10.30837/2522-9818.2024.4.005

12. Calzada-Garcia A., Victores J.G., Naranjo-Campos F.J., Balaguer C. (2025) A Review on Inverse Kinematics, Control and Planning for Robotic Manipulators With and Without Obstacles via Deep Neural Networks. Algorithms, 18, 23, https://doi.org/10.3390/a18010023

13. Han R., Sang H., Liu F., Huang F. (2024) State of the Art and Development Trend of Laparoscopic Surgical Robot and Master Manipulator. International Journal of Medical Robotics and Computer Assisted Surgery, 20(6), e70020, https://doi.org/10.1002/rcs.70020

14. Polishchuk L.K., Piontkevych O.V., Svietlov A.V., Adler O.O., Lozinskyi D. (2025) Development and optimization of the control devicefor the hydraulic drive of the belt conveyor. Informatyka, Automatyka, Pomiary w Gospodarce i Ochronie Środowiska, 15, 124-129, http://doi.org/10.35784/iapgos.7051

15. Petrov O., Kozlov L., Lozinskiy D., Piontkevych O. (2019) Improvement of the hydraulic units design based on CFD modeling. Lecture Notes in Mechanical Engineering, 653-660, https://doi.org/10.1007/978-3-030-22365-6_65

16. The Cabinet of Ministers of Ukraine (2004) Resolution No. 265 "Pro zatverdzhennia Prohramy povodzhennia z tverdymy pobutovymyvidkhodamy" ["On Approval of the Program for Solid Waste Management"]. URL: http://zakon1.rada.gov.ua/laws/show/265-2004-%D0%BF.

17. Lazea M., Constantin G.A., Stoica D., Voicu G. (2020) Analiza structurala cu elemente finite a pieselor de uzura de pe placa de contrapresiune a unei autogunoiere. Revista Romana de Materiale, 50(2), 283-293.

18. Qiu Z., Min R., Wang D., Fan S. (2022) Energy features fusion based hydraulic cylinder seal wear and internal leakage fault diagnosis method. Measurement, 195, 111042, https://doi.org/10.1016/j.measurement.2022.111042

19. Li H., Li Y. (2025) Finite element analysis and structural optimization design of multifunctional robotic arm for garbage truck. Frontiers in Mechanical Engineering, 11, 1543967, https://doi.org/10.3389/fmech.2025.1543967

20. Chernik D.V., Chernik K.N. (2020) Mathematical model of a combined manipulator of a forest machine. In IOP Conference Series: Materials Science and Engineering, 5(919), 052037,

https://doi.org/10.1088/1757-899X/919/5/052037

21. Kot T., Bobovský Z., Vysocký A., Krys V., Šafařík J., Ružarovský R. (2021) Method for robot manipulator joint wear reduction by finding the optimal robot placement in a robotic cell. Applied Sciences, 11(12), 5398, https://doi.org/10.3390/app11125398

22. Serebryanskii A. (2014) Except the negative reverse effect and automatically compensate for wear in the hinge manipulators. DOAJ – Lund University: Concept: Scientific and Methodological e-magazine, 4 (Collected works, Best Article).

23. Zadorozhnaya E., Levanov I., Kandeva M. (2018, May) Tribological research of biodegradable lubricants for friction units of machines and mechanisms: Current state of research. In International Conference on Industrial Engineering, 939-947, https://doi.org/10.1007/978-3-319-95630-5_98

24. Beisembayev A., Yerbossynova A., Pavlenko P., Baibatshayev M. (2023) Planning trajectories of a manipulation robot with a spherical coordinate system for removing oxide film in the production of commercial lead, zinc. Eastern-European Journal of Enterprise Technologies, 124(2), 80, https://doi.org/10.15587/1729-4061.2023.286463

25. Kargin R.V., Yakovlev I.A., Shemshura E.A. (2017) Modeling of workflow in the grip-container-grip system of body garbage trucks. Procedia Engineering, 206, 1535-1539, https://doi.org/10.1016/j.proeng.2017.10.727

19. Skyba M.Ye., Misiats O.V., Polishchuk A.O., Misiats V.P., Rubanka M.M. (2021). Systema adaptyvnoho chastotnoho keruvannia shvydkistiu obertannia asynkhronnoho tryfaznoho elektrodvyhuna pryvodu rotornoi drobarky [Adaptive frequency control system for the rotational speed of a three-phase asynchronous electric motor driving a rotary crusher]. Herald of of Khmelnytskyi National University. Technical Sciences, 2(295), 139-146, https://doi.org/10.31891/2307-5732-2021-295-2-139-146

27. Manoilenko O., Dvorzhak V., Horobets V., Panasiuk I., Bezuhlyi D. (2024) Assessing the impact of sewing machine thread take-up mechanism parameters on the magnitude and nature of thread take-up. Eastern European Journal of Enterprise Technologies, 2024, 6(1(132)), 64-75, https://doi.org/10.15587/1729-4061.2024.315129

28. Iskovich-Lototsky R., Kots I., Ivanchuk Y., Ivashko Y., Gromaszek K., Mussabekova A., Kalimoldayev M. (2019). Terms of the stability for the control valve of the hydraulic impulse drive of vibrating and vibro-impact machines. Przeglad Elektrotechniczny, 4(19), 19-23, https://doi.org/10.15199/48.2019.04.04

29. Bereziuk O.V., Yavorskyi V.Ye. (2025) Udoskonalena matematychna model roboty hidropryvodu mekhanizmu zavantazhennia tverdykh pobutovykh vidkhodiv u smittievoz iz urakhuvanniam znosu par tertia [Improved mathematical model of the hydraulic drive of the mechanism for loading solid household waste into a garbage truck, taking into account friction pair wear]. Scientific Works of Vinnytsia National Technical University, 1, 154-164, https://doi.org/10.31649/2307-5376-2025-1-154-164

30. Bereziuk O.V., Savulyak V.I., Kharzhevskyi V.O., Ivanov S.Cv., Yavorskyi V.Ye. (2025) Analytical study of a hydraulic drive model for a municipal waste container overturning mechanism in a garbage truck considering the wear of friction pairs. Problems of Tribology, 30(3/117), 30-49, https://doi.org/10.31891/2079-1372-2025-117-3-30-40

31. Bereziuk O.V., Savulyak V.I., Kharzhevskyi V.O., Serdiuk O.V., Yavorskyi V.Ye. (2024) Dependence of wear of friction pairs of the mechanism for loading solid household waste into a garbage truck on the characteristics of antifriction materials. Problems of Tribology, 29(3/113), 24-30, https://doi.org/10.31891/2079-1372-2024-113-3-15-23

32. Bereziuk O.V., Savulyak V.I., Kharzhevskyi V.O., Yavorskyi V.Ye. (2023) The influence of hingeswear on the dynamic load of the articulated boom of a garbage truck's manipulator. Problems of Tribology, 28(3/109), 18-24, https://doi.org/10.31891/2079-1372-2023-109-3-18-24

33. State Enterprise "Ukrainian Scientific and Research Center for Standardization, Certification and Quality" (UkrNDNC). (2010) DSTU EN 1993-1-1:2010. Eurocode 3. Design of steel structures. Part 1-1: General rules and rules for buildings. Kyiv: UkrNDNC.

34. Bereziuk O.V. (2021) Naukovo-tekhnichni osnovy proektuvannia pryvodiv robochykh orhaniv mashyn dlia zbyrannia ta pervynnoi pererobky tverdykh pobutovykh vidkhodiv [Scientific and technical grounds for designing drives for working bodies of machines for collecting and primary processing of municipal solid waste]. Doctor of Engineering Sciences Dissertation (Specialty 05.02.02 – Machine Science). Khmelnytskyi, 482 p.

Березюк О.В., Савуляк В.І., Харжевський В.О., S.Cv. Ivanov, Яворський В.Є. Удосконалений алгоритм інженерних розрахунків параметрів механізму перевертання контейнера у сміттєвоз із урахуванням зносу пар тертя

Стаття присвячена розробці на основі аналізу наукових літературних джерел науково-обґрунтованої удосконаленої методики проєктного розрахунку параметрів механізму перевертання контейнера з твердими побутовими відходами у сміттєвоз із урахуванням зносу пар тертя з метою визначення основних його геометричних, силових та швидкісних параметрів. Привод робочих органів механізму перевертання контейнера з твердими побутовими відходами у сміттєвоз – гідравлічний з джерелом живлення від насосної станції сміттєвоза. Використання запропонованої удосконаленої методики інженерного розрахунку параметрів механізму перевертання контейнера з твердими побутовими відходами у сміттєвоз із урахуванням зносу пар тертя дозволяє суттєво скоротити час проєктування, уникнути необґрунтованих витрат на трудомісткі експериментальні та теоретичні дослідження. За допомогою запропонованої науково-обґрунтованої удосконаленої методики проєктного розрахунку параметрів механізму перевертання контейнера з твердими побутовими відходами у сміттєвоз із урахуванням зносу пар тертя визначено основні його геометричні, силові та швидкісні параметри. Встановлено, що розробка удосконаленої методики проєктного розрахунку параметрів механізму повороту важеля маніпулятора під час завантаження твердих побутових відходів у сміттєвоз із урахуванням зносу пар тертя вимагає проведення подальших досліджень.

Ключові слова: алгоритм, методика проєктного розрахунку, урахування зносу, гідропривод, знос, вузли тертя, механізм перевертання контейнера, сміттєвоз, тверді побутові відходи.

ISSN 2079-1372 Problems of Tribology, V. 31, No 1/119-2026, 72-79

Problems of Tribology
Website: http://tribology.khnu.km.ua/index.php/ProbTrib
E-mail: tribosenator@gmail.com

DOI: https://doi.org/10.31891/2079-1372-2026-119-1-72-79

Development and Investigation of the Technology of Electro-Induction Surfacing of Parts of Working Bodies of Agricultural Machines

D.D. Marchenko* 0000-0002-0808-2923 **, K.S. Matvyeyeva** 0000-0003-0974-3022

**Mykolayiv National Agrarian University, Mykolayiv, Ukraine*
E-mail: marchenkodd@mnau.edu.ua

Received: 24 January 2026: Revised 10 February 2026: Accept: 28 February 2026

Abstract

This article examines ways to improve the wear resistance of agricultural machinery components operating under intense abrasive wear conditions. The study focused on cultivator shanks made of 50, 50KhGA, and 65G structural steels. The aim of the study is to develop and scientifically validate a technology for electro-induction surfacing of wear-resistant coatings based on Fe–Cr–C and Fe–Cr–C–B alloys, ensuring the formation of an optimal deposited layer structure and improving the performance of the components. A hardening process is proposed, including electro-induction surfacing of a hard-alloy material followed by pulsed high-energy heating, as well as the design of a special inductor that allows for simultaneous surfacing of the shanks' nose and hardening of their wings. The effect of chemical-thermal treatment (boriding) on the formation of a hardened surface layer is also studied. Field tests were conducted under cultivating conditions using pilot and control samples. Working tool wear was assessed based on changes in geometric parameters, overlap area, and mass loss. It was found that the relative wear of surface-hardened wingtip shanks ranged from 8–27%, while for standard parts hardened using traditional methods, it reached 25–40%. This indicates a 30–60% reduction in wear intensity. It was shown that the performance of wingtip shanks during operation is determined primarily by maintaining their overall arrowhead shape. For a more objective wear assessment, it was proposed to use integrated indicators including changes in the overlap area of the working tools and average mass loss. The developed technological solutions can increase the relative wear resistance of the working tools by 2.0–2.5 times, reduce traction resistance during soil operation by 6–8%, and improve the efficiency of agricultural processes.

Keywords: electro-induction surfacing, wear-resistant coatings, abrasive wear, arrow paw, working parts of agricultural machinery, boriding, alloys of the Fe–Cr–C system, alloys of the Fe–Cr–C–B system, surface hardening, wear resistance.

Introduction

Every year, as a result of abrasive wear, which occurs during soil cultivation and crop production processing, a significant loss of metal occurs. Even in parts subjected to hardening, the total volume of such losses reaches hundreds of thousands of tons. In order to increase the service life of parts and components operating under conditions of intense abrasive action, various hardening methods are used, one of which is surfacing of wear surfaces. Electro-induction surfacing using powder materials based on high-alloy chromium white cast irons and pseudoalloys of the Fe–Cr–C and Fe–Cr–C–B systems is considered a promising but still insufficiently studied direction. The study of the features of this process is devoted to the work of V.N. Tkacheva, M.M. Tenenbaum, A.I. Sydorov and other scientists. In the process of forming a hard alloy layer on the surface of structural and low-alloy steels, chemical and structural inhomogeneity of the coating occurs. As a result, the wear resistance of individual zones of the formed layer may differ and vary between 0.55 and 1.0 relative to each other. One of the ways to improve the reliability and durability of the working bodies of agricultural machines is the development of methods for controlling the structure and properties of wear-resistant coatings obtained by the method of electro-induction surfacing from white high-alloy chromium cast iron and pseudoalloys. The key stage of the electro-induction surfacing process is the formation of a durable wear-resistant layer on the surface of the parts, capable of working effectively under conditions of intense abrasive and shock-abrasive impact. To solve this problem, resource-saving technologies of electro-induction hardening of working bodies of agricultural machinery

are widely used. Currently, about 73% of all welding operations are performed by the method of electro-induction surfacing in tractor and agricultural machine building.

An analysis of the operating conditions of working parts of agricultural machines strengthened by electro-induction surfacing shows that their premature failure is often associated with the formation of an inhomogeneous structure of the surfacing layer. Such inhomogeneity occurs when applying wear-resistant coatings made of high-alloy chromium white cast iron and pseudoalloys to carbon and low-alloy steels.

The increase in production efficiency and the quality of manufactured products is directly related to the fuller use of the potential of materials and technologies for applying wear-resistant coatings to structural steel. In this regard, the study of the influence of physical, chemical and technological factors, as well as their complex impact on the formation of the structure, chemical and phase composition of alloys of the Fe–Cr–C and Fe–Cr–C–B systems during electro-induction surfacing, becomes especially relevant.

The implementation of this direction is possible due to alloying wear-resistant coated with carbide-forming elements, saturating them with boron, applying heating with an electromagnetic field of increased frequency, optimizing the composition of charge materials, as well as additional impact on the deposited layer with an electric arc of a carbon electrode. The use of the specified methods allows you to purposefully control the process of forming the primary structure of the deposited layer. The cumulative application of physical, chemical and technological effects opens up opportunities for obtaining new scientific and technical solutions aimed at significantly increasing the operational characteristics of hardened parts.

Literature review

Working bodies of agricultural machines in the process of operation are exposed to intensive abrasive wear, which occurs when metal surfaces interact with soil, sand and hard mineral inclusions. As a result, there is a gradual destruction of the surface layer of parts, a change in their geometric parameters and a decrease in the efficiency of the equipment. Abrasive wear is one of the main reasons for failure of such elements as ploughshares, cultivator paws, knives of tillage units and other parts of agricultural machines. Therefore, increasing their wear resistance and durability is an important task of modern agricultural engineering.

One of the most common ways to increase the service life of parts operating under conditions of intense abrasive action is the application of wear-resistant coatings. For this, various methods of surfacing are widely used, which allow to form a layer of material with increased hardness and wear resistance on the surface of the part. Coating technologies allow not only to improve the performance characteristics of new parts, but also to effectively restore worn-out machine elements, which has a significant economic value.

In recent years, researchers have paid considerable attention to surfacing materials based on the Fe–Cr–C system, which are widely used to obtain wear-resistant coatings. Such alloys are characterized by the formation of a structure containing solid carbide phases that provide high hardness and resistance to abrasive wear. However, a number of studies show that the traditional materials of this system do not always provide sufficient durability of the coating at high specific loads and cyclic impacts. This is due to the formation of a coarse-grained structure and non-uniform distribution of carbide phases, which can accelerate the wear process.

To improve the operational properties of the coating, researchers suggest alloying surfacing alloys with various elements, such as boron, titanium, molybdenum, and others. The introduction of boron contributes to the formation of solid boride phases in the structure of the coating, which significantly increase the hardness and wear resistance of the material. Studies show that with an increase in the boron content in iron-containing alloys, the share of borides increases, which leads to an improvement in microhardness and an increase in resistance to abrasive wear.

Considerable attention is paid to the issues of increasing the wear resistance of the working bodies of agricultural machines in modern studies of Ukrainian scientists. For example, in the works of T. Skoblo, O. Nanka, O. Saichuk, I. Rybalko, A. Tikhonov, and A. Zakharov, the effect of modifying additives on the structure and properties of welded layers used in the restoration of plowshares and cultivator paws was studied. The obtained results show that the introduction of carbide and oxide modifiers makes it possible to improve the mechanical and tribological characteristics of welded coatings.

Foreign researchers also made a significant contribution to the development of surface hardening technologies and wear-resistant coatings. Thus, in the works of V. Malikov, A. Ishkov, D. Shmykov, P. Androsov and others, methods of increasing the wear resistance of parts using electro-induction surfacing were studied. The authors have shown that the use of electro-induction heating makes it possible to form durable wear-resistant coatings and significantly increase the service life of machine parts.

A number of foreign studies are devoted to the study of the structure and properties of iron-based composite coatings obtained by the method of electro-induction surfacing. Experimental results show that such coatings have high hardness and resistance to wear due to the formation of carbide and boride phases in the structure of the coating.

In the field of development of modern functional coatings and technologies of surface engineering, the research of the German scientist Robert Vaßen is also well-known, whose work is devoted to the creation of high-temperature and wear-resistant coatings for various branches of mechanical engineering. His research contributed to the development of technologies for obtaining functional coatings with increased operational properties.

An important role in the formation of the structure and properties of wear-resistant coatings is also played by the technology of their application. Currently, various methods of obtaining such coatings are used, including arc surfacing, plasma spraying, laser surfacing and electro-induction surfacing. Among them, electro-induction surfacing is of considerable interest due to the possibility of local heating, high productivity of the process and relatively low energy consumption. In addition, this method makes it possible to obtain coatings with good adhesion to the base and a minimal zone of thermal influence.

Electro-induction surfacing is especially promising when using powder materials and high-alloy alloys. In the process of heating with a high-frequency electromagnetic field, the surfacing material is melted and a protective layer with specified properties is formed on the surface of the part. The structure of such a layer depends on the composition of the charge materials, heating modes and cooling rate. A number of studies have shown that the formation of a finely dispersed structure with a uniform distribution of carbides and borides contributes to a significant increase in the wear resistance of the coating.

Of special interest are wear-resistant coatings based on highly alloyed chromium white cast irons and pseudoalloys of the Fe–Cr–C and Fe–Cr–C–B systems. Such materials are characterized by high hardness due to the presence of chromium carbides and boride phases, which effectively prevent the development of abrasive wear. With an optimal ratio of components, it is possible to form a structure that provides a combination of high hardness and sufficient viscosity, which is especially important for parts that work under shock-abrasive conditions.

Despite a significant amount of research in the field of wear-resistant coatings, a number of issues related to the formation of the structure of the deposited layer and the management of its properties remain insufficiently studied. In particular, the tasks of optimizing the composition of surfacing materials, improving electro-induction heating modes, and developing combined surface treatment technologies are relevant.

Thus, the analysis of literary sources shows that the application of electro-induction surfacing using high-alloyed alloys and powder materials is a promising direction for increasing the durability of working bodies of agricultural machines. Further research should be directed to the study of the regularities of structure formation and phase composition of welded coatings, as well as to the development of technological solutions that provide an increase in their wear resistance and operational reliability.

Purpose

The purpose of the research is the development and scientific substantiation of the technology of electro-induction surfacing of wear-resistant coatings on parts of the working bodies of agricultural machines based on alloys of the Fe–Cr–C and Fe–Cr–C–B systems, which ensures the formation of the optimal structure of the deposited layer and increases the operational characteristics of parts operating under conditions of abrasive wear.

Research methodology

The subject of the study was the working parts of tillage machines – cultivator shanks made of 50, 50KhGA, and 65G structural steels. These materials were chosen due to their widespread use in the manufacture of working parts of agricultural machinery operating under conditions of intense abrasive wear.

The research aimed to increase the wear resistance of shanks by developing electro-induction surfacing and chemical-thermal hardening (boring) processes.

To strengthen the blade portion of shanks, a process was developed that included:

– applying a hard-alloy charge to the blade surface;
– electro-induction heating of the surfacing zone;
– forming a hardened layer;
– simultaneous hardening of the shanks' wings.

To implement this process, a special inductor was developed that simultaneously deposits the nose of the lance and hardens the working surface wings.

The inductor design includes:

– deposition coil;
– quenching coil;
– current conductor;
– connecting plate for connection to the generator;
– profiled tube for melting the charge.

Pulsed high-energy heating ensured localized melting of the carbide material and the formation of a hardened layer on the cutting edge.

Some of the experimental samples were additionally borided. Boriding was performed using special paste-like coatings of various compositions (coating codes I–VI). After coating application, the samples were heat-treated to form a boride layer of increased hardness.

The resulting hardened samples were used for further performance testing.

Field testing of the wingtip shares was conducted on a cultivator during soil cultivation. Experimental samples were installed in the first and second rows of working elements.

Control samples included production wingtip shares that had undergone bulk hardening, high-frequency hardening, and spark hardening.

The tests were conducted under identical agricultural conditions, with controlled tillage depth and operating modes.

Wear of the working parts was determined by changes in the geometric parameters of the wingtip sweep, which were measured before and after testing.

The following parameters were monitored:

l_B – wear along the nose width;

l_b – wear along the wing width;

l_l – wear along the blade length;

l_S – change in overlap area;

l_m – change in working part weight.

Relative wear was determined using the formula:

$$I = ((X_0 – X) / X_0) \times 100\%$$

where:

X_0 – initial parameter value;

X – parameter value after testing.

For a comprehensive characterization of wingtip sweep wear, it is proposed to use the following integrated indicators:

– change in working part overlap area (Js);

– change in average sweep weight.

This approach allows for a more objective assessment of the performance of wingtip sweeps, since maintaining their arrow-shaped shape is the main factor in meeting agricultural requirements.

The test results were processed using a comparative analysis of the experimental and control samples. Relative wear was determined for each hardening variant and compared with the control samples.

Research results

Modern constructions of the working bodies of agricultural machines and the applied methods of strengthening them must ensure a minimum level of wear and a reduction in traction resistance with mandatory observance of agrotechnical requirements. Fig. 1 shows the scheme of applying a hardening coating, which helps to reduce the intensity of wear.

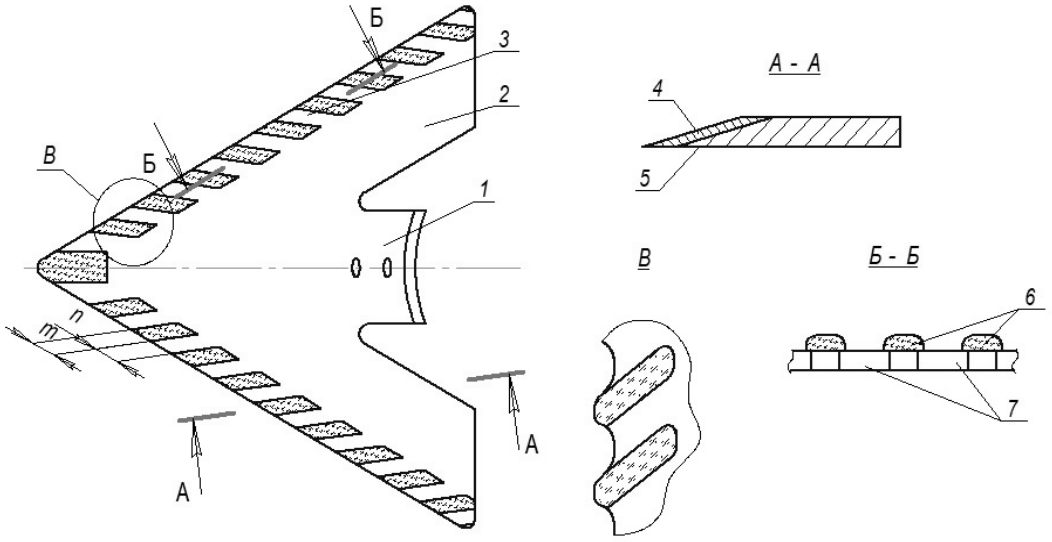

Fig. 1. Scheme of application of a hard alloy with subsequent high-energy heating (pulse heating): 1, 2 – shank and wing of the arrow paw; 3 – hardened layer on the cutting surface; 4 – cross section of the hardened layer; 5 – base metal

In this regard, the working body of the agricultural machine was developed, the design of which allows, with the gradual dulling and change of the geometry of the blade, arising as a result of abrasive wear during operation, to prevent a situation in which soil particles stop in front of the cutting edge and are pressed into the soil layer.

In addition, a technological process was proposed, which allows simultaneous surfacing of a hard alloy and hardening of individual parts of the working bodies of agricultural machines in a special inductor (Fig. 2).

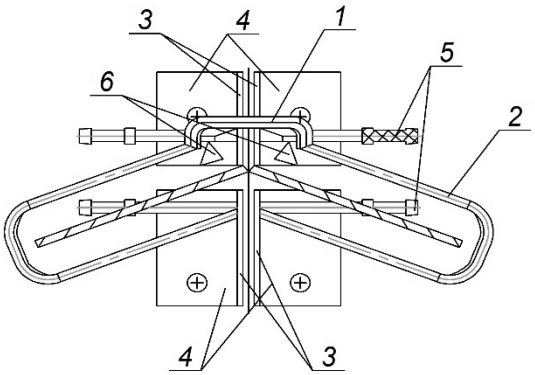

Fig. 2. Inductor for simultaneous surfacing of the nose part of the arrow paw and hardening of its wings: 1, 2 – naplavochny and zakalochny turns; 3 – current conduit; 4 – plate for connection to the generator; 5 – fitting; 6 – profiled tube for melting the charge material

The developed and manufactured inductor provides the necessary modes of hardening of both welded and stamped arrow legs when performing electro-induction surfacing of the nose part with simultaneous hardening of the wings. The working bodies, made of steel 50, 50KhGA and 65G, were subjected to the process of boronization, after which tests of the formed hardened layer were carried out in real field conditions of operation.

Table 1

Relative wear of surface-hardened arrow feet

Plastering code	Wear by parameter l_x, %					Installation diagram for a field (row-crop) cultivator
	B	b	l	S	m	
1-2-WP, O	12.1	17.2	20.7	33.8	28.6	first row
II-1-AP, O	12.7	27.9	21.5	33.4	34.5	second row
III-1-WP, O	12.3	16.8	20.9	34.9	28.6	first row
III-2-AP, O	19.1	22.4	29.6	41.2	33.3	second row
V-2-WP, C	9.9	8.8	13.7	23.5	19.1	first row
V-2-WP, C	9.3	16.3	13.2	25.2	25.0	second row
IV-1-WP, O	27.4	33.8	30.0	49.4	44.1	first row
IV-2-AP, O	28.2	52.3	33.3	51.8	55.9	second row
I-1-WP, O	8.4	11.1	13.6	23.5	20.2	first row
I-1-WP, C	13.4	13.1	18.9	31.1	22.6	second row
VI-2-AP, C	25.9	36.4	31.3	50.5	35.7	first row
Control	19.9	43.6	32.5	50.4	40.5	second row

The analysis of the data presented in Table 1 shows that the influence of the investigated technological factors on the intensity of wear of the hardened working body in real operating conditions is ambiguous. Regardless of the method of applying the coating to the surface of the arrow paws, in all samples with surface hardening, wear is recorded in the range of 8–27% according to individual dimensional parameters. At the same time, control arrow legs tested under similar conditions (both volume hardening and three-stage hardening) show significantly greater wear, which is 25–40%. The appearance of industrially manufactured arrow paws after operation is shown in Fig. 3. The obtained experimental results show that there is a definite relationship between the amount of wear and the parameters of the deposited layer of surface-hardened working bodies. At the same time, despite a significant change in some geometrical parameters (l_B, l_b, l_l), the arrow legs remained operational throughout the entire period of testing. This allows us to conclude that the performance of a worn arrow paw is largely determined not by a change in individual geometric dimensions, but by the ability of the working body to maintain a general arrow-shaped shape.

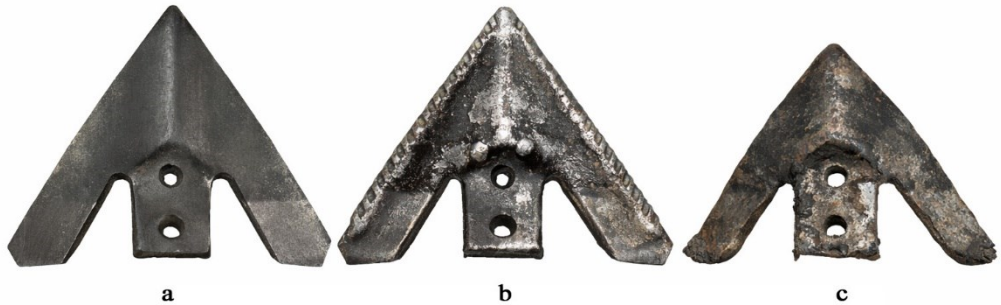

a b c

Fig. 3. Photos of worn arrow paws: a – initial paw; b – paw strengthened according to scheme IV-1-WP after testing; c – serial pawl subjected to volume hardening, surface high frequency currents hardening and electrospark hardening (HRCe ≈ 50) after testing

In this regard, it is proposed to estimate the wear of surface-reinforced arrow feet using integral indicators, such as the change in the overlapping area (J_S) and the average mass loss.

Conclusions

A technological process for hardening the shovel blades of tillage machines has been developed. This process involves electro-induction surfacing of a carbide material followed by pulsed high-energy heating, ensuring the formation of a localized wear-resistant layer on the most heavily loaded areas of the working element.

A special inductor design has been proposed that allows for the combined hardening of the shovel nose and the hardening of its wings, ensuring differentiated hardening of the working surfaces and increasing the technological efficiency of the hardening process.

Experimental studies have shown that the use of the developed coating compositions during boriding of working elements made of grades 50, 50KhGA, and 65G steels promotes the formation of a hardened surface layer with increased resistance to abrasive wear under operating conditions.

Field tests showed that the relative wear of surface-hardened wingtip tines, based on controlled geometric parameters, ranges from 8% to 27%, while the wear of standard wingtip tines hardened using traditional methods (bulk hardening, high-frequency hardening, and spark hardening) reaches 25% to 40%, indicating a 30% to 60% reduction in wear intensity.

It was established that the continued performance of wingtip tines during operation is determined primarily by the maintenance of the overall wingtip shape of the working element, rather than by individual geometric wear parameters. This is crucial for ensuring consistent tillage performance.

It is proposed to use integrated wear indicators, including changes in the overlap area of the working elements and average mass loss, which allow for a more objective assessment of the service life of surface-hardened working elements.

The research resulted in the proposal of new design solutions and technologies for hardening working parts, based on the use of electro-induction surfacing of high-chromium white cast irons and pseudoalloys on 65G and 50KhGA steel for components such as feed mill hammers, as well as welded and solid-stamped wing tines. Implementation of the developed technologies increases the relative wear resistance of the components by 2.0–2.5 times compared to traditional hardening methods, reduces traction resistance during movement in the working environment by 6–8%, and improves the efficiency of agricultural processes.

References

1. Berenji, K. R., Karagüzel, U., Özlü, E., & Budak, E. (2019). Effects of turn-milling conditions on chip formation and surface finish. CIRP Annals, 68, 113–116. https://doi.org/10.1016/j.cirp.2019.03.023.

2. Boivie, K., Karlsen, R., & Ystgaard, P. (2012). The concept of hybrid manufacturing for high performance parts. South African Journal of Industrial Engineering, 23, 106–115. https://doi.org/10.7166/23-4-361.

3. Brecher, C., & Özdemir, D. (2017). Integrative production technology: Theory and applications. Springer International Publishing. https://doi.org/10.1007/978-3-319-47452-6.

4. Ding, H. T., & Shin, Y. C. (2010). Laser-assisted machining of hardened steel parts with surface integrity analysis. International Journal of Machine Tools & Manufacture, 50, 106–114. https://doi.org/10.1016/j.ijmachtools.2009.09.008.

5. Garro, O., Martin, P., & Veron, M. (1993). Shiva, a multiarms machine tool. CIRP Annals, 42, 433–436. https://doi.org/10.1016/S0007-8506(07)61553-0.

6. Jeon, Y., & Lee, C. M. (2012). Current research trend on laser assisted machining. International Journal of Precision Engineering and Manufacturing, 13, 311–317. https://doi.org/10.1007/s12541-012-0178-6.

7. Khatir, F. A., Sadeghi, M. H., & Akar, S. (2021). Investigation of surface integrity in the laser-assisted turning of AISI 4340 hardened steel. Journal of Manufacturing Processes, 61, 173–189. https://doi.org/10.1016/j.jmapro.2020.12.021.

8. Lauwers, B., Klocke, F., Klink, A., Tekkaya, A. E., Neugebauer, R., & Mcintosh, D. (2014). Hybrid processes in manufacturing. CIRP Annals, 63, 561–583. https://doi.org/10.1016/j.cirp.2014.05.004.

9. Liu, J., Ye, C., & Dong, Y. (2021). Recent development of thermally assisted surface hardening techniques: A review. Advances in Industrial and Manufacturing Engineering, 2, 100006. https://doi.org/10.1016/j.aime.2021.100006.

10. Lobanov, D. V., Arkhipov, P. V., Yanyushkin, A. S., & Skeeba, V. Y. (2016). Research of influence electric conditions combined electro-diamond processing on specific consumption of wheel. IOP Conference Series: Materials Science and Engineering, 142, 012081. https://doi.org/10.1088/1757-899X/142/1/012081.

11. Lymar, O., & Marchenko, D. (2022). Prospects for the application of restoring electric arc coatings in the repair of machines and mechanisms. In Proceedings of the 2022 IEEE 4th International Conference on Modern Electrical and Energy System (MEES 2022). https://doi.org/10.1109/MEES58014.2022.10005709.

12. Marchenko, D., Matvyeyeva, K. (2023). Research of Increase of the Wear Resistance of Machine Parts and Tools by Surface Alloying. Problems of Tribology, 28(3/109), 32–40. https://doi.org/10.31891/2079-1372-2023-109-3-32-40.

13. Marchenko, D., Matvyeyeva, K., Kurepin, V. (2024). Increasing the wear resistance of plunger pairs of high-pressure fuel pumps using extreme pressure additives. Problems of Tribology, 29(4/114), 24–31. https://doi.org/10.31891/2079-1372-2024-114-4-24-31.

14. Marchenko, D., Matvyeyeva, K. (2024). Study of Wear Resistance of Cylindrical Parts by Electromechanical Surface Hardening. Problems of Tribology, 29(1/111), 25–31. https://doi.org/10.31891/2079-1372-2024-111-1-25-31.

15. Marchenko, D., Matvyeyeva, K., Lymar, O., Kurepin, V. (2025). Enhancing the reliability and wear resistance of high-speed cutting tools through the use of ionized air-oil lubrication media in machine part restoration. Problems of Tribology, 30(4/118), 72–78. https://doi.org/10.31891/2079-1372-2025-118-4-72-78.

16. Makarov, V. M. (2011). Well integrated technological systems: Prospects and problems of implementation. Repair. Innovation. Technology. Modernization, 6, 20–23.

17. Makarov, V. M., & Lukina, S. V. (2016). Unique synergy of hybrid machines. Repair. Innovation. Technology. Modernization, 8, 18–25.

18. Mitsuishi, M., Ueda, K., & Kimura, F. (2008). Manufacturing systems and technologies for the new frontier. Springer. https://doi.org/10.1007/978-1-84800-267-8.

19. Moriwaki, T. (2008). Multi-functional machine tool. CIRP Annals, 57, 736–749. https://doi.org/10.1016/j.cirp.2008.09.001.

20. Mühl, F., Jarms, J., Kaiser, D., Dietrich, S., & Schulze, V. (2020). Tailored bainitic-martensitic microstructures by means of inductive surface hardening for AISI4140. Materials & Design, 195, 108964. https://doi.org/10.1016/j.matdes.2020.108964.

21. Nagae, A. (2005). Development trend of multi-tasking machines. Proceedings of JSPE Semester Meeting, 2005S, 430. https://doi.org/10.2493/jspe.2005S.430.

22. Sales, W. F., Schoop, J., Silva, L. R. R., & Machado, Á. R., Jawahir, I. S. (2020). A review of surface integrity in machining of hardened steels. Journal of Manufacturing Processes, 58, 136–162. https://doi.org/10.1016/j.jmapro.2020.08.031.

23. Skoblo, T. S., Nanka, O. V., Saichuk, O. V., Rybalko, I. M., Markov, O. V., & Zakharov, A. V. (2021). Theoretical evaluation of structure formation features with the introduction of carbon-containing powder compositions in coatings. Industry in Focus, 5(101), 52–56. [in Ukrainian]

24. Skeeba, V., Pushnin, V., Erohin, I., & Kornev, D. (2015). Integration of production steps on a single equipment. Materials and Manufacturing Processes, 30, 1408–1411. https://doi.org/10.1080/10426914.2014.951679.

25. Rybalko, I. M., Tikhonov, O. V., & Zakharov, A. V. (2021). Development of a method to increase the wear resistance of cultivator arrow-shaped shovels. In Abstracts of the VIII International Scientific and Technical Conference “Kramarovsky Readings” (pp. 68–71). Kyiv: NUBiP of Ukraine. [in Ukrainian]

26. Rybalko, I. M., Saichuk, O. V., & Zakharov, A. V. (2022). Electroslag surfacing of product surfaces with composite wear-resistant additives. In Abstracts of the IX International Scientific and Technical Online Conference “Kramarovsky Readings” (pp. 56–59). Kyiv: NUBiP of Ukraine. [in Ukrainian]

27. Yang, Y., Gong, Y., Qu, S., Rong, Y., Sun, Y., & Cai, M. (2018). Densification, surface morphology, microstructure and mechanical properties of 316L fabricated by hybrid manufacturing. International Journal of Advanced Manufacturing Technology, 97, 2687–2696. https://doi.org/10.1007/s00170-018-2127-2.

28. Yamazaki, T. (2016). Development of a hybrid multi-tasking machine tool: Integration of additive manufacturing technology with CNC machining. Procedia CIRP, 42, 81–86. https://doi.org/10.1016/j.procir.2016.02.016.

29. Yanyushkin, A. S., Lobanov, D. V., & Arkhipov, P. V. (2015). Research of influence of electric conditions of the combined electro-diamond machining on quality of grinding of hard alloys. IOP Conference Series: Materials Science and Engineering, 91, 012051. https://doi.org/10.1088/1757-899X/91/1/012051.

30. You, K., Yan, G., Luo, X., Gilchrist, M. D., & Fang, F. (2020). Advances in laser assisted machining of hard and brittle materials. Journal of Manufacturing Processes, 58, 677–692. https://doi.org/10.1016/j.jmapro.2020.09.025.

Марченко Д.Д., Матвєєва К.С. Розробка та дослідження технології електроіндукційного наплавлення деталей робочих органів сільськогосподарських машин

У статті розглянуто питання щодо підвищення зносостійкості робочих органів сільськогосподарських машин, що експлуатуються в умовах інтенсивного абразивного зношування. Об'єктом дослідження були стрілчасті лапи культиваторів, виготовлені з конструкційних сталей 50, 50ХГА та 65Г. Метою роботи є розробка та наукове обґрунтування технології електроіндукційного наплавлення зносостійких покриттів на основі сплавів систем Fe–Cr–C та Fe–Cr–C–B, що забезпечує формування оптимальної структури наплавленого шару та підвищення експлуатаційних характеристик робочих органів. Запропоновано технологічний процес зміцнення, що включає електроіндукційне наплавлення твердосплавного матеріалу з наступним імпульсним високоенергетичним нагріванням, а також конструкція спеціального індуктора, що дозволяє одночасно виконувати наплавлення носової частини стрілчастої лапи та загартування її крил. Додатково досліджено вплив хіміко-термічної обробки (борування) на формування зміцненого поверхневого шару. Польові випробування проводилися в умовах обробки ґрунту на культиваторі з використанням дослідних та контрольних зразків. Знос робочих органів оцінювався щодо зміни геометричних параметрів, площі перекриття та втрати маси. Встановлено, що відносне зношування поверхнево-зміцнених стрілчастих лап становить 8–27%, тоді як у серійних деталей, зміцнених традиційними методами, він досягає 25–40%. Це свідчить про зниження інтенсивності зношування на 30–60%. Показано, що працездатність стрілчастих лап у процесі експлуатації визначається переважно збереженням їхньої загальної стрілоподібної форми. Для більш об'єктивної оцінки зношування запропоновано використовувати інтегральні показники, що включають зміну площі перекриття робочих органів та середню втрату маси. Розроблені технологічні рішення дозволяють підвищити відносну зносостійкість робочих органів у 2,0–2,5 рази, знизити тяговий опір при їх роботі у ґрунті на 6–8 % та підвищити ефективність агротехнічних процесів.

Ключові слова: електроіндукційна наплавка, зносостійкі покриття, абразивний знос, стрілчаста лапа, робочі органи сільськогосподарських машин, борування, сплави системи Fe–Cr–C, сплави системи Fe–Cr–C–B, зміцнення поверхні, зносостійкість.

ISSN 2079-1372 Problems of Tribology, V. 31, No 1/119-2026, 80-85

Problems of Tribology
Website: http://tribology.khnu.km.ua/index.php/ProbTrib
E-mail: tribosenator@gmail.com

DOI: https://doi.org/10.31891/2079-1372-2026-119-1-80-85

Study of tribotechnical characteristics of composite coatings formed by the method of electrospark alloying

O. Mikosianchyk[1*]0000-0002-2438-1333, V. Shamrai[1]0000-0002-1746-5213, L. Lopata[2]0000-0003-2019-0609, R. Mnatsakanov[1]0000-0001-5035-2432, P. Nosko[1]0000-0003-4792-6460, I. Semak[1]0000-0001-9742-3226

[1]*National University «Kyiv Aviation Institute», Ukraine*
[2]*G.S. Pisarenko Institute for Problems of Strength of National Academy of Sciences of Ukraine*
**E-mail: oksana.mikos@ukr.net*

Received: 30 January 2026: Revised 20 February 2026: Accept: 05 March 2026

Abstract

The results of studying the tribotechnical characteristics of composite coatings formed by the electric spark alloying (ESA) method are presented. It has been established that the key factor in controlling the stress-strain state of the "coating-base" system is the optimization of the thickness and continuity of the strengthened layer. Using the finite element method, it was demonstrated that for coatings with a thickness of 100 μm, the minimum stress concentration is achieved when the coating continuity is within 60–80%. Deviations from these values (less than 50% or greater than 80%) lead to an increase in local stresses. Modeling showed that the maximum equivalent stresses are localized at depths up to 30 μm for BK8 coatings and up to 50 μm for KHN25 coatings (with a total layer thickness of 120 μm), which reduces the stress–strain state of the substrate under external loading. Experimental abrasive wear tests in an environment with loosely fixed abrasive particles showed that the minimum weight loss is achieved when the coating continuity is 55–75%, with an optimal value of 70% and a ratio of strengthened to unstrengthened areas of 2:1. Comparative analysis of materials revealed that coatings made of WC-8Co alloy (microhardness 10000 MPa) exhibit 1.8–2 times higher weight wear compared with KHN25 alloy (microhardness 8500 MPa). This is explained by the increased fragility of WC-8Co and the low content of the cobalt matrix, which leads to chipping and groove formation when in contact with abrasive particles up to 250 μm in size. The obtained results make it possible to scientifically justify the selection of ESA modes and electrode material compositions for the restoration of machine parts operating under conditions of intensive abrasive action.

Ключові слова: electric spark alloying, coating, wear resistance, abrasive wear, stress–strain state, tribotechnical characteristics.

Introduction

Ensuring the operational reliability and competitiveness of modern mechanical engineering depends on the development of effective methods for strengthening working surfaces. Since significant material losses are caused by friction and premature wear of tribological units, the search for technologies for forming wear-resistant structures is a priority task [1]. A promising tool for surface modification is the ESA method. It allows not only the creation of layers with high hardness and corrosion resistance but also the effective restoration of worn parts while minimizing thermal loads on the substrate. Due to its low energy consumption and the possibility of local control over the properties of the formed coatings, ESA meets modern environmental and economic requirements. The study of the micromechanical characteristics of such layers opens the way to scientifically grounded control of wear kinetics and improvement of technologies for creating composite protective coatings.

Literature review

A key stage in designing the technological process of electric spark alloying is the scientifically justified selection of electrode materials, since they determine the final functional parameters of the coating. According to

an analysis of scientific studies [2–4], the efficiency of forming composite layers depends on a complex of factors, among which the leading role is played by the physicochemical compatibility of the anode with the substrate surface, the features of reverse mass transfer, and the specifics of structure formation on the working surfaces of electrodes.

Since alloying elements are transferred directly under the action of electrical discharges, the composition of the selected material directly correlates with the wear resistance and anticorrosion characteristics of the strengthened part [5, 6]. Modern criteria for electrode selection require high electrical conductivity to stabilize discharge processes, as well as thermal and mechanical resistance to extreme loads in the processing zone. Particular attention in research is paid to the ability of materials to form stable phases, which is a critical factor for ensuring high adhesion and durability of protective coatings under complex operating conditions [7–9].

The choice of components of composite materials is limited by their compatibility [10]. Solving the problem of regulating the compatibility of components within a single coating makes it possible to fully utilize the tribotechnical properties of composite coatings. When selecting composite coatings, it is necessary to consider the ability of the part material to physically and mechanically interact with the coating material. The coefficients of thermal expansion of the strengthened part material and the coating material should differ minimally to ensure maximum adhesion strength between the coating and the surface of the part.

Under conditions of modern development of materials science, the electric spark alloying method is gaining particular relevance as a highly effective technology for surface modification that opens new opportunities for the functional improvement of parts in leading industries. Modern ESA research is focused on the development of innovative electrode materials, particularly those based on refractory compounds and nanostructured additives [12], which significantly expand the application limits of this method for extreme operating conditions.

To improve the tribotechnical properties of parts, it is advisable to use metal-matrix composite materials with ceramic fillers [11]. The choice of metal-matrix composites is justified by high values of strength characteristics, elastic modulus, and their stability up to the melting temperatures of the base metal. The main function of ceramic fillers is to strengthen the metal matrix of composite materials and the composite coating as a whole.

The study of tribotechnical properties of composite coatings makes it possible to scientifically control wear processes and improve technologies for creating protective coatings.

Purpose

To evaluate the tribotechnical properties of composite electric spark coatings (ESC), taking into account the physicomechanical interaction between the material of the material and the coating.

Objects of research and experimental conditions

The electric spark alloying process was carried out using an “Elitron-22” installation at a discharge energy of 0.5 J, operating current I = 0.5…1.5 A, voltage U = 25…55 V and electrode cross-section of 4–16 mm². During coating formation, the electrode was moved relative to the tool surface at a speed of 1…5 m/s.

During electric spark alloying of steels, electrodes made of tungsten carbide hard alloy WC-8Co and composite powder material KHN-25 were used (Table 1).

Table 1

Composition of composite powder KHN-25 (wt.%)

Alloy grade	Chromium carbide (%)	Nickel (%)
KHN-25 (Cr-Ni-C)	73..75	22…25

By varying the voltage and current during electric spark alloying, it is possible to control the ratio between coating continuity and thickness. This ratio determines the operational reliability of strengthened surfaces and improves the tribotechnical properties of the strengthened surface layer. The choice of EAS modes, electrode material, and material of the part to be strengthened is presented in Table 2.

Table 2

Selection of base material, electrode material, and ESA regimes

No.	Base material	Electrode material	Current (A)
1	40Cr13	KHN25	2.5
2	65G	WC-8Co	3.7

Experimental evaluation of coating wear resistance was performed on a specialized test stand according to GOST 23.208-79, which correlates with the international standard ASTM G65. The experiment simulated surface destruction under the action of loosely fixed abrasive particles with grain size up to 250 μm.

Analysis of the main results

As a result of modeling the stress - strain state of the electric-spark coating–substrate system using the finite element method in the licensed software package MSC Visual Nastran for Windows, it was established that for electric-spark coatings with a discontinuous structure, a reduction of shear loading in the substrate material can be achieved by increasing the continuity of the coating. An increase in coating continuity ensures the localization of shear stress within local regions of the coating. A reduction in the shear component of the load and an optimal distribution of the specific normal load over the contact zone can be achieved by decreasing the size of the coating contact areas with the part surface and by applying the coating with a continuity of 60…80%. In this case, the value of the specific normal distributed load increases less than the shear load decreases.

When the coating continuity increases to >80% (i.e., the distance between coating parts decreases) or decreases to <50%, stress concentration increases. For coatings of different thicknesses, the maximum reduction in stresses is observed at a coating continuity of 60…80% (Figure 1, 2).

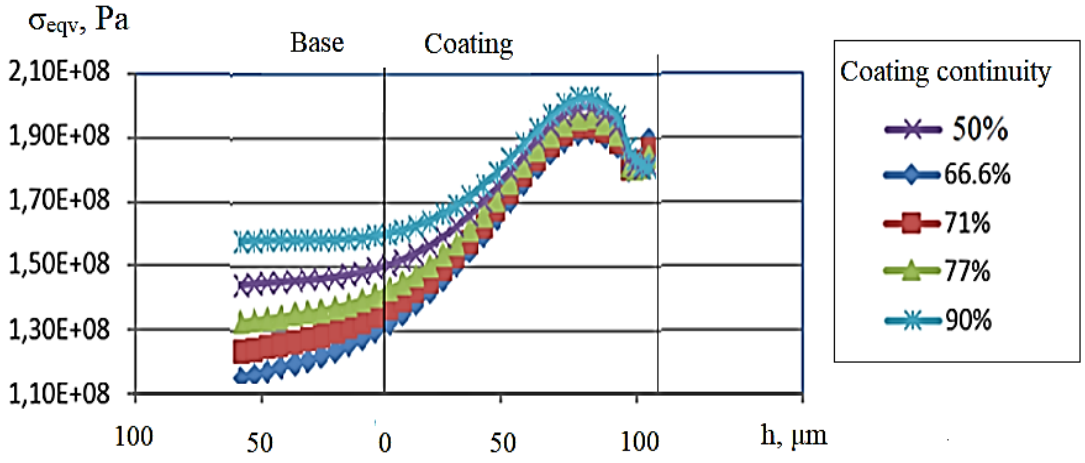

Fig. 1. Equivalent stresses along the depth from the coating surface into the substrate (65G steel) as a function of the continuity of the WC-8Co coating (coating thickness (h) 120 μm).

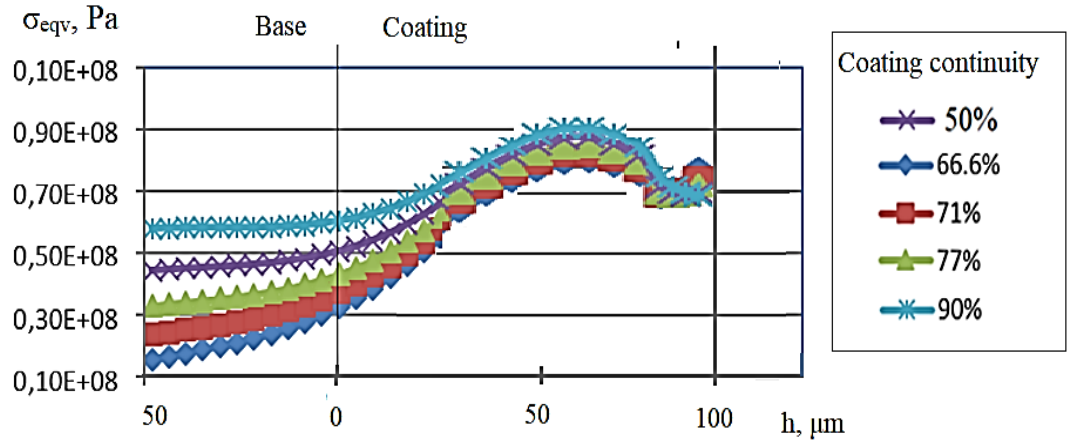

Fig. 2. Equivalent stresses along the depth from the coating surface into the substrate as a function of the continuity of the KHN25 coating (coating thickness (h) 120 μm).

It was established that the harder WC-8Co material forms a coating that ensures localization of the maximum equivalent stresses along the depth up to 30 μm, while a coating of lower hardness, KHN25, ensures localization of the maximum equivalent stresses at a depth of up to 50 μm for a coating thickness of 100…300 μm. Regardless of the coating type, the maximum equivalent stresses develop within the coating itself, which reduces the stress–strain state of the substrate.

The use of electric-spark composite coatings with an optimal combination of thickness and continuity makes it possible to improve the tribological performance of strengthened and restored components.

Applying a coating with variable continuity is achieved by changing the electrode movement speed. During ESA, moving the electrode allows the formation of different topographies of the coating on the strengthened surface of the part. By adjusting the current and voltage, it is possible to control the ratio of coating continuity to its thickness.

Composite coatings with variable continuity were formed in the form of microzones (up to 1.0 mm) by changing the electrode movement speed, allowing control of the coating continuity within the range of 20…90%.

To select the optimal continuity of the coatings, which would provide high abrasive resistance, experiments were conducted in an abrasive environment under sliding conditions. Figure 3 shows the dependence of the weight wear of the coating on its continuity (ψ).

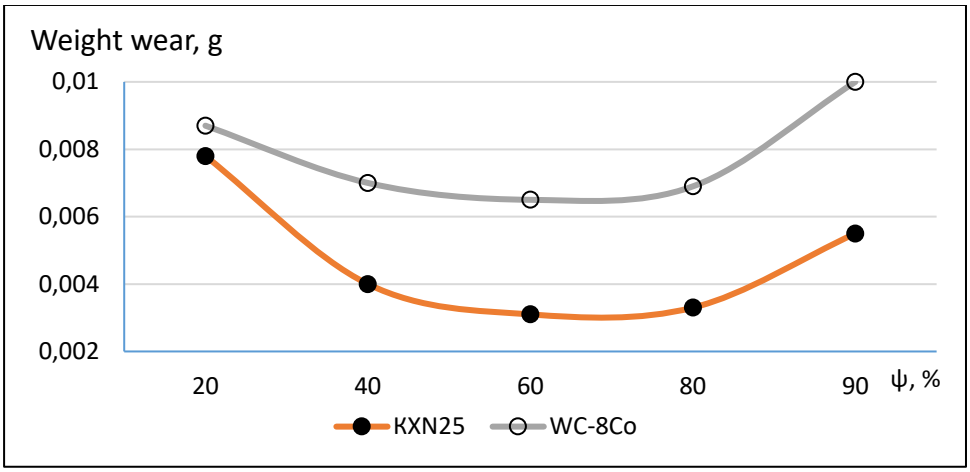

Fig. 3. Dependence of the weight wear of experimental samples with ESA coatings on the coating continuity.

At a continuity of ψ = 55…75%, minimal abrasive wear of the electrical discharge coatings is observed, regardless of the type of coating studied. It has been determined that the best quality indicators of the reinforced surfaces are obtained at a continuity of ψ = 70% and with a ratio of reinforced to non-reinforced areas of the coating of 2:1.

For ESC WC-8Co, the mass loss under the action of loose abrasive particles is 1.8–2 times higher than the mass loss of ESC KHN25. This is related to the fact that the microhardness of ESC WC-8Co is 1.3 times higher than that of the KHN25 coating (microhardness of WC-8Co – 10000 MPa, KHN25 – 8500 MPa), which causes brittleness of this coating. Additionally, the high microhardness of the BK8 coating leads to a decrease in resistance to abrasive wear due to a reduction in tangential shear resistance when a hard abrasive particle penetrates, which is explained by the low fraction of the matrix component (cobalt) in the structure of the BK8 hard alloy. The friction tracks of ESC WC-8Co are characterized by the presence of large grooves and signs of chipping (Fig. 4). For ESC KHN25, the friction tracks are characterized by a uniform structure, indicating a high degree of resistance of ESC to the penetration of abrasive particles.

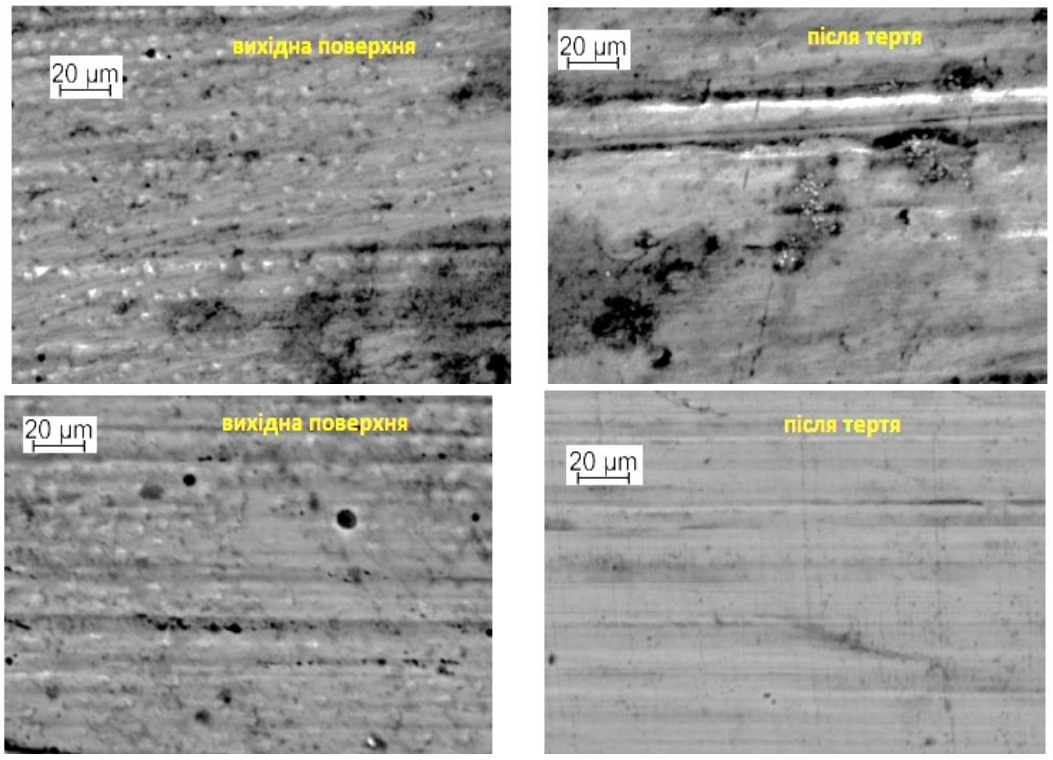

Fig. 4. Appearance of the initial surface and the surface after friction under the influence of loose abrasive particles: a) – WC-8Co, b) – KHN25.

Thus, the established dependencies allow scientifically justified control of wear kinetics by varying alloying regimes to achieve an optimal balance between continuity, thickness, and toughness of composite coatings.

Conclusions

1. Finite element modeling showed that the minimum stress–strain state of electric spark coatings can be achieved by selecting optimal values of coating thickness and continuity. When continuity exceeds 80% or drops below 50%, stress concentration increases. Maximum stress reduction occurs at 60..80% continuity.

2. It was determined that the minimum abrasive wear of discrete electric spark coatings occurs at a continuity of 55..75%. KHN25 coatings demonstrated the highest resistance to abrasive particle penetration.

3. For ESC (electric spark coating) WC-8Co coatings, weight wear under loose abrasive particles is 1.8-2 times higher than for KHN25 coatings, due to the higher microhardness (1.3 times greater), increased brittleness, reduced tangential shear resistance during abrasive penetration, and the low cobalt matrix content in the WC-8Co alloy.

References

1. Mikosianchyk O. O., Skvortsov O. O., Kornienko A. O. Improving the wear resistance of structural steels by electrospark deposition. *Проблеми тертя та зношування,* 2025. 2 (107). С.40-47. https://doi.org/10.18372/0370-2197.2(107).20145

2 C. Barile, C. Casavola, G. Pappalettera, G. Renna Advancements in Electrospark Deposition (ESD) Technique: A Short Review. *Coatings.* 2022. 12 (10). P. 1536. DOI: https://doi.org/10.3390/coatings12101536

3. Storozhenko M.S., Umansky O.P., Sheludko V.E., Gubin Yu.V., Kurinna T.V. Development of technologies and materials for electric spark coating with the aim of increasing service life and reliability of parts of technological and power equipment and tools. *Automatic Welding*. 2020. №10. P. 21-25. DOI: https://doi.org/10.37434/as2020.10.04

4. Wang J., Zhang M., Dai S., Zhu L. Research Progress in Electrospark Deposition Coatings on Titanium Alloy Surfaces: A Short Review. *Coatings* 2023. *13*. 1473. https://doi.org/10.3390/coatings13081473

5. Holubets V.M., Pashechko M.I., Borc J., Tisov O.V., Shpuliar Y.S. Wear Resistance of Electrospark-Deposited Coatings in Dry Sliding Friction Conditions. *Powder Metallurgy and Metal Ceramics*. 2021. vol.60. P.90-96. https://doi.org/10.1007/s11106-021-00218-0

6. V.B. Tarelnyk, O.P. Gaponova, G.V. Kirik et al. Cementation of steel details by electrospark alloying. *Metallofiz. Noveishie Tekhnol*. 2020. Vol. 42 (5). P. 655–667. DOI: https://doi.org/10.15407/mfint.42.05.0655

7. Kozak, F. V., Prunko, I. B., Fedenko, V. Y., Gladun, M. R. Optimization of the process of application of electrospark coatings when strengthening automotive parts of the “shaft” type. *Oil and Gas Power Engineering*. 2024. (2(40). P. 66–72. https://doi.org/10.31471/1993-9868-2023-2(40)-66-72

8. Habibi F., Samadi A. In-situ formation of ultra-hard titanium-based composite coatings on carbon steel through electro-spark deposition in different gas media. *Surface and Coatings Technology*. 2024. Vol. 478. 130472 https://doi.org/10.1016/j.surfcoat.2024.130472

9. Skvortsov O., Mikosianchyk O. The dependence of the wear resistance of electro-spark coatings in an abrasive environment on the strengthening phases. *Problems of friction and wear*. 2024. No. 3(104). P.78-90. https://doi.org/10.18372/0370-2197.3(104).18983

10. Lopata L., Kachynska I., Solovykh A., Katerinich S. Creation of wear-resistant composites coated on the basis of powder-based self-flowing alloys by electro-contact sintering. *Problems of friction and wear*. 2024. (3(104). P. 15–22. https://doi.org/10.18372/0370-2197.3(104).18974

11. Marchenko, D., Matvyeyeva, K. Increasing the Wear Resistance of Restored Car Parts by Using Electrospark Coatings. *Problems of Tribology*. 2023. 28(1/107). С. 65–72. https://doi.org/10.31891/2079-1372-2023-107-1-65-72

12. Gildersleeve, E.J., Vaßen, R. Thermally Sprayed Functional Coatings and Multilayers: A Selection of Historical Applications and Potential Pathways for Future Innovation. *J Therm Spray Tech. 2023.* 32. P. 778–817. https://doi.org/10.1007/s11666-023-01587-1

Мікосянчик О. О., Шамрай В.Б., Лопата Л.А., Мнацаканов Р.Г., Носко П.Л., Семак І.В. Дослідження триботехнічних характеристик композиційних покриттів, сформованих методом електроіскрового легування

Представлено результати дослідження триботехнічних характеристик композиційних покриттів, сформованих методом електроіскрового легування. Встановлено, що ключовим фактором керування напружено-деформованим станом системи «покриття — основа» є оптимізація товщини та суцільності зміцненого шару. За допомогою методу скінченних елементів доведено, що для покриттів товщиною 100 мкм мінімальна концентрація напружень досягається при суцільності в межах 60–80%. Відхилення від цих значень (менше 50% або більше 80%) призводить до зростання локальних напружень. Моделювання показало, що максимальні еквівалентні напруження локалізуються на глибині до **30 мкм** для ВК8 та до **50 мкм** для КХН25 (при загальній товщині шару 120 мкм), що знижує напружено-деформований стан основи в умовах дії зовнішнього навантаження. Експериментальні випробування на абразивне зношування в середовищі нежорстко закріпленим абразивом показали, що мінімальний ваговий знос забезпечується при суцільності покриття 55–75%, з оптимальним показником 70% та співвідношенням зміцненої і незміцненої ділянок 2:1. Порівняльний аналіз матеріалів виявив, що покриття зі сплаву ВК8 (мікротвердість 10000 МПа) має у 1,8–2 рази вищий ваговий знос порівняно зі сплавом КХН25 (мікротвердість 8500 МПа). Це пояснюється підвищеною крихкістю ВК8 та низьким вмістом кобальтової матриці, що призводить до викришування та утворення борозен при контакті з абразивними частками розміром до 250 мкм. Отримані дані дозволяють науково обґрунтовано підбирати режими ЕІЛ та склад електродних матеріалів для відновлення деталей машин, що працюють в умовах інтенсивного абразивного впливу.

Ключові слова: електроіскрове легування, покриття, зносостійкість, абразивне зношування, напружено-деформований стан, триботехнічні характеристики.

ISSN 2079-1372 Problems of Tribology, V. 31, No 1/119-2026, 86-91

Problems of Tribology
Website: http://tribology.khnu.km.ua/index.php/ProbTrib
E-mail: tribosenator@gmail.com

DOI: https://doi.org/10.31891/2079-1372-2026-119-1-86-91

Equipment and technology for gas fluorination of polymers to improve their wear resistance under micro-impact loads

A. Martyniuk*[1][0000-0001-8277-1308], **M. Stechyshyn[1]**[0000-0001-5780-2790], **V. Fedoriv[1]**[0000-0002-4499-0910], **P. Yaroshenko[2]**[0000-0003-0112-0963], **V. Liukhovets[1]**[0000-0002-6978-7820]

[1]Khmelnytskyi National University, Ukraine
[2]Sumy National Agrarian University, Ukraine
**E-mail: avmart@khmnu.edu.ua*

Received: 05 February 2026: Revised 25 February 2026: Accept: 10 March 2026

Abstract

The article addresses the problem of improving the cavitation–erosion wear resistance of polymer materials operating under micro-impact loads in corrosive environments. It is shown that material degradation under such conditions has a complex mechano-corrosive nature, while corrosion processes can significantly accelerate the degradation of surface layers. In this regard, the use of polymers with high chemical resistance and inertness to aggressive media is relevant. However, the application of such highly resistant polymers is often economically impractical, which necessitates the development of methods for surface modification of available structural polymers to improve their performance properties. he aim of this work is to develop and scientifically substantiate a laboratory installation and technological parameters of the direct gas fluorination process for polymer materials in order to form a modified surface layer without altering the surface microgeometry and to increase their wear resistance. Polypropylene grade 21060, widely used in mechanical engineering, agricultural machinery, and food equipment due to its sufficient strength, chemical resistance, and processability, was selected as the object of the study. A laboratory installation for direct gas fluorination of polymers was designed using a gas mixture of 1% F_2 and 99% Ar followed by treatment with nitric oxide to neutralize active radicals. Experimental studies showed the formation of a modified surface layer about 5 μm thick with increased chemical inertness. It was established that fluorination significantly reduces the intensity of cavitation–erosion wear of polypropylene in various environments, confirming the effectiveness of the method for improving the durability of polymer components.

Keywords: gas fluorination, polypropylene, surface modification, cavitation–erosion wear, aggressive environments, micro-impact loads.

Introduction

The cavitation–erosion wear resistance of metallic alloys in corrosive environments is determined by both mechanical and corrosion-related factors of material degradation. Corrosion itself does not usually cause significant mass loss; however, it acts as a catalyst for fatigue failure of metallic surfaces subjected to micro-impact loading in corrosive media. Therefore, corrosion resistance, and in many cases complete chemical inertness to aggressive environments, has stimulated the interest of researchers and practitioners in the use of polymer components that operate in contact with corrosive media, particularly under friction and cavitation conditions [1].

On the other hand, polymers characterized by high chemical resistance or complete chemical inertness are relatively expensive and their application is often limited at elevated temperatures [2]. Therefore, from an economic perspective it is advantageous to manufacture equipment components from inexpensive and readily available polymers and subsequently modify only their surface layer in order to obtain the required performance characteristics [3]. One of the effective methods of surface modification of polymers is the method of direct gas fluorination [3].

The term direct fluorination of polymers usually refers to the process of heterogeneous interaction between polymer surfaces and gaseous molecular fluorine (F_2) or gas mixtures containing fluorine together with N_2, He, Ar, O_2, etc. Direct fluorination has several important practical advantages: the process occurs at room temperature with a sufficiently high rate and does not require heating or additional activation by ultraviolet

radiation, catalysts, or γ-radiation. At the same time, only a thin surface layer of polymers with a thickness of approximately 0.01–10 μm is modified, while the geometric dimensions of the polymer remain unchanged [3].

The direct fluorination process is widely used on an industrial scale to improve the barrier properties and chemical resistance of polymer automotive fuel tanks [3–5]. However, studies investigating the effect of direct fluorination on improving the cavitation–erosion resistance of polymers under cavitation–erosion wear are practically absent.

On the other hand, in the food industry and the agro-industrial sector, polyethylene and polypropylene (polyolefins) and their modifications are most widely used for manufacturing equipment components [6]. This is explained by the fact that polypropylene, in particular, exhibits high chemical inertness, is approved for full contact with food products, and can be readily processed both by machining and by molding [6].

Therefore, the aim of this work is to develop and scientifically substantiate the design of an installation and the technological parameters of the gas fluorination process for polymer materials in order to form a modified surface layer without altering the surface microgeometry and to increase their wear resistance under micro-impact loading in corrosive environments.

Materials and Methods for Experimental Studies

Polypropylene grade 21060 (hereinafter referred to as PP) was selected for the study because this material is one of the most widely used structural thermoplastics. It is extensively applied in mechanical engineering, agricultural machinery, and transport equipment due to its combination of sufficient mechanical strength, chemical resistance, low density, and good processability. Polypropylene is characterized by relatively low surface energy and limited wear resistance under impact–friction loading, which makes modification of its surface layer advisable. Gas fluorination enables modification of the chemical composition and structure of the polymer surface without significantly affecting its bulk properties, making polypropylene a promising material for investigating the effectiveness of such modification aimed at improving wear resistance under micro-impact loading.

For cavitation–erosion testing, a laboratory setup with a magnetostrictive vibrator (MSV) was designed and manufactured. The system includes an ultrasonic vibration generator UZDN-A, a container for the working media with a specimen mounting unit, and a cooling system. The generator power is 130 W, the operating frequency is 22 kHz, and the amplitude of the concentrator oscillations ranges from 22 to 65 μm (Fig. 1) [6].

For experiments in aggressive environments, the container for the working media (1) and the specimen mounting unit (2) were made of fluoroplastic F4. Two coil-type heat exchanger circuits with counter-directional flows of tap water were installed inside the container (Fig. 1). The first heat exchanger (3) maintains stabilization of the average temperature of the working medium throughout the entire volume of the container, while the second heat exchanger (4) is located directly in the cavitation zone. To increase the heat transfer coefficient, the pitch of the turns of circuit 4 was experimentally selected to be 4–5 mm (Fig. 1). This pitch ensures free movement of differently heated volumes of the working medium between the turns of the coil during different phases of incident and reflected ultrasonic waves. In addition, the opposite directions of the coil turns provide counterflow of cooled and heated volumes of the working solution. As a result, countercurrent flow is achieved, increasing the heat transfer coefficient and improving the efficiency of temperature stabilization of the working medium [1,6,7].

Stabilization of the temperature in the cavitation zone at the ambient temperature increases the reliability and accuracy of evaluating cavitation–erosion wear resistance, bringing the experimental conditions closer to the real operating conditions of components and assemblies of hydraulic machines [1,6-8].

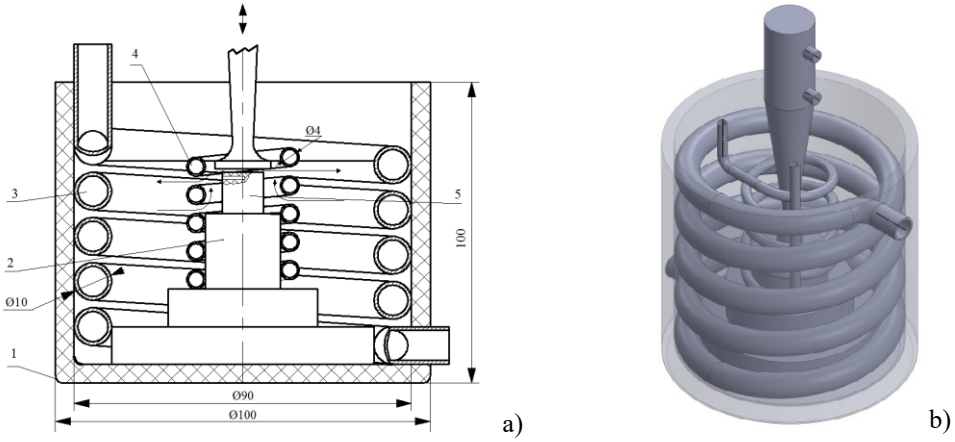

Fig. 1. Capacity for working environments with a sample attachment unit and a two-circuit cooling system: a) installation diagram; b) general view of the installation. 1 – container, 2 – sample attachment unit, 3 – external cooling circuit, 4 – internal cooling circuit, 5 – sample.

The wear resistance of the samples was tested in neutral (3% sodium chloride solution), alkaline (calcium oxide CaO – 250 g/L + sucrose – 15% by mass of CaO), and acidic (disodium phosphate Na_2HPO_4 – 10 g/L + citric acid $C_6H_8O_7$ – 5 g/L) environments, which are typical model solutions used in the food industry and the agro-industrial sector [7].

Results and Discussion

A laboratory setup for direct gas fluorination of polymers was designed and fabricated for the experimental studies (Fig. 2).

The model of the designed setup is shown in Fig. 2. The installation operates as follows: the reactor 2 (fluorination chamber), made of stainless steel 12X18H10T (hereinafter stainless steel), is mounted on the platform 1. The gas mixture is supplied to the reactor through the inlet pipe 3 and evacuated through a cascade of filters for fluorine neutralization by a fore-vacuum pump via the outlet pipe 4.

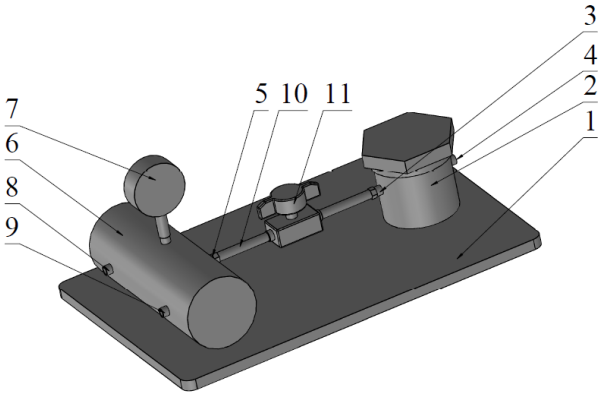

Fig. 2. Model of the laboratory setup: 1 – mounting plate; 2 – reactor; 3 – flange for fluorinating mixture inlet; 4 – flange for fore-vacuum pump; 5 – flange for fluorination supply; 6 – mixing container; 7 – pressure sensor; 8 – flange for Ar and NO supply; 9 – flange for F_2 supply; 10 – connecting pipes; 11 – valve.

The fluorinating mixture is prepared in the container 6, with gas pressure monitored by a manometer 7. Gases are fed into the container through inlet pipes 8 (Ar and NO) and 9 (F_2). Check valves installed in pipes 8 and 9 prevent backflow of the mixture after disconnecting the supply lines.

Once the mixture is prepared, the container is placed on the platform, and via pipe 10 it is connected from the outlet flange 5 (valve not shown in the figure) to valve 11 (type Ду), which is fixed on the frame and connected to the reactor via a stainless steel pipe.

Inside the reactor (Fig. 3), four polymer samples 2 are installed into copper sleeves 1 soldered with silver into the reactor body. This configuration ensures that only the wear surface of each sample is fluorinated. Such placement significantly reduces fluorine (F_2) consumption and also serves as a heat sink and catalyst for the sample during fluorination.

After the samples are installed, the reactor 3 is closed with a lid 5 sealed with a fluoroplastic gasket 4. Additionally, the threaded connection between the lid and reactor body is sealed with a fluoroplastic tape (FUM tape). Flanges 6 and 7 for mixture supply and evacuation are soldered to the reactor body with silver.

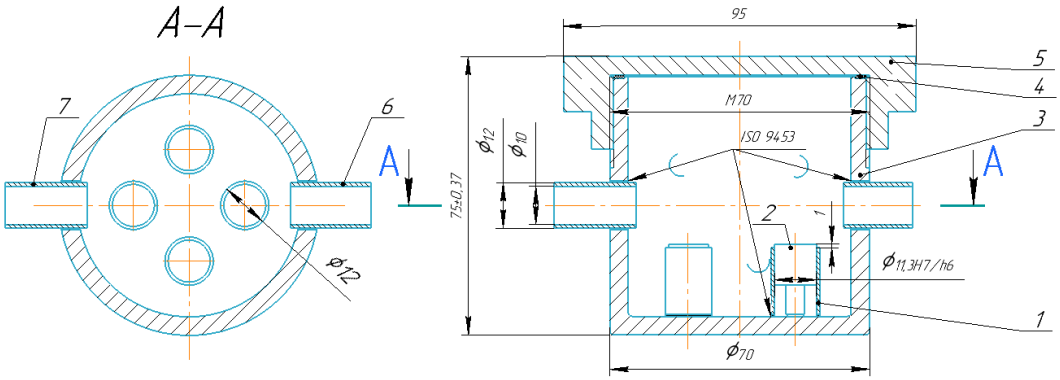

Fig. 3. Reactor (fluorination chamber) of the fluorination setup: 1 – sleeve; 2 – sample; 3 – reactor body; 4 – fluoroplastic gasket; 5 – lid; 6, 7 – outlet and inlet pipes, respectively.

The laboratory setup is equipped with two interchangeable containers (Fig. 2, position 6), which serve for preparing the fluorination mixture and for storing nitric oxide (NO), respectively.

The samples were treated with nitric oxide for 20 minutes to neutralize free radicals formed during the fluorination process. This treatment was carried out at atmospheric pressure and room temperature [3].

For the fluorination process, a fluorine–argon gas mixture was used, consisting of 1% F_2 (fluorine) and 99% Ar (argon) [9]. Argon was chosen due to its relatively low cost and because it ensures a more stable reaction during mixture preparation [9]. Before introducing the fluorinating mixture into the reactor, air was evacuated from the reactor to a residual pressure of (3–4) × 10^{-2} Pa. The reactor was then filled with the fluorine-containing mixture. Experimental conditions (fluorination area, reactor volume, etc.) were selected so that the fluorine consumption did not exceed 5% of the reactor volume.

After a set period, the fluorinating mixture was removed from the reactor, and the fluorine was neutralized in a filter. The pressure was again reduced to the same residual level, and nitric oxide was introduced into the chamber to neutralize remaining free radicals. Afterward, the NO was evacuated, the pressure stabilized, and the samples were extracted for further testing.

All parts of the laboratory setup that come into contact with fluorine or its gas mixtures are made of stainless steel and copper. Pipes and their connections are made of fluoroplastic F4, and all metal and threaded connections are sealed with fluoroplastic FUM tape [9-10]. To ensure safe operation with fluorine and nitric oxide, the setup was installed inside a specially equipped fume hood.

Cavitation–erosion wear resistance tests were performed on two types of samples: original polypropylene 21060 and polypropylene after surface fluorination. Tests were conducted in three environments: alkaline, acidic, and neutral. The thickness of the modified fluorinated layer was approximately 5 μm.

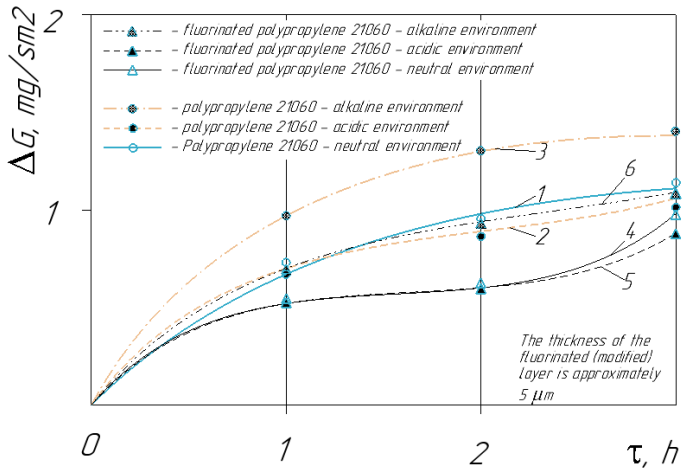

Fig. 4. Wear resistance kinetics of polypropylene 21060 and fluorinated polypropylene 21060 under micro-impact loading in neutral, acidic, and alkaline environments

The analysis of the experimental data (Fig. 4) shows that for all tested samples, the mass loss ΔG increases systematically with the duration of cavitation loading in neutral, acidic, and alkaline environments. The change in ΔG is nonlinear, reflecting the characteristics of the cavitation–erosion wear processes in the polymer material. In the initial stage, ΔG increases relatively rapidly due to active destruction of the surface layer caused by micro-impacts generated during the collapse of cavitation bubbles. Subsequently, the mass loss rate gradually decreases, indicating partial stabilization of the surface and the approach of the wear process to a quasi-stationary regime.

It was found that unfluorinated polypropylene 21060 exhibits the highest intensity of cavitation–erosion wear in an alkaline environment. Under such conditions, the polymer matrix interacts more actively with the components of the medium, and in combination with micro-impact loads induced by cavitation, this leads to accelerated surface degradation. In acidic environments, surface degradation occurs less intensively, resulting in a more moderate increase in ΔG. In neutral media, the mass loss also gradually increases, with wear intensity intermediate between alkaline and acidic conditions. These results demonstrate the significant influence of the chemical nature of the environment on the cavitation–erosion behavior of polypropylene 21060.

Distinct trends were observed for polypropylene samples modified by direct gas fluorination. In all tested environments, ΔG values for fluorinated samples were lower than for the unmodified material, indicating increased resistance to cavitation–erosion wear due to surface modification. In alkaline media, mass loss of fluorinated samples occurs much more slowly, demonstrating the effectiveness of the modified layer in resisting simultaneous micro-impact and chemically aggressive action. Similar trends were observed in acidic and neutral media, where cavitation–erosion processes proceed more stably and less intensively.

Comparative analysis confirms that surface fluorination reduces cavitation–erosion wear intensity in all tested environments. This effect is attributed to the formation of a thin fluorinated layer on the polymer surface, which exhibits increased chemical inertness, lower permeability to aggressive components, and a reduction of free

radicals in the near-surface layer. This layer decreases surface destruction under micro-impacts and slows diffusion and chemical processes at the polymer interface.

Furthermore, the most intense cavitation–erosion wear occurs during the initial stage of cavitation exposure. The subsequent decrease in mass loss rate may be associated with changes in surface morphology and the establishment of quasi-stationary wear conditions.

Thus, the results confirm the effectiveness of surface fluorination as a promising method for enhancing the resistance of polypropylene to cavitation–erosion wear in various aggressive environments. This modification method reduces surface degradation under cavitation and increases the service life of polymer components during operation.

Conclusions

1. It was established that under cavitation loading, polypropylene 21060 exhibits a systematic increase in mass loss with increasing cavitation duration. The cavitation–erosion wear process is nonlinear, with more intensive mass loss occurring during the initial stage of testing.

2. The chemical nature of the environment significantly affects the intensity of cavitation–erosion degradation of polypropylene. The highest wear intensity for unfluorinated samples is observed in alkaline media, while in acidic and neutral environments, degradation processes occur less intensively.

3. Surface modification of polypropylene by direct gas fluorination reduces the intensity of cavitation–erosion wear in all tested environments. This effect is due to the formation of a thin fluorinated layer on the material surface, which has increased chemical inertness and a stable structure.

4. A laboratory setup for surface fluorination of polymer materials was developed, providing controlled gas-phase processing and enabling surface modification of samples with minimal fluorine consumption.

5. The proposed reactor design and fluorination technology ensure localized surface treatment of samples, efficient heat removal, and neutralization of active radicals after fluorination, which enhances the operational resistance of polymer materials to cavitation–erosion wear.

References

1. Martyniuk A. V., Stechyshyn M. S., Tsepenyuk M. I., Borys M. M., Bandura V. M., Mykhalevskyi V. Ts. Cavitation-Erosion Wear of Aminoplast in Simulated Environments of Sugar Production. Materials Science. 2024. Vol. 59, No. 6. P. 673–678. - https://doi.org/10.1007/s11003-024-00827-1.

2. Jaye, J.A., Sletten, E.M. Recent advances in the preparation of semifluorinated polymers // Polymer Chemistry. – 2021. – Vol. 12. – P. 6515–6526. - https://doi.org/10.1039/D1PY01024G

3. Yasuo E., Sugiyama M., Ishibashi Y., Hommura S., Okazoe T., Kuwamoto S., Ohta N., Kawaguchi D. Direct Fluorination of Ethylene–Tetrafluoroethylene Copolymer Films in Liquid Media // Macromolecules. – 2026. – https://doi.org/10.1021/acs.macromol.5c03120

4. Uno M., Sugiyama M., Okazoe T., Kawaguchi D. Polynorbornenes Bearing Cyclic Fluoroalkyl Side Groups for Achieving High Glass Transition Temperature and Low Refractive Index // Macromolecules. – 2025. – Vol. 58, No. 6. – P. 3221–3230. - https://doi.org/10.1021/acs.macromol.4c03185.

5. McCloskey, C. B., Yip, C. M., & Santerre, J. P. (2002). Effect of fluorinated surface-modifying macromolecules on the molecular surface structure of a polyether. Macromolecules, 35(3), 924–933. - https://doi.org/10.1021/ma010283v.

6. Li, X., Pan, J., Macedonio, F., Ursino, C., Carraro, M., Bonchio, M., Drioli, E., Figoli, A., Wang, Z., & Cui, Z. (2022). Fluoropolymer Membranes for Membrane Distillation and Membrane Crystallization. Polymers, 14(24), 5439. - https://doi.org/0.3390/polym14245439..

7. Zhang Y., Li B., Wang S., et al. Prediction of micro wear depth between engineering polymers // Journal of Manufacturing Processes. – 2024. – Vol. 124. – P. 1124–1134. - https://doi.org/10.1016/j.jmapro.2024.07.024.

8. Wang X., Wang Y., Liang Q., Zhang Y. Fundamentals of Single Cavitation Bubble Dynamics // SpringerBriefs in Energy. – 2024. - https://doi.org/10.1007/978-3-031-75041-0.

9. Seyedtaghi Mousavi, John G. Hardy. In-situ Microscopy and Digital Image Correlation to Study the Mechanical Characteristics of Polymer-Based Materials // Discover Materials. – 2025. – Vol. 5, Article 41.- https://doi.org/10.1007/s43939-025-00208-8.

10. Yang K., Zhang J., Wang S., et al. Thickness Effects of Surface Direct Fluorination and Plasma Treatments on Polymer Materials: Kinetics and Surface Properties // Materials and Manufacturing Processes. – 2023.- https://doi.org/10.1002/mame.202200557.

Мартинюк В., Стечишин, М., Федорів В., Ярошенко П., Люховець В. Установка та технологія газового фторування полімерів для підвищення їх зносостійкості при мікроударних навантаженнях

У статті розглянуто проблему підвищення кавітаційно-ерозійної зносостійкості полімерних матеріалів, що працюють в умовах мікроударних навантажень у корозійно-активних середовищах. Показано, що руйнування матеріалів у таких умовах має складний механіко-корозійний характер, а корозійні процеси можуть значно прискорювати деградацію поверхневих шарів. У зв'язку з цим актуальним є застосування полімерів із високою хімічною стійкістю та інертністю до агресивних середовищ. Проте використання таких матеріалів часто є економічно недоцільним, що обумовлює необхідність модифікації поверхні доступних конструкційних полімерів. Метою роботи є розроблення та наукове обґрунтування лабораторної установки і технологічних параметрів процесу прямого газового фторування полімерів для формування модифікованого поверхневого шару без зміни мікрогеометрії поверхні та підвищення їх зносостійкості. Об'єктом дослідження обрано поліпропілен марки 21060, який широко застосовується у машинобудуванні, сільськогосподарській техніці та харчовому обладнанні. У роботі спроектовано лабораторну установку для прямого газового фторування полімерів із використанням суміші 1% F_2 та 99% Ar з подальшою обробкою монооксидом азоту. Експериментальні дослідження показали формування модифікованого шару товщиною близько 5 мкм, що характеризується підвищеною хімічною інертністю. Встановлено, що фторування суттєво знижує інтенсивність кавітаційно-ерозійного зношування поліпропілену в різних середовищах, підтверджуючи ефективність методу для підвищення довговічності полімерних деталей.

Ключові слова: газове фторування, поліпропілен, поверхнева модифікація, кавітаційно-ерозійне зношування, агресивні середовища, мікроударні навантаження.

ISSN 2079-1372 Problems of Tribology, V. 31, No 1/119-2026, 92-98

Problems of Tribology
Website: http://tribology.khnu.km.ua/index.php/ProbTrib
E-mail: tribosenator@gmail.com

DOI: https://doi.org/10.31891/2079-1372-2026-119-1-92-98

Surface deformation relief as an indicator of fatigue damage under two-step loading sequences

M. Karuskevych* 0000-0003-1698-0296, **T. Maslak** 0000-0001-8320-8613, **O. Karuskevych** 0009-0009-7496-0075, **V. Korchuk** 0009-0006-0063-1656

National University «Kyiv Aviation Institute», Ukraine
**E-mail: mykhailo.karuskevych@npp.kai.edu.ua*

Received: 12 February 2026: Revised 28 February 2026: Accept: 14 March 2026

Abstract

The study investigates the possibility of predicting the residual fatigue life of clad structural aluminum alloys based on the quantitative evaluation of surface deformation relief formed during cyclic loading. Fatigue damage accumulation in metallic structures is accompanied by microstructural transformations caused by dislocation motion along crystallographic planes. These processes lead to the formation of characteristic surface features such as slip bands, extrusions, and intrusions. Although these structures are three-dimensional, their development can be effectively assessed using two-dimensional optical microscopy images, enabling quantitative analysis of the deformation relief evolution during fatigue loading. The research focuses on clad aluminum alloys widely used in aircraft structures, including D16ATV, V95, 2024-T3, and 7075-T6. A damage parameter D was introduced to characterize the saturation level of the deformation relief. This parameter is defined as the ratio of the surface area occupied by deformation relief features to the total observation area. Experimental observations were carried out using metallographic microscopy at magnifications of 200–400×. The obtained data allowed regression models to be developed that relate the damage parameter to the relative residual fatigue life. The proposed approach was extended from regular cyclic loading to simple irregular loading regimes, specifically two-step loading sequences of the "low–high" and "high–low" types. The results were compared with predictions based on Miner's linear fatigue damage summation rule. Experimental fatigue tests on D16ATV alloy specimens demonstrated that the accuracy of residual life prediction using the deformation relief based damage parameter depends on the stress range. Within a certain range of cyclic stresses, the developed regression model provides prediction accuracy comparable to, and in some cases exceeding, that obtained using Miner's rule. The results confirm that the saturation of surface deformation relief can serve as a structurally sensitive indicator of accumulated fatigue damage. The proposed methodology can be applied both to direct monitoring of clad aluminum structural components and to the fatigue indicators for metal structures of aircraft, bridge, pressure vessels.

Key words: fatigue, alclad alloy, deformation relief, Miner's rule, residual life, fatigue indicators.

Introduction

The phenomenon of fatigue damage in metallic structures is studied with the aim of preventing catastrophic failures, optimizing maintenance, and developing methods for technical condition diagnostics. The existence of a large number of diverse approaches to assessing accumulated fatigue damage indicates that current understanding of the fatigue process mechanisms remains insufficiently developed and that further accumulation of experimental data is required for subsequent generalization. The process of fatigue damage accumulation consists of structural transformations in the metal which, for a number of metals, exhibit features that can be observed using relatively simple surface examination methods. As a result of dislocation motion along crystallographic planes, extrusions, intrusions, and slip bands can be observed on the surface of many metals, forming a deformation relief. These surface structures are three-dimensional; however, even a two-dimensional digital optical image obtained using a metallographic microscope makes it possible to quantitatively assess their saturation level and evolution during cyclic loading. The general form of cyclic loading is irregular loading, i.e., loading in which the cycle parameters

are not constant during the service life of the structure. This is a typical situation for aircraft structures, which are subjected to loads of different origins and, accordingly, of different amplitudes, load ratio (cycle asymmetry), mean stress, sequence of applied loads, uniaxial and multiaxial loading, as well as in-phase and out-of-phase loading. An analytical assessment of accumulated fatigue damage for such structures under such loading conditions has not yet been fully resolved. The use of simplified models requires large safety factors, while instrumental monitoring methods are still under development and have not yet found widespread practical application. One of the reasons for the imperfection of existing methods is the insufficient attention paid to damage indicators that are not merely accompanying effects of metal fatigue (such as changes in electrical resistance), but that directly reflect the nature of the phenomenon – namely, changes in the metal structure resulting from dislocation motion. Below, key stages of a research cycle devoted to studying the evolution of deformation relief during cyclic loading are presented. The possibility of quantitative evaluation of the deformation relief of the cladding layer surface of widely used structural aluminum alloys is demonstrated for both regular and stepwise cyclic loading.

1. Deformation Relief of Metal Surfaces Formed under Cyclic Loading

As a result of cyclic loading, a deformation relief is formed on the surface of many pure metals and alloys. The deformation relief caused by the crystallographic slip includes extrusions, intrusions, and rotational structures of the surface layer of the metals. Detail description of relief components has been done in papers [1, 2]. Extrusions, intrusions and their role in the fatigue cracks forming and propagating in polycrystalline copper considered in the paper [3]. In the paper [4] it was shown that cyclic loading results in well-developed slip markings in the fully pearlitic steel. In the research [5] the evaluation of the extrusion/intrusion structure was conducted by the measuring surface roughness thus predicting location of the fatigue crack initiation. It was found by the authors of [6] in the results of in situ observations and characterization of the formation of Persistent Slip Bands (PSB) in micrometer-sized Ni single crystals, that a relatively large number of cycles (>106) was necessary to nucleate PSBs in microcrystals compared with bulk scale, and correspondingly, extreme fatigue lifetimes were exhibited at the micrometer scale. The PSB surface have an inherent roughness immediately on formation; then the roughness of the PSB remains stable with further cyclic loading. The slip traces formed in the first ~10 cycles are also found to identify the locations where PSBs and cracks form. The grain size effect and initial dislocation density on surface roughness evolution in Face Centered Cubic (FCC) Ni single crystals during the early number of cycles of mechanical cyclic loading has been simulated by the authors of the work [7]. For the number of cycles modeled, larger crystals showed a uniform surface step distribution compared to smaller crystals where the surface roughness was more localized in surface slip bands. In the work [8] the surface roughness of specimens made of Medium-Carbon Steel 42CrMo4 (SAE 4140) was measured using a confocal microscope to confirm the surface roughness evolution. The surfaces of the specimens changed during fatigue testing, moreover, the roughness evolution of the specimens at several applied stress amplitudes might correlate with the lifetime. Extrusions and intrusions under cyclic loading do not form in all materials. They were not observed in exploratory experiments on unclad D16 alloy conducted within the framework of the present study. At the same time, the cladding layer, formed from commercially pure aluminum or some of its ductile alloys, is sensitive to cyclic loading and exhibits the formation of surface deformation relief that reflects the process of deformation localization in the crystal at the micro-, meso-, and macro-levels.

2. Formation and Evolution of Surface Deformation Relief in Clad Aluminum Alloys

The surface deformation relief of clad aluminum alloys was investigated in order to develop a method for evaluating accumulated fatigue damage. The deformation relief that forms on the surface of aluminum alloys D16ATV, V95, 2024-T3, and 7075-T6 was studied. A typical appearance of the deformation relief on the polished surface of D16ATV alloy specimens after cyclic loading is shown in Fig. 1. The number of loading cycles and the percentage of the consumed fatigue life are indicated.

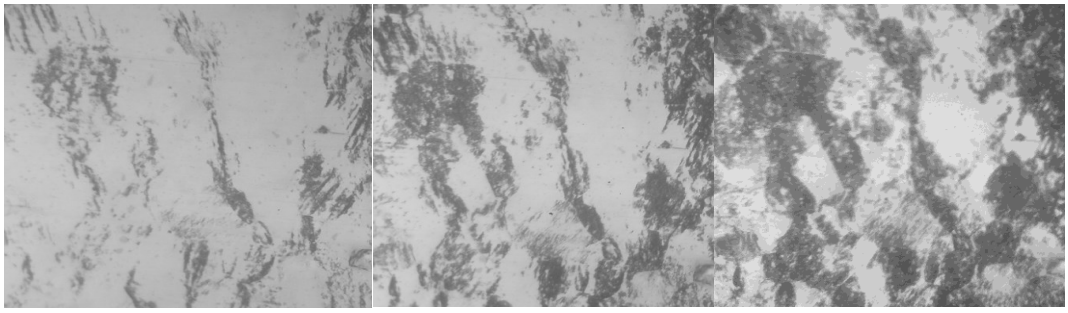

a) b) c)

Fig.1. Evolution of the surface deformation relief in the process of the cyclical loading: a) N= 30000 cycles (1.9%); b) N= 100000 cycles (6,3%); c) N= 400000 cycles (25,2%). R=0; σ_{max}=147,0 MPa

For the quantitative evaluation of the saturation of the deformation relief and the corresponding accumulated fatigue damage, a damage parameter was proposed. This parameter is defined as the ratio of the surface area exhibiting features of deformation relief to the observation area. The size of the observation area was 0.3 × 0.3 mm. In the present study, optical images were obtained at magnifications in the range of 200× – 400×.

The deformation relief was investigated during fatigue testing of aluminum alloy specimens under uniaxial tension and cantilever bending with different loading cycle parameters, under biaxial loading with in-phase and out-of-phase conditions, and under simple block-type irregular loading regimes. Typical curves describing the evolution of the deformation relief are shown in Figs. 2 and 3.

Experimental data on the evolution of the damage parameter during cyclic loading made it possible to obtain regression models for predicting the critical state, in which the relative remaining number of cycles $\overline{N_R}$ is considered as a function of the damage parameter.

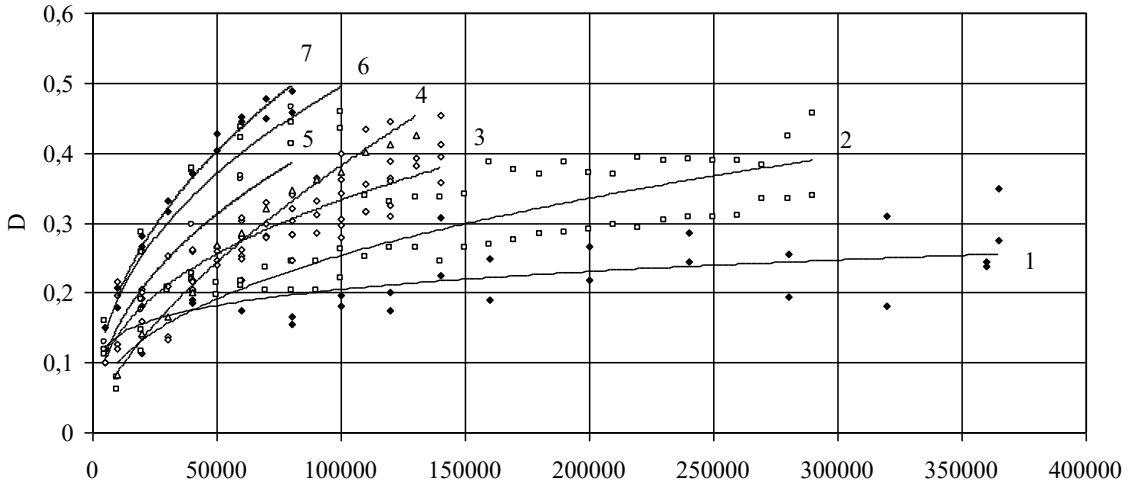

Fig.2. Dependence of the damage parameter *D* on maximum sress of the cycle under the axial cyclical loading: 1 - σ_{max}=76,9 MPa; 2 - σ_{max}=81,7 MPa; 3 - σ_{max}=96,2 MPa; 4 - σ_{max}=105,8 MPa; 5 - σ_{max}=115,4 MPa; 6 - σ_{max}=129,8 MPa, 7 - σ_{max}=134,6 MPa. Stress ratio *R*=0

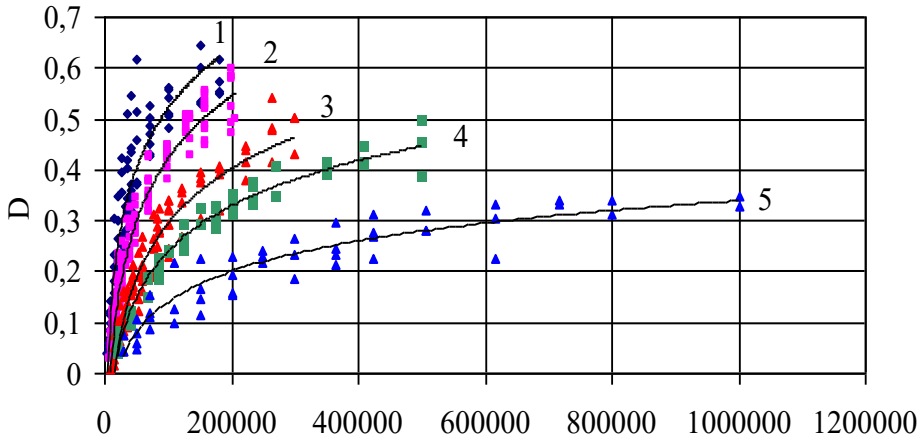

Fig.3. Evolution of the damage parameter *D* at the fatigue test by cantilever bending: 1 – *R* =0; 2 - *R* =0,3; 3 –*R* =0,42; 4 – R = 0,5; 5 – *R*=0,6

The model for predicting the residual fatigue life can be constructed by transforming the model of the evolution of the parameter D during cyclic loading. To estimate the residual life, the following correlation relationship was obtained: $N_R, \% = 119{,}29 - 226{,}3D$. The corresponding experimental values are shown in Fig. 4.

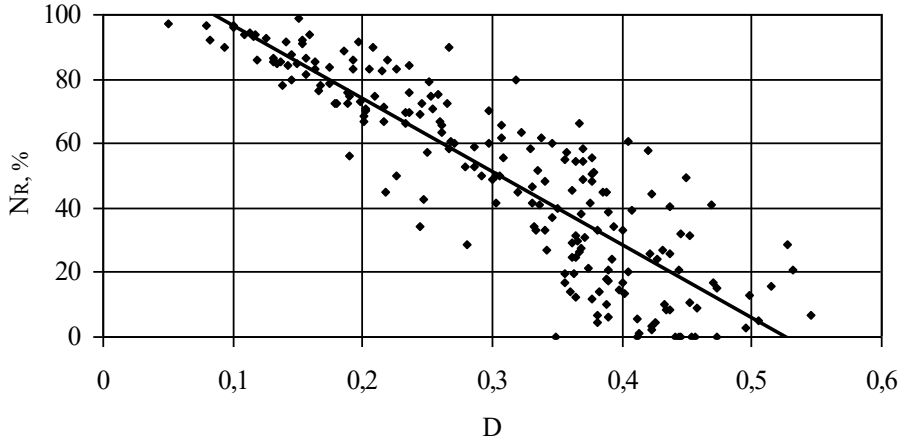

Fig.4. Dependence of the residual life N_R on the damage parameter D

3. Evaluation of accumulated damage and residual fatigue life under stepped irregular loading.

The summation of accumulated fatigue damage in simplified engineering calculations is most often performed according to the linear Miner's rule or its modifications. It is well known that one of the shortcomings of Miner's rule is that it does not take into account the sequence of the applied loads. In an experiment conducted on specimens of the D16AT aluminum alloy under a tensile cyclic loading condition, a comparison was made between the results of residual life evaluation obtained using the linear fatigue damage accumulation rule and those obtained using parameters of the deformation relief. The programmed fatigue tests included the implementation of two-step loading sequences: "high–low" and "low–high" (Fig. 5). The selection of stress levels was based on durability data obtained under regular loading regimes.

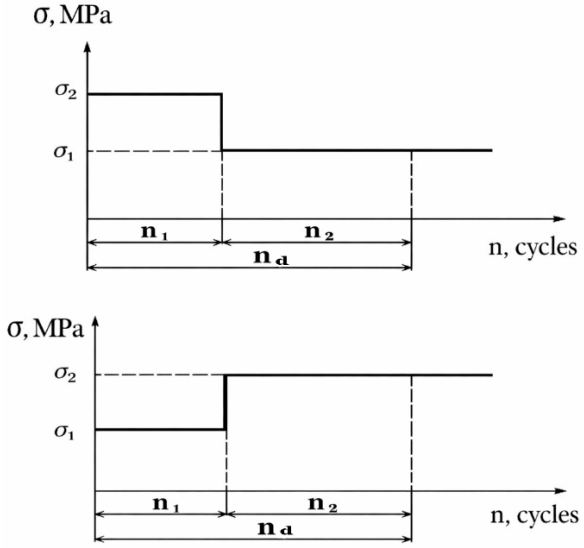

Fig.5. Scheme of two step block loading: n_1 – number of cycles at first step; n_2 – number of cycles at second step; n_d – number of cycles at which the damage was assessed

After the implementation of two loading steps, the tests were continued while recording the number of cycles up to the initiation of a fatigue crack and up to complete failure. The following quantities were determined: the damage parameter D and the corresponding residual life at a given cyclic loading level according to the regression model presented above; the relative damage according to the Miner rule and the corresponding residual life; the relationship between these quantitative indicators and the sequence of loading application; and the assessment of the adequacy of the Miner rule and of the method for determining accumulated damage based on the deformation relief state. The relative damage and the sum of relative damages were determined with respect to the moment of formation of a crack with a length of 1.0 mm. The basis for calculating the relative damages according to Miner's theory was the previously obtained fatigue curves. Two series of tests were carried out: with a transition from a lower stress level to a higher one, and from a higher stress level to a lower one. In the first series, the "low" stress level was 79.0 MPa and the "high" stress level was 108.0 MPa. In the second series, the "low" stress level was 79.0 MPa and the "high" stress level was 133.0 MPa. The selection of stress levels was based on data on fatigue life under regular loading conditions and on the results of monitoring the deformation

relief. Conditions were taken into account under which the exhaustion of the fatigue life is determined by the damage parameter *D*, regardless of the level of cyclic stress, as well as conditions under which the determination of this parameter is not sufficient for reliable prediction of the remaining number of loading cycles. The loading regimes of both steps in the first series of programmed tests corresponded to the stress range in which the exhaustion of fatigue life can be determined by the damage parameter *D* regardless of the level of cyclic stress, whereas the loading regimes of the second series of tests were partly outside this range. In tests performed according to the "low–high" scheme (79.0 MPa – 108.0 MPa), the average value of the sum of relative damages was $\sum n/N = 1.089$**.** In tests according to the "high–low" scheme (108.0 MPa – 79.0 MPa), the average value of the sum of relative damages was $\sum n/N = 1.138$**.** As can be seen, loading with a transition from a lower stress level to a higher one produces a greater damaging effect than loading with a transition from a higher stress level to a lower one, which, according to data reported by other authors, may exhibit a strengthening effect. The features of the damage accumulation process were also considered for loading regimes outside the range from 70.0 MPa to 120.0 MPa, within which the damage parameter is determined by the relative cyclic life and does not depend on the stress level. In tests performed according to the "low–high" scheme (79.0 MPa – 133.0 MPa), the average value of the sum of relative damages was $\sum n/N = 0.796$. In tests performed according to the "high–low" scheme (133.0 MPa – 79.0 MPa), the average value of the sum of relative damages was $\sum n/N = 1.605$.

Table 1 presents the results of calculating the residual fatigue life both according to Miner's rule and using the damage parameter.

Table 1

Results of residual fatigue life evaluation under a two-step loading program

Loading scheme	Residual life according to Miner's rule n_{resM}, cycles	Mean value of the residual fatigue life according to the damage parameter *D*, n_{resD}, cycles	Mean value of the residual fatigue life according to the experiment, n_{res}, cycles	Mean value of the prediction error when using Miner's rule	Mean prediction error when using the damage parameter *D*
79MPa-108 MPa	61596	69547	68380	9,82	-1,806
108 MPa -79 MPa	119 148	131488	166800	28,36	20,78
133 MPa -79 MPa	115 582	131501	216933	45,36	37,3
79 MPa - 133 MPa	34 531	34654	27166	-52,43	51,21

The results of the residual life calculations presented in Table 1: a) according to the Miner rule; b) according to the damage parameter D determined by the developed methodology after two stages of programmed loading and the corresponding regression model of life consumption, as well as the actual fatigue lives obtained experimentally, make it possible to conclude that within a certain range of loading regimes the obtained regression model of life consumption allows the residual life to be determined with an accuracy that exceeds the accuracy of life estimation according to the Miner rule. The agreement of the residual life calculation methods, both according to the Miner rule and according to the prediction methodology based on the damage parameter D, decreases with increasing levels of the applied stresses.

At the same time, the prediction obtained by both methods gives an overestimated result for loading according to the "low–high" scheme and an underestimated result for loading according to the "high–low" scheme. Thus, the regression model of life consumption developed on the basis of regular fatigue tests makes it possible to evaluate the residual life of aircraft structural elements without the use of additional calculations within a certain range of programmed loading regimes.

4. Implementation of the Surface Deformation Relief Phenomenon in Fatigue Damage Indicators for Metal Structures

One of the applications of data concerning the evolution of the surface deformation relief of clad aluminum alloys is a method that involves installing fatigue indicators for metal structures (FIMS) on loaded structural elements of various purposes. The need to use such indicators arises from the fact that a significant number of structural materials do not exhibit the formation of surface deformation relief under cyclic loading and do not possess a cladding layer that belongs to PSB (Persistent Slip Band) metals, i.e., metals on whose surface extrusions, intrusions, and slip bands can be observed during cyclic loading. The results of this work demonstrated that the surface deformation relief can be considered an indicator of fatigue damage. When such an indicator is attached to the surface of loaded structural elements, a correlation can be established between the damage in the indicator and the damage in the structure, making it possible to assess the exhaustion of the fatigue life of the structure. For many structures, another solution is more optimal, namely, the use of structural alloys with a cladding layer instead of single crystals. The basic configuration is an indicator specifically developed for aircraft fatigue monitoring (Fig. 6). In this case, the cladding layer of the indicator serves as the fatigue damage indicator, whose sensitivity to cyclic loading was demonstrated above. The sensitivity of the indicators is determined by their geometry. The

loading regimes of some other engineering structures indicate the possibility and expediency of using structurally-sensitive fatigue damage indicators.

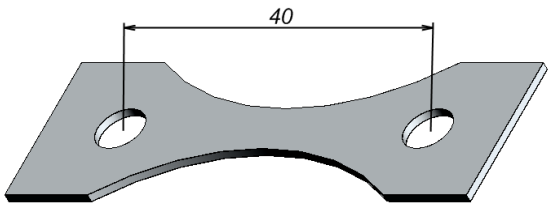

Fig. 6. Basic configuration of the Fatigue Indicator for Metal Structures

After analyzing the deformation of elements of steel bridges [10], it was established that indicators manufactured from 2024-T3 clad alloy (Alclad) are capable of responding to the service deformations of bridge elements made of S275 and S355 steels through the formation of a surface deformation relief [18]. Another potential application of fatigue indicators for metal structures is the monitoring of fatigue damage in oil and gas transportation systems, for example for Compressed Natural Gas (PNG) pressure cylinders [12, 13].

Conclusions

The study of the evolution of the surface deformation relief of clad aluminum structural alloys indicates a close correlation between the density of the deformation relief and the accumulated fatigue damage within a certain range of cyclic stresses and the corresponding strains. Under irregular two steps cyclic loading, this phenomenon makes it possible to predict the residual life with an accuracy that is not inferior to, and within a certain range even exceeds, the accuracy of prediction based on the Miner rule.

The obtained conclusions can be implemented both in the direct monitoring of the technical condition of structures made of clad aluminum alloys and in the application of fatigue indicators for metal structures.

References

1. Polák J., Mazánová V., Heczko M., Petráš R., Kuběna I., Casalena L., Man J.. The role of extrusions and intrusions in fatigue crack initiation. Engineering Fracture Mechanics. 2017. Vol. 185. P. 46–60. DOI: https://doi.org/10.1016/j.engfracmech.2017.03.006.

2. Polák J. Role of Persistent Slip Bands and Persistent Slip Markings in Fatigue Crack Initiation in Polycrystals. Crystals. 2023. Vol. 13. Article 220. DOI: https://doi.org/10.3390/cryst13020220

3. Polák J., Babinský T., Vražina T. and Kruml T. The Role of Extrusions and Intrusions in the Initiation and Intergranular Growth of Fatigue Cracks. Advanced Engineering Materials. 2024. Vol. 26. Article 2400313. DOI: https://doi.org/10.1002/adem.202400313

4. Vogt J.-B., Costa I. M. O. A., Addad A., Bouquerel J. Fatigue intrusion-extrusion in a fully pearlitic steel. Materials Letters. 2020. Vol. 267. Article 127539. DOI: https://doi.org/10.1016/j.matlet.2020.127539

5. Hao R., Lin W. Evolution of surface roughness of notched steel details under fatigue loading. Structures. 2023. Vol. 58. Article 105441. DOI: https://doi.org/10.1016/j.istruc.2023.105441

6. Lavenstein S. et al. The heterogeneity of persistent slip band nucleation and evolution in metals at the micrometer scale. Science. 2020. Vol. 370. eabb2690. DOI: https://doi.org/10.1126/science.abb2690

7. Hussein A. M., El-Awady J. A. Surface roughness evolution during early stages of mechanical cyclic loading International Journal of Fatigue. 2016. Vol. 87. P. 339–350. DOI: https://doi.org/10.1016/j.ijfatigue.2016.02.022

8. Seensattayawong P., Kerscher E. The Evolution of Surfaces on Medium-Carbon Steel for Fatigue Life Estimations. Coatings. 2024. Vol. 14. Article 1077. DOI: https://doi.org/10.3390/coatings14081077

9. Pejkowski Ł., Karuskevich M., Maslak T. Extrusion/intrusion structure as a fatigue indicator for uniaxial and multiaxial loading. Fatigue and Fracture of Engineering Materials and Structures. 2019. Vol. 42, № 10. P. 2315–2324. DOI: https://doi.org/10.1111/ffe.13066

10. Design and Evaluation of Steel Bridges for Fatigue and Fracture. Publication No. FHWA-NHI-16-016. Washington: Federal Highway Administration, 2016.

11. Karuskevych M., Maslak T., Karuskevych O., Vlasenko Y. Fatigue indicator for metal structures: from aircraft to bridges. Aviation. 2025. Vol. 29, Issue 3. P. 174–182. DOI: https://doi.org/10.3846/aviation.2025.24532

12. Cok L., Busetto P., De Zotti L., Dorigo S., Angelini S. GASVESSEL – CNG Sea Transportation Project. Technology and Science for the Ships of the Future. 2018. P. 681–690. DOI: https://doi.org/10.3233/978-1-61499-870-9-681

13. Kwak H. S., Park G. Y., Kim C. Design of Compressed Natural Gas Pressure Vessel (Type II) to Improve Storage Efficiency and Structural Reliability. Journal of Pressure Vessel Technology. 2020. Vol. 142, № 1. 011303. DOI: https://doi.org/10.1115/1.4045027

Карускевич М.В. , Маслак Т.П. , Карускевич О.М. , Корчук В.І. Деформаційний рельєф поверхні як індикатор втомного пошкодження при ступінчатому циклічному навантажуванні

У роботі досліджено можливість прогнозування залишкового ресурсу втоми плакованих конструкційних алюмінієвих сплавів на основі кількісної оцінки поверхневого деформаційного рельєфу, що формується під час циклічного навантаження. Накопичення втомних пошкоджень у металевих конструкціях супроводжується мікроструктурними перетвореннями, зумовленими рухом дислокацій уздовж кристалографічних площин. У результаті цих процесів на поверхні металу утворюються характерні структурні елементи, зокрема смуги ковзання, екструзії та інтрузії. Хоча ці структури мають тривимірний характер, їх розвиток може ефективно оцінюватися за допомогою двовимірних оптичних зображень, отриманих за допомогою металографічного мікроскопа, що дозволяє кількісно аналізувати еволюцію деформаційного рельєфу під час втомного навантаження. Дослідження присвячене плакованим алюмінієвим сплавам, які широко застосовуються в авіаційних конструкціях, зокрема сплавам Д16АТВ, В95, 2024-Т3 та 7075-Т6. Для характеристики ступеня насичення деформаційного рельєфу було введено параметр пошкодження *D*. Цей параметр визначається як відношення площі поверхні, зайнятої елементами деформаційного рельєфу, до загальної площі спостереження. Експериментальні спостереження проводилися за допомогою металографічної мікроскопії при збільшенні 200–400$^{\times}$. Отримані експериментальні дані дали змогу побудувати регресійні моделі, що пов’язують параметр пошкодження з відносним залишковим ресурсом втоми. Запропонований підхід було поширено з умов регулярного циклічного навантаження на прості режими нерегулярного навантаження, зокрема на двоступеневі програми навантаження типу «низький–високий» та «високий–низький». Отримані результати порівнювалися з прогнозами, виконаними за правилом лінійного підсумовування втомних пошкоджень Майнера. Експериментальні випробування зразків зі сплаву Д16АТВ показали, що точність прогнозування залишкового ресурсу на основі параметра деформаційного рельєфу залежить від діапазону напружень. У певному інтервалі циклічних напружень розроблена регресійна модель забезпечує точність прогнозування, яка є не гіршою, а в окремих випадках навіть перевищує точність оцінювання за правилом Майнера. Отримані результати підтверджують, що ступінь насичення поверхневого деформаційного рельєфу може розглядатися як структурно чутливий індикатор накопичених втомних пошкоджень. Запропонована методика може бути використана як для безпосереднього моніторингу технічного стану конструкцій із плакованих алюмінієвих сплавів, так і для індикаторів втоми металевих конструкцій літаків, мостів, посудин під тиском.

Ключові слова: втома, плаковані сплави, деформаційний рельєф, залишковий ресурс, індикатори втоми.

ISSN 2079-1372 Problems of Tribology, V. 31, No 1/119-2026, 99-105

Problems of Tribology
Website: http://tribology.khnu.km.ua/index.php/ProbTrib
E-mail: tribosenator@gmail.com

DOI: https://doi.org/10.31891/2079-1372-2026-119-1-99-105

Electromechanical wear of the contact wire–current collecting insert pair in electric transport systems

O.S. Kovtun*[0009-0000-6036-6723], **A.O. Polishchuk**[0000-0001-7887-7169]

[1]*Khmelnytskyi National University, Ukraine*
**E-mail: alkovt1982@gmail. com*

Received: 15 February 2026: Revised 28 February 2026: Accept: 15 March 2026

Abstract

The article considers the processes of current collection and wear in the sliding electrical contact system "contact wire - current collection insert" of a trolleybus. It is shown that the destruction of contact surfaces has a complex electromechanical nature and is caused by the simultaneous action of mechanical, electrical and thermal factors. The main mechanisms of electrical and mechanical wear of contact elements are analyzed, in particular, electroerosion, abrasive, fatigue and molecular-mechanical wear. The influence of contact pressure, current collector speed, traction current magnitude and properties of contact pair materials on the intensity of destruction of surface layers is considered. It is shown that the uneven distribution of current in the contact zone leads to local overheating of the surface and the formation of electric arcs, which accelerate the electroerosion destruction of contact elements. It is established that the formation of a thin graphite film on the surface of the contact wire can partially reduce the friction coefficient and wear intensity. The results obtained can be used to increase the durability of current-collecting elements of electric transport and optimize their operating modes.

Keywords: current collection; current collection insert; contact wire; electrical wear; mechanical wear; electrical erosion; sliding electrical contact; electric transport.

Introduction

Electric transport, in particular trolleybuses, is widely used in urban transport systems due to its high energy efficiency and environmental friendliness. One of the most important elements of such systems is the contact network, through which electrical energy is transmitted from the power supply network to the rolling stock. The transmission of current from the contact wire to the electrical equipment of the vehicle occurs through pantographs equipped with current-collecting inserts that are in constant sliding contact with the contact wire (Fig. 1).

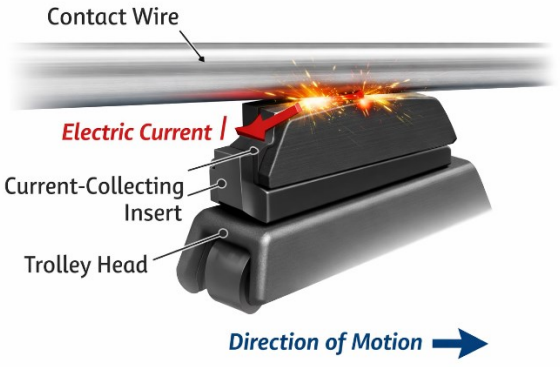

Fig. 1. Tribocontact pair "contact wire-current collector insert"

During operation, a complex interaction of mechanical, electrical and thermal processes occurs in the contact zone of the contact wire and the current collector insert. Under the action of contact pressure, electric current and friction forces, the surface layers of materials are subjected to intense plastic deformation, local heating and electrical erosion. This leads to the gradual destruction of the contact surfaces, which manifests itself in the form of wear of the contact wire and current collector elements. The intensity of wear of the contact pair largely depends on the design parameters of the contact network, the stability of the contact pressure of the current collector, the speed of the vehicle and the magnitude of the electric current. An important role is also played by the physical, mechanical and electrophysical properties of the materials of the contact elements, in particular their electrical conductivity, hardness, thermal conductivity and melting point. The study of wear processes in a sliding electrical contact allows us to determine the main mechanisms of destruction of contact surfaces and develop effective methods for increasing the durability of current collector elements. This is important for reducing the costs of maintenance of the contact network and increasing the reliability of electric transport. In this regard, the purpose of this work is to analyze the main mechanisms of electrical and mechanical wear of the contact pair "contact wire - current collector insert" and determine the factors that most affect the intensity of destruction of contact surfaces during the operation of trolleybus transport.

Literature review

The problem of wear of the contact pair "contact wire - current collector insert" of electric transport is important for ensuring the reliability of current collection systems and the stability of the operation of the contact network. It is known that in a sliding electrical contact, mechanical, electrical and thermal processes simultaneously operate, which determine the intensity of destruction of the contacting surfaces [1].

Studies of the characteristics of a sliding electrical contact in the "current collector - contact wire" system have shown that the stability of current collection is largely determined by the parameters of contact pressure, electric current and temperature in the contact zone. At the same time, a change in these parameters leads to an uneven distribution of current over the contact surface and an increase in contact resistance [1,7].

Experimental studies of the tribological interaction of current-collecting inserts with the contact wire have shown that the wear mechanism is complex and includes abrasive, adhesive and electroerosion processes. As a result of local overheating of the surfaces in the contact zone, electric arcs may occur, causing melting of the material and the formation of craters on the surface of the contact wire [3,10].

The speed of movement and the electrical load play an important role in the wear processes. It has been shown that with increasing current, the intensity of electrical erosion of contact surfaces increases, while an increase in contact pressure leads to an increase in the mechanical component of wear [3,4].

A number of works have investigated the influence of geometric and dynamic parameters of current collectors on the processes of destruction of contact elements. It has been established that uneven contact pressure and oscillations of the current collector can cause local overloads of the contact zones and accelerate the wear of current collection inserts [4,5].

Considerable attention in modern research is paid to predicting the service life of contact inserts. The proposed mathematical models and machine learning methods allow assessing the influence of the main operational parameters on the wear rate and predicting the moment of reaching the limit state of contact elements [6].

A review of modern research shows that the wear of the contact pair "pantograph - contact wire" is a complex electromechanical process that depends on the material of the contact surfaces, the operating mode and the parameters of the contact network [7].

An important direction for increasing the reliability of current collection systems is the improvement of contact insert materials. Studies have shown that the use of composite materials based on graphite with metal additives allows improving electrical conductivity and reducing the intensity of wear of contact surfaces [8].

Some works are devoted to increasing the wear resistance of contact elements by restoring and strengthening their surface layers. It has been shown that the use of modern technologies for restoring and modifying the surface allows to significantly increase the service life of contact units of electric transport [9].

Thus, the literature analysis shows that the wear process of the contact pair "contact wire - current collector insert" is determined by the complex interaction of mechanical, electrical and thermal factors. Despite a significant amount of research in this area, the issues of increasing the wear resistance of current collector inserts and predicting their resource remain relevant and require further research.

Main material

Electrical wear of sliding contact

Electrical wear of a sliding contact is mainly caused by electrical erosion. Electrical erosion is the destruction of contacting materials associated with the melting and transfer of metal in a gaseous and liquid (in the form of small droplets) state from one contacting surface to another under the action of electrical discharges. Electrical erosion is especially significant in DC circuits. It can lead to the formation of growths and craters on

the contact surfaces. The higher the value of the specific heat capacity, melting point, specific heat of fusion and sublimation temperature of the contacting materials, the lower their electrical erosion. It was noted above that more thermal energy is required to melt aluminum than to melt the same mass of copper, although copper has a higher melting point. This is explained by the fact that the specific heat capacity and specific heat of fusion of aluminum are higher than those of copper.

The intensity of electrical wear of sliding contact materials depends not only on their nature, but also on the current density, contact pressure force and contact design. The surfaces of breaking and sliding contacts always have irregularities (roughness) as a result of mechanical processing, wear, plastic deformation. In addition, they are covered with a film of oxides and sulfides formed under the influence of atmospheric oxygen, ozone and sulfur-containing gases and liquids, as well as various accidental pollutants. The thickness of such a film depends on many factors and is usually $10^{-6}…10^{-5}$ mm; its specific electrical resistance is not less than 10^3 Ohm m. The distribution of current over the contacting surfaces is uneven, since the structure of the surfaces is inhomogeneous.

The surface structure of an electrical contact consists of four main types of contact areas (spots) (Fig. 2): contact spots with a metal contact (1), through which electric current flows without noticeable transition resistance; contact spots covered with adhesive and chemisorbed monomolecular films are quasi-metallic contacts (2), which easily pass electric current due to the tunneling effect; contact spots covered with electrically insulating relatively thick films of oxides and sulfides (3) and do not pass electric current; non-contact areas 4.

The contact parts touch only in areas 1, 2, forming a real contact surface. In areas g, there is no contact pair. The total area of the electrical contact consists of the sum of the areas of all spots (1+2 + 3+4) and is an imaginary contact surface formed by the crushing of the roughness protrusions of the contact surfaces under the action of contact pressure (pressure). At low voltages, the electric current actually passes only through areas (spots) and 2 of the real contact surface. In strong electric fields, due to the breakdown of thick films of oxides and sulfides (areas) and air layers (areas 4), they also become electrically conductive. In this case, part of the electrical energy is transmitted in contact through arc discharges, which cause electrical wear of the contacting surfaces and determine the efficiency and quality of current collection. Therefore, the smaller the contact pressure, the larger the area of non-contact areas, the higher the power of the electric arc and the more intense the electrical wear.

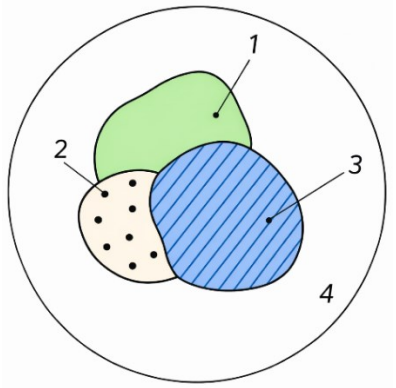

Fig. 2. Scheme of the contact surface: 1 - metal spots (areas); 2 - quasi-metallic spots; 3 - spots of insulating thick films of oxides and sulfides; 4 - non-contact areas

Since the electric current in the contact passes only through metallic and quasi-metallic areas, the current lines are distributed unevenly over the entire geometric surface of the contact. They are contracted to areas with metallic and quasi-metallic conductivity and are bent. As a result, the current density in these areas increases, which leads to the emergence of the resistance of the current lines to contract *Rcon* (constriction resistance). In this regard, the total contact (transition) resistance *Rc* consists of the resistance of the conductive microcontacts and the resistance arising from the contraction of the current lines. The contact pressure force *F*, the state of the contacting surfaces, and the magnitude of the current I directly affect the value of *Rcon* and, accordingly, the total contact resistance *Rc* and the heating temperature of the contacts when an electric current flows. With an increase in the contact pressure *F*, a decrease in the roughness of the contact surfaces and the proportion of areas covered with insulating oxide and sulfide films, the value of the contact resistance Rc can significantly decrease.

Due to the heating of the contact wire during interaction with the current-collecting elements, recrystallization and strengthening of copper occur to a certain depth (0.54-0.16 mm) within several days of operation. Later, when the contact wire wears out to the limit value, the strengthening of the surface layer in depth remains constant.

In the operating conditions of the trolleybus contact network, the electrical wear of the contact pair "contact wire - current collector insert" is largely determined by the instability of the electrical contact and the occurrence of short-term electric arcs. Such phenomena can occur when the contact is locally broken due to surface irregularities, current collector oscillations, changes in contact pressure or contamination of the contact wire surface. At the moment of microcontact rupture between the conductive sections, an electric arc is formed, which leads to local heating, melting and evaporation of the material of the contacting surfaces.

At the same time, characteristic microcraters, molten metal inflows and oxidation products are formed on the surface of the contact wire and current-collecting insert, which change the microgeometry of the surface and increase the contact resistance. This subsequently leads to an even greater current concentration on individual areas of the contact surface and intensification of electrical erosion. These processes are especially intense at high current values, unstable contact pressure and increased speeds of rolling stock.

Additionally, it should be taken into account that the electrical resistance in the contact area is largely determined by the phenomenon of current line contraction in the microcontact area. According to the classical Holm theory of electrical contacts, the contact resistance of one microcontact can be estimated by the formula:

$$R_c = \frac{\rho}{2a},$$

where ρ is the electrical resistivity of the contact material, *a* is the radius of the contact spot.

When an electric current flows through microcontacts, their local heating occurs, which can be estimated using the Joule–Lenz law:

$$Q = I^2 R_c t$$

where *I* is the current strength, *Rc* is the contact resistance, *t* is the current flow time.

Local heat release in the microcontact zone causes an increase in the temperature of the surface layers of the material, which can lead to their melting, the formation of microcraters and the intensification of electroerosion wear of the contact pair.

In addition, an important role in the process of electrical wear is played by the electrophysical properties of the current collector insert material, in particular electrical conductivity, thermal conductivity, melting point and the ability to form stable protective films on the surface. The use of graphite-based composite materials allows reducing the intensity of electrical erosion due to their ability to form a thin graphite film on the contact wire, which partially stabilizes the contact and reduces the local current density.

Mechanical wear of sliding contact

Mechanical wear of contact wires and current-collecting elements occurs as a result of friction of surfaces that contact and slide relative to each other. The main types of mechanical wear of materials in sliding contact are oxidative, fatigue, abrasive and molecular-mechanical. Oxidative wear is associated with the destruction of thin oxide films on friction surfaces and their formation again. Fatigue wear is associated with deformation, cracking and removal of a heavily hardened (hardened) layer of rubbing surfaces. Abrasive wear is caused by the ingress of solid particles from the outside (dust, sand, etc.) between the rubbing surfaces, as well as wear products (metal oxides and particles from the destroyed heavily hardened layer). Molecular-mechanical wear is explained by the processes of seizing, tearing and tearing out of particles of contact materials. This causes deformation and heating, which causes the contact surfaces to oxidize. The lubricant significantly reduces molecular-mechanical wear.

In sliding contact, under the influence of processes caused by friction, plastic deformation and hardening of the surface layer of the contact wire occurs. As a result, the density of dislocations and the heterogeneity of their distribution increase in the surface layer of the contacting surface, which leads to the formation of microregions. During further operation, the formed microregions are crushed and disoriented. Outside their boundaries, the concentration of internal stresses increases, which lead to the formation of microcracks. Behind them, the destruction of the surface layers occurs with the separation of mechanical particles that participate in the abrasive wear of the contacting surface of the contact wire. The intensity of the formation of microregions and the subsequent destruction of the contacting surface increases with increasing speed of movement and the force of pressing the current collector on the contact wire.

Destructive processes caused by plastic deformation and hardening of the surface layer, as well as abrasive wear, largely depend on the nature of the contact wire metal. In a contact wire made of alloyed copper, the plastic deformation of the surface layer is less than in pure copper, therefore, there are fewer and further destructive processes. As a result, the resistance of the contact wire to mechanical wear increases. In alloyed copper, the tendency to set is also reduced. Since the hardness and hardening temperature of copper increase during alloying, the resistance to abrasive wear increases and the upper limit of the operating temperature increases.

The intensity of mechanical wear increases with increasing contact pressure, and decreases with improving the quality of the lubricant in the contact. Therefore, this indicator is greatly influenced by the nature of the materials of the contact pair and, first of all, their hardness. The most unfavorable in this respect are contact pairs made of the same material (for example, the contact pair "copper contact wire - copper current-collecting plate").

The dependence of the degree of wear of the contact surface of contact wires made of bronze of CuAg0.1 and CuMg0.5 grades on the speed of movement (up to 50 km/h), contact pressure (up to 300 N) and current load (up to 1000 A) was investigated. Studies have shown that at constant contact pressure (250 N) and constant current load (300 A), the maximum wear of the contact wire surface occurs at a speed of movement of about 50 km/h. At constant speed of movement (50 km/h) and constant current load (300 A), with increasing contact pressure, the wear of the contact wire surface increases. At a constant speed (50 km/h) and constant contact pressure with a force of 75 or 150 N, with increasing current load, the wear of the contact wires increases, and at a contact pressure

with a force of 300 N and with an increase in current load from 100 to 150 A, the wear of the contact wires disappears.

Studies show that when moving at high speed, with an increase in current load and contact pressure, the service life of contact wires can be extended. With an increase in traction current to a certain value, other things being equal, the intensity of contact wire wear decreases. This is explained by the "lubricating" effect of the current, which occurs as a result of the formation of a graphite film on the surface of the contact wire. When normalizing the speed of movement, it is possible to obtain a contact wire wear value of 1 mm per 100,000 pantograph passes. It also follows from these works that with an increase in current load, the electrical form of contact wire wear increases, and with an increase in contact pressure, the mechanical form of wear.

When contact wires interact with current-collecting elements as a result of heating of the contacting surfaces under the influence of high current loads, the surface layer of the contact wire can be strengthened to a depth of 0.54...1.16 mm. The weakened layer of copper (bronze) that has formed will be subject to more intense mechanical wear (abrasive and molecular-mechanical). Thus, structural changes in the metal (alloy) of the contact wire caused by electrical wear increase the intensity of its mechanical wear.

Based on the above, it can be concluded that the intensity of electromechanical wear of contact wires and current-collecting elements, in addition to their design and technical condition, mainly depends on: the uniformity of the contact suspension of the wire in the span; the amplitude of the force of pressing the moving current collector on the contact wire; the magnitude of the consumed current; the nature of the materials of the friction surfaces and the quality of the lubricant.

One of the most important and largely determining the efficiency of electric traction parameters is the cost associated with the cost of repairing worn contact wires and replacing them with new ones. These costs consist not only of the cost of new contact wires (minus the cost of the material of the worn wires) and the labor costs for their replacement, but also of losses due to delays in the traffic schedule, which are necessary for the performance of basic works.

Under conditions of sliding electrical contact of the contact wire and the current-collecting insert, mechanical wear is closely related to thermomechanical processes occurring in the surface layers of materials. Under the action of contact pressure and tangential friction forces, significant local stresses arise in the contact zone, which lead to intensive plastic deformation of the surface layer. As a result, a riveted layer with a changed microstructure, increased dislocation density and increased hardness is formed.

During long-term operation of the contact pair, cyclic loading of the surface layers of materials occurs, which leads to the development of microcracks due to contact fatigue. Further propagation of such microcracks causes the separation of small particles of material, which accumulate in the contact zone and can act as abrasive particles. In this case, the wear mechanism switches to a mixed mode, which includes elements of abrasive and fatigue wear.

An important factor affecting the intensity of mechanical wear is the microgeometry of the surface of the contact wire and the current-collecting insert. With increasing surface roughness, the number of local contacts between the protrusions of micro-irregularities increases, which leads to an increase in contact stresses and intensification of plastic deformation processes. At the same time, the probability of the formation of micro-interference between the surfaces increases, which contributes to the development of adhesive wear.

In the contact pair "copper contact wire - graphite or composite current collector insert" an important role is played by the formation on the surface of the contact wire of a thin layer of wear products containing graphite and metal oxides. Such a layer can act as a solid lubricating coating, reducing the coefficient of friction and the intensity of mechanical wear. At the same time, with excessive accumulation of wear products or ingress of solid abrasive particles from the external environment (dust, sand), this layer can turn into an abrasive medium, which accelerates the destruction of the surface of the contact wire.

In addition, it should be taken into account that mechanical wear in a sliding electrical contact is inextricably linked to electrical and thermal processes. Heating of the contact zone under the action of a current load can lead to a decrease in the strength of the surface layer of the contact wire material, which increases its susceptibility to plastic deformation and accelerates the development of mechanical wear. Thus, the real process of destruction of materials in the contact pair "contact wire - current-collecting insert" has an electromechanical nature and is determined by the complex action of mechanical, electrical and thermal factors.

Conclusions

1. It is shown that the wear of the contact pair “contact wire – current-collecting insert” is of an electromechanical nature and is determined by the complex action of mechanical, electrical and thermal processes in the sliding contact zone.

2. It has been established that electrical wear of contact surfaces is mainly caused by electrical erosion, which occurs as a result of local electrical discharges and uneven current distribution between surface microcontacts.

3. It is shown that mechanical wear of contact elements occurs as a result of abrasive, fatigue and molecular mechanical processes and largely depends on the contact pressure, the speed of movement of the current collector and the properties of the materials of the contact pair.

4. It has been established that the use of composite graphite materials for current-collecting inserts contributes to the formation of a thin protective film on the surface of the contact wire, which reduces the friction coefficient and the intensity of wear of the contact surfaces.

References

1. Wu, G., Wu, J., Wei, W., Zhou, Y., Yang, Z., & Gao, G. (2018). Characteristics of the sliding electric contact of pantograph/contact wire systems in electric railways. Energies, 11(1), 17. https://doi.org/10.3390/en11010017

2. Pieniak, D., Walczak, M., & Niewczas, A. (2025). Tests of operational wear of trolleybus traction wires. Applied Sciences, 15(23), 12716. https://doi.org/10.3390/app152312716

3. Ding, T., Xuan, W., He, Q., Wu, H., & Xiong, W. (2011). Study on friction and wear properties of pantograph strip–copper contact wire for high-speed train. Tribology International, 44(4), 437–444. https://doi.org/10.1016/j.triboint.2010.12.005

4. Zhang, W., Zhou, N., & Mei, G. (2016). Dynamic performance and wear behavior of pantograph contact strips in high-speed railway systems. Wear, 366–367, 220–229. https://doi.org/10.1016/j.wear.2016.06.018

5. Song, D., Jiang, Y., & Zhang, W. (2017). Effects of contact strip wear on service performance of pantograph system. Journal of Southwest Jiaotong University, 52(3). https://doi.org/10.3969/j.issn.0258-2724.2017.03.003

6. Kuźnar, M., Burek, J., & Zając, J. (2021). A method of predicting wear and damage of pantograph sliding strips using artificial neural networks. Materials, 14(24), 7612. https://doi.org/10.3390/ma14247612

7. Wu, G., Gao, G., Yang, Z., & Zhou, Y. (2022). Pantograph–catenary electrical contact system of high-speed railways: A review. Railway Engineering Science, 30, 1–15.https://doi.org/10.1007/s40534-022-00281-2

8. Zhi, X., Zhou, N., Wei, H., Cheng, Y., Zhang, W., & Chen, G. (2025). Study on wear performance and mechanism of pantograph contact strip under different environmental conditions. Friction. https://doi.org/10.26599/FRICT.2025.9441101

9. Kovtun, OS, Dytyniuk, VO, Staryi, AL, & Fasolia, VO (2024). Restoration and wear resistance of electric transport sliding contacts. Problems of Tribology, 29(2/112), 58–66. https://doi.org/10.31891/2079-1372-2024-112-2-58-66

10. Yang, H., Chen, G., & Gao, G. (2015). Experimental research on friction and wear properties of pantograph contact strips. Journal of Shanghai Jiaotong University (Science), 20(1), 79–84. https://doi.org/10.1007/s12204-015-1603-4

Ковтун О.С., Поліщук А.О. Електромеханічне зношування пари «контактний провід – струмознімальна вставка» електротранспорту

У статті розглянуто процеси струмознімання та зношування в системі ковзного електричного контакту «контактний провід – струмознімальна вставка» тролейбуса. Показано, що руйнування контактних поверхонь має складний електромеханічний характер і зумовлюється одночасною дією механічних, електричних та теплових факторів. Проаналізовано основні механізми електричного та механічного зношування контактних елементів, зокрема електроерозію, абразивне, втомне та молекулярно-механічне зношування. Розглянуто вплив контактного натискання, швидкості руху струмоприймача, величини тягового струму та властивостей матеріалів контактної пари на інтенсивність руйнування поверхневих шарів. Показано, що нерівномірність розподілу струму у зоні контакту призводить до локального перегріву поверхні та утворення електричних дуг, які прискорюють електроерозійне руйнування контактних елементів. Встановлено, що формування на поверхні контактного дроту тонкої графітової плівки може частково знижувати коефіцієнт тертя та інтенсивність зношування. Отримані результати можуть бути використані для підвищення довговічності струмознімальних елементів електричного транспорту та оптимізації режимів їх експлуатації.

Ключові слова: струмознімання; струмознімальна вставка; контактний провід; електричне зношування; механічне зношування; електрична ерозія; ковзний електричний контакт; електротранспорт.